



IRANIAN JOURNAL OF NUCLEAR MEDICINE

Iranian Journal of Nuclear Medicine is a peer-reviewed biannually journal of the Research Center for Nuclear Medicine, Tehran University of Medical Sciences, and is a fully open access journal with no author's charge of submission/publication fee covering basic and clinical nuclear medicine sciences and relevant applications such as molecular imaging, functional and metabolic investigation of disease, radiobiology, dosimetry, radiopharmacy, radiochemistry, instrumentation and computer sciences, etc. The journal particularly welcomes original articles reflecting the local or worldwide growing materials as well as common critical problems and interests in the field of nuclear medicine. Also systematic reviews, meta-analyses, general reviews, mini-reviews, short communications, editorials, case reports and letters to the editor in this subject will be accepted. The aim of this journal is to contribute to the education of physicians, technologists, and other relevant specialists and to provide an opportunity for the exchange of scientific information for national and international nuclear medicine community. The journal has been published in Persian (Farsi) from 1993 to 1994, in English and Persian [with English abstract] from 1994 to 2008 and only in English language from the early of 2008. The journal has an international editorial board and accepts manuscripts from scholars working in different countries.

Chairman & Chief Editor: Saghari, Mohsen; MD

Associate Editor and Executive Manager: Beiki, Davood; PhD

Scientific Affairs: Eftekhari, Mohammad; MD and Fard-Esfahani, Armaghan; MD

Editorial Board

Ahmadzadehfar, Hojjat; MD (Germany)	Grammaticos, Philip C.; MD (Greece)
Alavi, Abbas; MD (USA)	Jalilian, Amir Reza; PhD (Austria)
Ay, Mohammad Reza; PhD (Iran)	Mirzaei, Siroos; MD (Austria)
Beheshti, Mohsen; MD (Austria)	Rahmim, Arman; PhD (USA)
Beiki, Davood; PhD (Iran)	Rajabi, Hossein; PhD (Iran)
Cohen, Philip; MD (Canada)	Saghari, Mohsen; MD (Iran)
Eftekhari, Mohammad; MD (Iran)	Sarkar, Saeed; PhD (Iran)
Fard-Esfahani, Armaghan; MD (Iran)	Zakavi, Seyed Rasoul; MD (Iran)

Editorial Office

Iranian Journal of Nuclear Medicine,
Research Center for Nuclear Medicine,
Shariati Hospital, North Kargar Ave. 1411713135, Tehran, Iran

Tel: ++98 21 88633333, 4

Fax: ++98 21 88026905

E-mail: irjnm@tums.ac.ir

Website: <http://irjnm.tums.ac.ir>

Indexed in/Abstracted by

SCOPUS, ESCI (Emerging Sources Citation Index), EMBASE, ISC, DOAJ, Academic Resource Index, Scientific Indexing Services, ULRICHSWEB, Index Copernicus, EBSCO, IMEMR, SID, IranMedex, Magiran, CIVILICA

Vol 28 , Supplement 1

2020

INSTRUCTION TO AUTHORS

Aims and Scope

Iranian Journal of Nuclear Medicine is a peer-reviewed biannually journal of the Research Center for Nuclear Medicine, Tehran University of Medical Sciences, covering basic and clinical nuclear medicine sciences and relevant applications such as molecular imaging, functional and metabolic investigation of disease, radiobiology, dosimetry, radiopharmacy, radiochemistry, instrumentation and computer sciences, etc.

The journal particularly welcomes original articles reflecting the local or worldwide growing materials as well as common critical problems and interests in the field of nuclear medicine. Also systematic reviews/meta-analyses, general reviews, mini-reviews, short communications, editorials, case reports and letters to the editor in this subject will be accepted. The aim of this journal is to contribute to the education of physicians, technologists, and other relevant specialists and to provide an opportunity for the exchange of scientific information for national and international nuclear medicine community.

Manuscript submission

There are no charges for publication in this journal and all manuscripts should be submitted via journal, URL: <http://irjnm.tums.ac.ir>, easy to use and easy to track, thus by conducting all procedures electronically your submission will be done rather faster. Once you submit an article, it will be forwarded to one of the editors and afterwards to at least two of the peer-reviewers. At once after submission, the author will be notified of both the submission process by means of email and the follow-up ID code. It is recommended to save the sent ID code for all the future correspondence regarding each article separately.

Conditions and Ethics

Manuscripts are considered with the understanding that they are submitted solely to the "Iran J Nucl Med" and have not been published elsewhere previously either in print or electronic format, and are not under consideration by another publication or electronic medium. Submission of an article for publication implies the transfer of the copyright from the authors to the "Iran J Nucl Med" upon acceptance. The final decision of acceptance rests with the Editor. Authors are responsible for all statements made in their papers. All accepted papers become the permanent property of the "Iran J Nucl Med" and you may not modify copy, distribute, transmit, display, or publish elsewhere without written permission from the "Iran J Nucl Med". Authors should refrain from contacting the mass media about papers that are being peer reviewed or in press; the Editor reserves the right to withdraw an article from publication if it is given media coverage at any stage of the review/publication process.

Peer review and publication processes

1- All submitted manuscripts are subject to peer review and editorial approval. For paper submission, author should refer to the journal website and register himself/herself as an author using the "Register" link. After receiving their username and password via e-mail, the author could use the "Submit paper" link, log in, and submit the manuscript.

2- If the received manuscript is not written according to the journal format (considering the format in sectioning, the number of words in abstract, references, etc....) and/or the English language does not meet the required quality, the manuscript will be sent back to the corresponding author for revision and re-submission.

3- Manuscripts having the above-mentioned criteria are referred to the related section editor. If the paper fits to the specified fields of the journal and has innovation, then it will be sent to two or more national and international referees, expert in that specific field. The corresponding author could also suggest potential reviewers to the journal at the time of submission. However, the editor reserves the right to select or refuse to use the suggested potential reviewers.

4- If the nature of the work and the results necessitates deep statistical analysis, by suggestion of the Editor-in-Chief and/or referees, the manuscript is reviewed by a statistics expert as well.

5- Each reviewer suggests alteration/corrections or additional work to be done, asks questions to be answered by the author, and makes an overall opinion about the manuscript as being: acceptable as it is, acceptable after minor/major revision, or not acceptable. The reviewers' comments are then sent to the corresponding author.

6- After receiving the modified version of the manuscript and/or author's answers to the reviewers' questions, it will be sent to a final reviewer. If the modifications and/or answers are not adequate, it will be sent back to the corresponding author with a specified deadline to send the final corrected version.

7- The final corrected version of the manuscript is sent back to the same final reviewer. Then, the comments and the overall opinion of the final reviewer are evaluated by the Editor, and the final decision (the acceptance letter or a letter informing the author of not accepting the manuscript) will be sent to the corresponding author.

8- Authors will be able to check the progress of their manuscript through the submission system at any time by logging into the journal website.

Ethical considerations will be taken into account in the assessment of papers that have experimental investigations of human or animal subjects. Authors should state in the Methods section of the manuscript that informed consent was obtained from all human adult participants and from the parents or legal guardians of minors and an appropriate institutional review board approved the project. Those

investigators without such review boards should ensure that the principles outlined in the Declaration of Helsinki have been followed.

Manuscript categories

Original articles

These include controlled trials, interventional studies, studies of screening and diagnostic tests, outcome studies, cost-effectiveness analyses, and large-scale epidemiological studies. Each manuscript should clearly state an objective; the design and methodology; the essential features of any interventions; the main outcome measures; the main results of the study; a discussion placing the results in the context of published literature; and the conclusions which can be drawn based on the study. The text should not exceed 4000 words, the number of tables, figures, or both should not be more than six, and references not more than 40.

Review articles

These are, in general, invited papers, but unsolicited reviews, if of good quality, may be considered. Reviews are systematic critical assessments of literature and data sources pertaining to clinical topics, emphasizing factors such as cause, diagnosis, prognosis, therapy, or prevention. The text should not exceed 6000 words, the number of tables, figures, or both should not be more than ten, and references not more than 120. All articles and data sources reviewed should include information about the specific type of study or analysis, population, intervention, exposure, and test or outcomes. All articles and data sources should be selected systematically for inclusion in the review and critically evaluated, and the selection process should also be described in the paper.

Case reports

Case reports will be accepted only if they deal with a clinical problem that is of sufficient interest. The text should not exceed 2500 words; the number of tables, figures, or both should not be more than four; references should not be more than 25.

Editorials/Commentaries

Commentaries on current topics or on papers published elsewhere in the issue. Length should not exceed 2000 words; tables or figures are allowed only exceptionally; references should not be more than 40.

Letters to the editor

Letters discussing a recent article in the "Iran J Nucl Med" are welcome and should be sent to the Editorial Office by e-mail within 6 weeks of the article's publication. Letters that do not refer to an "Iran J Nucl Med" article may also be considered. The text should not exceed 1000 words, have no more than two figure or table, and 10 references.

Short communications

Short communications are suitable for the presentation of research that extends previously published research, including the reporting of additional controls and confirmatory results in other settings, as well as negative results, small-scale

clinical studies, clinical audits and case series. Authors must clearly acknowledge any work upon which they are building, both published and unpublished.

Systematic reviews/meta-analyses

Authors should report systematic reviews and meta-analyses in accordance with the PRISMA (Preferred Reporting Items for Systematic Reviews and Meta-Analyses) statement.

Criteria for manuscripts

Manuscripts submitted to the "Iran J Nucl Med" should meet the following criteria: the content is original; the writing is clear; the study methods are appropriate; the data are valid; the conclusions are reasonable and supported by the data; the information is important; and the topic has general medical interest. Manuscripts will be accepted only if both their contents and style meet the standards required by the "Iran J Nucl Med".

Manuscript preparation

Authors should refer to a current issue of the "Iran J Nucl Med" and to the Uniform Requirements for Manuscripts Submitted to Biomedical Journals for guidance on style, a copy of which can be found at www.icmje.org. To distinguish different parts of the article, it is recommended to use the font Times New Roman size 12 for the body, size 12 bold for subheadings, size 14 for headings and size 14 bold for the title. Please double check the article for spelling, structure and format mistakes. Use Arabic numerals for numbers above nine, for designators (e.g. case 5, day 2, etc) and for units of measure; numbers should be spelled out if below 10, at the beginning of sentences, and for fractions below one. Manuscripts should be word-processed double-spaced.

The manuscript (complete with tables and figures) should be submitted via journal URL: <http://irjnm.tums.ac.ir>

The manuscript should be accompanied by the following statements, signed by all the authors: "No work resembling the enclosed article has been published or is being submitted for publication elsewhere. We certify that we have each made a substantial contribution so as to qualify for authorship and that we have approved the contents. We have disclosed all financial support for our work and other potential conflicts of interests." Use System International (SI) measurements only, except when "Dual report" is indicated in the SI unit conversion table.

Use generic names of drugs, unless the specific trade name of a drug used is directly relevant to the discussion. When generic names are not available, brand names which take an initial capital can be used. In Original articles, the maker of the study drug must be given. Do not use abbreviations and symbols in the title or abstract and limit their use in the text. Standard abbreviations may be used and should be defined on first mention in the text unless they are the standard units of measurement. In general, terms should not be abbreviated unless they are used repeatedly and the abbreviation is helpful to the reader.

Arrangement

Title page-This page should contain (1) the title, (2) names and surnames of authors, with their degrees [maximum two] and affiliations; if an author's affiliation has changed since the work was done, list the new affiliation as well, (3) the full address, phone and fax numbers, and e-mail address of the corresponding author, and (4) a short running head of no more than 40 characters.

Abstract-The abstract should not exceed 250 words for structured (Original articles) or unstructured abstracts (Review articles, Case reports). The abstract should be concise, summarizing the purpose, basic procedures, main findings (giving specific data and their statistical significance, if possible), and principal conclusions of the investigation. Structured abstract headings should be as follows: Introduction, Methods, Results, Conclusion.

Key words-At the end of the abstract, authors should provide no more than five key words to assist with cross-indexing of the paper. Key words should be taken from Medical Subject Headings (MeSH) list of *Index Medicus*:

(<http://www.nlm.nih.gov/mesh/MBrowser.html>).

Introduction-The rationale for the study should be summarized and pertinent background material outlined. The Introduction should not include findings or conclusions.

Methods-The methods section should include the design of the study, the type of materials involved, a clear description of all comparisons, and the type of analysis used, to enable replication. These should be described in sufficient detail to leave the reader in no doubt as to how the results are derived.

Results-These should be presented in logical sequence in the text, tables, and illustrations; repetitive presentation of the same data in different forms should be avoided. This section should not include material appropriate to the Discussion. Results must be statistically analyzed where appropriate, and the statistical guidelines of the International Committee of Medical Journal Editors should be followed.

Discussion-Data given in the Results section should not be repeated here. This section should consider the results in relation to any hypothesis/es advanced in the Introduction. This may include an evaluation of methodology and of the relationship of new information to the existing body of knowledge in that field. Conclusions should be incorporated into the final paragraph and should be commensurate with-and completely supported by-data in the text.

Note: The Results and Discussion sections may be broken into subsections with short, informative headings. The Results and Discussion may also be combined into a single section.

Conclusion-This should state clearly the main conclusions of the research and give a clear explanation of their importance and relevance. Summary illustrations may be included.

Acknowledgement-All contributors who do not meet the criteria for authorship should be covered in the acknowledgement section. It should include persons who provided technical help, writing assistance and departmental head who only provided general support. Financial and material support should be acknowledged.

References-Number references in the order they appear in the text; do not alphabetize. References should follow the Vancouver style and should appear in the text, tables, and legends as Arabic numerals in square brackets. Only articles, datasets and abstracts that have been published or are in press, or are available through public e-print/preprint servers, may be cited; unpublished abstracts, unpublished data and personal communications should not be included in the reference list, but may be included in the text and referred to as "unpublished observations" or "personal communications" giving the names of the involved researchers. Obtaining permission to quote personal communications and unpublished data from the cited colleagues is the responsibility of the author. Footnotes are not allowed. Journal abbreviations follow *Index Medicus*/MEDLINE. Citations in the reference list should include all named authors, up to the first 30 before adding '*et al.*'.

Any *in press* articles cited within the references and necessary for the reviewers' assessment of the manuscript should be made available if requested by the editorial office. Authors are responsible for the accuracy of references and must verify them against the original documents.

The following are sample references:

Standard journal article

List all authors, up to the first 30 before adding '*et al.*':

Mackness MI, Mackness B, Durrington PN, Fogelman AM, Berliner J, Lusic AJ, Navab M, Shih D, Fonarow GC. Paraoxonase and coronary heart disease. *Curr Opin Lipidol*. 1998 Aug;9(4):319-24.

Article, no author given:

Cancer in South Africa. *S Afr Med J*. 1994 Dec;84(12):15.

In press article:

Kharitonov SA, Barnes PJ: Clinical aspects of exhaled nitric oxide. *Eur Respir J*, in press.

Published abstract:

Zvaifler NJ, Burger JA, Marinova-Mutafchieva L, Taylor P, Maini RN: Mesenchymal cells, stromal derived factor-1 and rheumatoid arthritis [abstract]. *Arthritis Rheum* 1999;42:s250.

Thesis:

Kohavi R: Wrappers for performance enhancement and oblivious decision graphs. PhD thesis. Stanford University, Computer Science Department; 1995.

Chapter in a book:

Phillips SJ, Whisnant JP. Hypertension and stroke. In: Laragh JH, Brenner BM, editors. *Hypertension: pathophysiology, diagnosis, and management*. 2nd ed. New York: Raven Press; 1995. p. 465-78.

Book, personal author(s):

Ringsven MK, Bond D. Gerontology and leadership skills for nurses. 2nd ed. Albany (NY): Delmar Publishers; 1996.

Book, editor(s) as author:

Norman IJ, Redfern SJ, editors. Mental health care for elderly people. New York: Churchill Livingstone; 1996.

Book, Organization as author and publisher:

Institute of Medicine (US). Looking at the future of the Medicaid program. Washington: The Institute; 1992.

Article in electronic form:

Morse SS. Factors in the emergence of infectious diseases. *Emerg Infect Dis* [serial online] 1995 Jan-Mar [cited 1996 Jun 5];1(1):[24 screens]. Available from: <http://www.cdc.gov/ncidod/EID/eid.htm>

Conference proceedings:

Kimura J, Shibasaki H, editors. Recent advances in clinical neurophysiology. Proceedings of the 10th International Congress of EMG and Clinical Neurophysiology; 1995 Oct 15-19; Kyoto, Japan. Amsterdam: Elsevier; 1996.

Conference paper:

Bengtsson S, Solheim BG. Enforcement of data protection, privacy and security in medical informatics. In: Lun KC, Degoulet P, Piemme TE, Rienhoff O, editors. MEDINFO 92. Proceedings of the 7th World Congress on Medical Informatics; 1992 Sep 6-10; Geneva, Switzerland.

Tables

Each table should be numbered and cited in sequence using Arabic numerals (i.e. Table 1, 2, 3 etc.). Tables should also have a title (above the table) that summarizes the whole table. Detailed legends may then follow, but they should be concise. Tables should always be cited in text in consecutive numerical order. Tables considered to be integral to the manuscript can be pasted into the end of the document text file, in A4 portrait or landscape format. These will be typeset and displayed in the final published form of the article. Such tables should be formatted using the 'Table object' in a word processing program to ensure that columns of data are kept aligned when the file is sent electronically for review; this will not always be the case if columns are generated by simply using tabs to separate text. Columns and rows of data should be made visibly distinct by ensuring that the borders of each cell display as black lines. Commas should not be used to indicate numerical values. Color and shading may not be used; parts of the table can be highlighted using symbols or bold text, the meaning of which should be explained in a table legend. All non-standard abbreviations used in each table should be defined in the footnotes, in alphabetical order. Statistical measures of variations such as standard deviation, standard error of the mean, or confidence interval should be identified in headings. Tables should not be embedded as figures or spreadsheet files.

Figures

Figures must be submitted as separate files. We will NOT accept any images with resolution below 300 dpi. Illustrations include photographs, photomicrographs, charts, and diagrams, and these should be camera-ready. Professional medical illustrators should be consulted when figures are prepared; freehand or typewritten lettering is unacceptable. Letters, numbers, and symbols should be clear and of sufficient size to retain legibility when reduced. The diagram should not lose clarity on reduction; it is generally simplest to aim for a 50% linear reduction. Titles and detailed explanations should be confined to legends and not included in illustrations. Number illustrations consecutively in the order of their first citation in the text.

Please note that it is the responsibility of the author(s) to obtain permission from the copyright holder to reproduce figures or tables that have previously been published elsewhere.

Typography

- 1- Please use double line spacing.
- 2- Type the text justified, without hyphenating words at line breaks.
- 3- Use hard returns only to end headings and paragraphs, not to rearrange lines.
- 4- Capitalize only the first word, and proper nouns, in the title.
- 5- All pages should be numbered.
- 6- Use the Iran J Nucl Med reference format.
- 7- Footnotes are not allowed.
- 8- Please do not format the text in multiple columns.
- 9- Greek and other special characters may be included. If you are unable to reproduce a particular special character, please type out the name of the symbol in full. *Please ensure that all special characters used are embedded in the text, otherwise they will be lost during conversion to PDF.*

The Final Checklist

The authors must ensure that before submitting the manuscript for publication, they have taken care of the following:

- 1- Title page should contain title, short running title, name and surname of author/co-authors, their qualifications, designation and institutions they are affiliated with and mailing address for future correspondence, e-mail address, phone and fax number.
- 2- Abstract in structured format up to 250 words.
- 3- References mentioned as stated in the "Guide for Authors" section.
- 4- Do not submit tables as photographs. Make sure for heading of the table, their number.
- 5- Photographs/illustrations along with their captions. Titles and detailed explanations should be confined to legends and not included in illustrations.
- 6- Disclosure regarding source of funding and conflict of interest if any besides approval of the study from respective Ethics Committee/Institution Review Board.
- 7- Covering Letter
- 8- Copyright Transfer Form

Sample Cover Letter

Dear Editor

On behalf of my co-authors, I would like to submit our manuscript entitled "-----" for consideration of publication by your Journal. This manuscript has not been published in this or any similar form (in print or electronically, including on a web site), nor accepted for publication elsewhere, nor is under consideration by another publication. All authors offer the copyright to the "Iran J Nucl Med" and each author has contributed significantly to the submitted manuscript. Also it should be mentioned that, there is no conflict of interest in connection with the submitted article.

"Corresponding Author's Signature"

Copyright Transfer Form

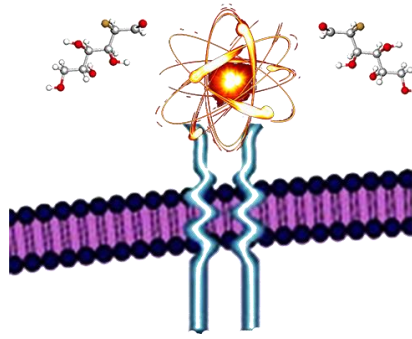
The Iranian Journal of Nuclear Medicine is pleased to publish your manuscript entitled: "-----".

Upon acceptance by *The Iranian Journal of Nuclear Medicine*, all copyright ownership for the article named above is transferred to *The Iranian Journal of Nuclear Medicine*. We, the undersigned coauthors of this article, have contributed to (1) data design, analysis, or interpretation; (2) writing or critiquing drafts of the manuscript; and (3) approval of the final manuscript before publication. We share in the responsibility for the release of any part or all of the material contained within the article noted above. We also affirm that the manuscript has been seen and approved by all authors. The undersigned stipulate that the material submitted to *The Iranian Journal of Nuclear Medicine* is new, original and has not been submitted to another publication, be it print or electronic, for concurrent consideration; likewise, this manuscript has not been published elsewhere either in part or in its entirety.

We also attest that any human and/or animal studies undertaken as part of the research from which this manuscript was derived are in compliance with regulations of our institution(s) and with generally accepted guidelines governing such work.

We further attest that we have herein disclosed any and all financial or other relationships that could be construed as a conflict of interest and that all sources of financial support for this study have been disclosed and are indicated in the acknowledgments.

Corresponding Author's Signature	Date
Author's Signature	Date
Author's Signature	Date
Author's Signature	Date
Author's Signature	Date
Author's Signature	Date
Author's Signature	Date



ABSTRACTS

23rd Iranian Nuclear Medicine Annual Congress

27-29 November 2019

Tehran, IRAN

Head of the Congress: Mohsen Saghari, MD

Scientific Chairman: Saeed Farzanehfar, MD

Executive Chairman: Mehrshad Abbasi, MD

Clinical Nuclear Medicine Committee

Scientific Chairman: Saeed Farzanehfar

Mohsen Saghari
Mehrshad Abbasi
Yalda Salehi
Alireza Zakani
Rasoul Zakavi
Vahid Reza Dabbagh
Ramin Sadeghi
Babak Shafiei
Majid Asadi
Shahram Dabiri

Medical Physics Committee

Scientific Chairman: Peyman Sheikhzadeh

Mohammad Reza Ay
Arman Rahmim
Ahmad Bitarfan Rajabi
Pardis Ghafarian
Parham Geramifar
Alireza Kamali Asl
Mehdi Sadeghi
Davood Khezerlo
Hojjat Mahani
Ali Shabestani Monfared
Ali asghar Parach

Reza Paydar

Jalil Pirayesh Eslamian

Radiopharmacy Committee

Scientific Chairman: Nasim Vahidfar

Davood Beiki
Mehdi Shafiee Ardestani
Tahereh Firuzyar
Seyed Jalal Hosseinimehr
Soraya Shahhosseini
Zohreh Noaparast
Mostafa Erfani
Kayvan Sadri
Ayoub Aghanejad
Fariba Johari Daha

Executive Committee

Marzieh Peyman
Ali Hoseini
Sedigheh Hoseini Shabanan
Abbas Monsef
Poorya Nakhaei
Zahra Kalaei
Narges Aghakhan Olia
Maryam Vaghefi
Abolfazl Salarian Zade

Posters (Nuclear Medicine)

P 001

The relationship between Ga-68 PSMA PET CT scan and serum PSA in patients with biochemical recurrence prostate cancer

Vahid Khalili, Mahasti Amoui, Elahe Pirayesh

Shahid Beheshti University of Medical Sciences, Tehran, Iran

Background: Early diagnosis of prostate cancer is very important and will be effective in controlling the disease as well as targeted selection of therapies.

Objective: To evaluate the Ga-68 PSMA scan of PET in patients with prostate cancer and its relationship with serum PSA.

Methods: This cross-sectional study was performed on patients with prostate cancer with biochemical recurrence (increase in PSA $>$ 0.2 ng/ml after prostatectomy or three successive increases in serum PSA levels after the initial treatment). Finally, the diagnostic power of the PSMA-Ga68 scan was determined and its association with serum PSA values was analyzed.

Results: Mean and SD of the levels of PSA in 72 patients in the first and second turns were observed for 34 patients, 1.96, 5.6, 3.53, and 8.7, respectively. Out of 39 patients with PSA Serum less than 2 ng/ml had positive diagnostic results for 25 (64%) patients, while for those with serum PSA greater than 5, out of 20 patients had positive results for all patients. The general sensitivity of PETCT was 79%.

Conclusion: Our study shown that with the increase in serum PSA level, the PET CT scan detection increased significantly. Also, the accuracy of PET CT was higher than other conventional methods, such as MRI and CT scan.

P 002

A challenging case of differentiated follicular thyroid carcinoma – an individual approach by different PET tracers – a case report

Mohsen Beheshti, Reyhane Manafi-Farid

PET-CT Center, St. Vincent's Hospital, Ordensklinikum, Linz, Austria

Research Center for Nuclear Medicine, Tehran University of Medical Sciences, Tehran, Iran

Differentiated thyroid carcinoma (DTC) has been successfully managed with thyroidectomy and radioiodine (RAI) therapy for decades. Nevertheless, infrequent cases of RAI refractory patients have always been challenging. In case of negative whole-body iodine scan, an alternative method should be employed to localize tumoral foci. F-18 fluorodeoxyglucose positron emission tomography/computed tomography (¹⁸FDG-PET/CT) is a widely accepted modality in this concept. However, a limited number of cancers do not exhibit significant metabolic activity to be pictured by ¹⁸FDG-PET/CT. Also, tumor visualization with a number of other non-specific PET-tracers has been demonstrated. Somatostatin receptor imaging has shown encouraging results in iodine negative DTC. More importantly, peptide receptor radionuclide therapy has been employed in the management of these patients. Furthermore, prostate-specific membrane antigen (PSMA) expression has been documented in the neovasculature of thyroid malignancies. In this report, a 79-year-old patient with a long history of follicular thyroid carcinoma is presented, who suffers from RAI refractory metastatic disease. Afterwards, an intriguing pattern of different PET-tracers uptake, including Gallium-68 dodecane tetraacetic acid Nal3-octreotide (⁶⁸Ga-DOTANOC) and ⁶⁸Ga-PSMA, is discussed, which sheds light on a hypothesis of taking advantage of the novel theranostic radio-ligand, PSMA, in the treatment of DTC.

P 003

Systematic review of PET/CT Scan in oncology

Masoume Gity, Rana farshbaf Aghaeinejad

Emam Khomeini Hospital, Tehran University of Medical Science, Tehran, Iran

Background: Despite developments in surgical treatment, radiation therapy, and chemotherapy protocols, tumor recurrence and metastasis are still major problems in breast cancer management. The aim of the present report was to review and compare the performance of PET/CT with some of the conventional imaging modalities in detection of breast cancer recurrence

Methods: A literature search was performed in PubMed, Embase and ScienceDirect databases with no search restriction for the date of publication. The most important current clinical applications of 18F-FDG PET/CT in breast cancer patients are for the detection and evaluation of recurrent or metastatic disease

Results and Conclusion: 60 studies including a total of 1378 patients with prior breast cancer and clinical suspicion of recurrence that assessed the sensitivity, specificity, and accuracy of PET/CT and other conventional imaging methods in followed up by treated breast cancer and presented the results in systematic review format. The information extracted from each article included the first author, publication year, number of patients and their characteristics, index test(s), sensitivity, specificity, positive predictive value (PPV), negative predictive value (NPV), and accuracy.

P 004

Screening of first-degree family members of thyroid cancer patients for evaluation of the prevalence of benign and malignant thyroid disease in comparison with normal community persons

Zahra Kiamanesh, Farrokh Seilanian Tousi, Narjess Ayati, Seyed Rasoul Zakavi

Nuclear Medicine Research Center, Mashhad University of Medical Sciences, Mashhad, Iran

Background: Thyroid cancer is known as the most common endocrine malignancy with an incidence of 298,000 cases per year. A literature survey shows that the risk of this cancer is higher in first-degree relatives of differentiated thyroid cancer patients. It should be noted that based on some investigations, the familial thyroid carcinoma shows more aggressive behavior; on the other hand, other researchers claim that the intensity or prognosis of the familial and sporadic types are similar.

Objective: Because of the available controversy and absence of a consensus on the necessity of performing a screening program in first-degree relatives of an affected patient, we are motivated to compare thyroid disease incidence between these groups and persons without a familial history of thyroid cancer.

Methods: We conducted a case-control study including 127 first-degree relatives of 40 patients with differentiated thyroid cancer as the case group and 127 controls matched by sex and age. After collecting demographic data, the persons underwent thyroid disease screening with the physical examination, thyroid function tests, and thyroid ultrasonography.

Results: The number of 127 subjects in the case group were compared with 127 persons in the control group. The mean age at screening was 40.11 ± 13.6 years (18-79 years) in cases and 42.96 ± 12.9 years (27-75 years) in controls. Each of the case and control groups comprises 83 female and 44 male persons. A personal history of thyroid disease has no significant statistical differences between the two groups; nevertheless, thyroid dysfunctions were higher in the person with a history of differentiated thyroid cancer in first-degree relatives. Besides, these individuals had a greater probability of having thyroid nodules; however, the size of the nodules, as well as the thyroid imaging reporting and data system (TIRADS) score or the American thyroid association (ATA) risk of the nodules, is not greater in comparison with the control group.

Conclusion: The obtained results of the present work show a thyroid disorder encompassing thyroid function abnormality and nodule formation in thyroid cancer patient's family. The study provides evidence of a genetic predisposition in the family of affected persons. This issue needs more clarification in subsequent studies.

P 005

Comparison of visual and quantitative interpretation of ^{99m}Tc-TRODAT SPECT in differentiation of early Parkinson's disease from non-parkinsonian tremor

Mohammad Reza Hossein-Tehrani, Etrat Hooshmandi, Leila Kalhor, Amin Abolhasani Foroughi, Tahereh Ghaedian, Vahid Reza Ostovan

Clinical Neurology Research Center, Shiraz University of Medical Sciences, Shiraz, Nuclear Medicine and Molecular Imaging Research Center, Namazi Teaching Hospital, Shiraz University of Medical Sciences, Shiraz, Iran

Medical Imaging Research Center, Shiraz University of Medical Sciences, Shiraz, Iran

Epilepsy Research Center, Shiraz University of Medical Sciences, Shiraz, Iran

Objective: The clinical differentiation of Parkinson's disease (PD) from non-Parkinsonian tremor made a challenge in neurology. This study aimed to compare the specificity and sensitivity of visual and quantitative report in dopamine transporter (DAT) scans for differentiating PD from non-Parkinsonian tremor in the early stages of disease. The aim of this study is to compare the sensitivity and specificity of visual analysis of DAT scan with quantitative analysis.

Methods: This study included 34 patients younger than 70 years-old with less than 3 years of extrapyramidal symptoms. Demographic and clinical history of the patients were gathered including age, sex and disease duration. Disease severity was assessed using Unified Parkinson's Disease Rating Scale (UPDRS). For all patients, 99mTc-TRODAT single-photon emission computed tomography (SPECT) was performed. Patients were followed up for one year and examined for final diagnosis.

Results: According to quantitative 99mTc-TRODAT analysis, both right and left specific binding ratio (SBR) were significantly higher in non-Parkinsonian patients. Also, the results indicated a high sensitivity and specificity for both visual and quantitative 99mTc-TRODAT analysis which showed higher sensitivity for visual scan result in comparison with quantitative results (94.1% as compared to 82.4% in left SBR and 70.6% in right SBR, respectively). However, the specificity of quantitative analysis showed comparable results with higher specificity only for right SBR (88.2%, in left SBR and 100% in right SBR, respectively as compared to 88.2% for visual interpretation). Furthermore, the accuracy of visual analysis in diagnosis of PD was 91% which is slightly higher than that of quantitative results (AUC: 0.87 for both SBRs).

Conclusion: Visual and quantitative 99mTc-TRODAT both, have high accuracy in differentiation of early PD from non-Parkinsonian conditions particularly essential tremor (ET). But results showed that visual analysis due to higher sensitivity, can diagnose early PD more accurate than quantitative analysis, but in case of concerning about a specificity of test, quantitative results can help with visual interpretation.

p 006

Effect of Proton pump inhibitor on stomach wall uptake in ^{99m}Tc-methoxy-isobutyl-isonitrile (MIBI) cardiac imaging

Azin Asadzadeh, Elahe Pirayesh

Nuclear Medicine Department, Shohadaye Tajrish Medical Center, Shahid Beheshti University of Medical Sciences, Tehran, Iran

Background: Stomach wall uptake (SWU) in Tc99m -Sestamibi cardiac imaging occasionally leads to some diagnostic artifacts and subsequent reduction of the diagnostic accuracy (1, 2). The possible effects of proton pump inhibitors (PPIs) on the gastric uptake are matter of debate. Accordingly, this study was conducted to determine the effect of proton pump inhibitor on the stomach wall uptake in Tc99m -Sestamibi cardiac imaging.

Methods: In this before-after study, 291 consecutive patients undergoing Tc99m -Sestamibi cardiac imaging were enrolled into 3 groups: control group (n = 84, not on any gastroprotective drug), PPI group (n = 84, on PPI treatment in both phases) and intervention groups (N = 65, patients on PPI treatment in rest phase, discontinued it for at least 3 days before stress phase).

Results: In rest phase, 2.1%, 95.5% and 98.5% of patients in control, PPI and intervention groups had SWU respectively. In the stress phase, gastric uptake was noted in 3%, 96.4%, and 24.6% of patients in these three groups, respectively. (P < 0.0001)

Conclusion: To reduce the incidence of significant SWU of Tc99m -Sestamibi associated with PPI therapy, discontinue PPIs for at least three days can be effective.

p 007

Multiple non-malignant iodine uptake in a ¹³¹I whole body scan of a patient with Papillary Thyroid Carcinoma: importance of SPECT/CT: A case report

Hamideh Abbasain, Farshad Emami, Farnaz Banezhad, Ramin Sadeghi

Nuclear Medicine Research Center, Ghaem Hospital, Mashhad University of Medical Science, Mashhad, Iran

Nuclear Medicine & Molecular Imaging Department, Imam Reza International University, Mashhad, Iran

After thyroidectomy in papillary thyroid carcinoma (PTC) patients, whole body radioiodine scan (WBIS) is necessary for localization of any abnormal radioiodine avid lesions. However false-positive radioiodine uptake in WBIS can be problematic. We reported a 32 years old female patient with PTC. After thyroidectomy and radioiodine therapy WBIS was performed. In her post therapy WBIS, there were zones of radioiodine uptake in the chest, mediastinum, and pelvis regions. In SPECT/CT, we encountered simultaneous uptake of radioiodine in breast, thymus, adnexa and intrauterine device (IUD) site. SPECT/CT images could identify these potential false positive uptakes as benign accumulations of the tracer.

p 008

¹⁸FDG PET/CT in pulmonary carcinosarcoma and brain metastasis (A case report)

Hamideh Abbasain, Ramin Sadeghi, Farshad Emami, Vahid Reza Dabbagh Kakhki

Nuclear Medicine Research Center, Ghaem Hospital, Mashhad University of Medical Science, Mashhad, Iran

Nuclear Medicine & Molecular Imaging Department, Imam Reza International University, Razavi Hospital, Mashhad, Iran

Pulmonary carcinosarcoma is a rare malignant neoplasm. We report a case of pulmonary carcinosarcoma and its ¹⁸F-FDG PET/CT findings. A 61-year-old male patient presented with brain symptoms including headache, nausea, right hemiplegia, and sometimes seizure. Brain lesion seen on the anatomical imaging was resected and pathology was carcinosarcoma. Based on anatomical imaging and evidence of pulmonary lesion, the patient underwent ¹⁸FDG PET/CT and left lung lesion biopsy. We found a large lesion in the left lung which pulmonary carcinosarcoma is confirmed by tissue sampling.

p 009

Evaluating the correlation of serum leptin and adiponectin levels with evidence of coronary artery disease on myocardial perfusion SPECT

Tahereh Ghaedian, Tahereh Firuzyar, Sina Ghanizadeh, Saeedeh Amirzadegan

Nuclear Medicine and Molecular Imaging Research Center, Namazi teaching Hospital, Shiraz University of Medical Sciences, Shiraz, Iran

Background: Cardiovascular disease is currently the most common cause of death worldwide. Several risk factors have been identified for cardiovascular diseases, including hypertension, hyperlipidemia, and diabetes. Adipokines were also recently claimed to have association with coronary artery disease. Leptin is a peptide hormone which act as a pro-inflammatory cytokine and has variety effects in hemostasis and metabolism and adiponectin is an insulin sensitizer and low level of adiponectin is associated with coronary artery disease. Given the controversial role of adiponectin in coronary artery disease, the aim of this study was to determine the relationship between the concentration of adiponectin and leptin with evidence of coronary artery disease in the myocardial perfusion scan.

Method: This cross-sectional study was conducted on all patients suspected of coronary artery disease, referring to the nuclear medicine department during a 6-months period for myocardial perfusion SPECT. All patients were classified according to the visual scan findings (normal or

abnormal scan). Then, leptin and adiponectin level as well as other CAD risk factors were compared between these groups, and also the correlation of the serum adiponectin and leptin level with the quantitative perfusion parameters of MPI SPECT were calculated.

Results: The mean age of the patients was 57.83 ± 10.64 years with a range of 28-87 years. The results of our study showed that both serum adiponectin and leptin levels in patients with normal and abnormal nuclear scans were not significantly different, but the level of adiponectin was significantly lower in diabetic and female patients. None of quantitative scan parameters showed significant correlation with leptin or adiponectin.

Conclusion: Our findings showed that there was no significant correlation between myocardial perfusion parameters and serum adiponectin or leptin levels. However, significantly lower serum level of adiponectin in diabetic patients as a risk factor for CAD, warrants further investigation on the mechanism of this relationship.

P 010**Psychological status and quality of life associated with radioactive iodine treatment in patients with differentiated thyroid cancer: Results of hospital anxiety and depression scale and short form (36) health survey**

Seyed Shahab Banihashem, Mohsen Qutbi

Department of Psychosomatic Medicine, School of medicine, Shahid Beheshti University of Medical Sciences, Tehran, Iran

Department of Nuclear Medicine, School of medicine, Shahid Beheshti University of Medical Sciences, Tehran, Iran

Background: Treatment and follow up of patients with differentiated thyroid cancers (DTCs) are seriously challenging for healthcare practitioners and may exert a massive impact on the psychological status and quality of life (QoL) of patients. To date, evidence regarding impact of radioactive iodine (RAI) treatment on QoL in patients with DTCs using standard questionnaires is scarce.

Objective: The objective is to investigate psychological status and QoL using Hospital Anxiety and Depression Scale (HADS) and Short Form (36) Health Survey (SF-36) questionnaires in patients with proven DTC who are referred for RAI ablation before, during and after treatment.

Methods: Of patients who underwent total thyroidectomy with a pathologically-proven DTC (papillary and follicular types) referred for RAI treatment to our department in 2018, 150 in whom the diagnosis was newly established and were referred for the first course of RAI treatment were consecutively enrolled in the study. The patients received an oral dose of radioiodine (100 or 150 mCi). For evaluation of anxiety, depression and QoL, all patients are given two standard questionnaires, HADS and SF-36, and are requested to answer them at 4 time points. First one was at one month before RAI, second was at the time of RAI treatment. Third and fourth ones were one week and 6 months later respectively.

Results: Mean age of patients was $39.17 (\pm 12.95)$ and 121 (80.7%) were female and 29 (19.3%) male. Values of HADS and SF-36 scores at corresponding time points were significantly correlated using Pearson correlation (HADS and SF-36 scores at 1 month before RAI: $r = -0.56$, $P < 0.001$; at time of RAI: $r = -0.71$, $P < 0.001$; 6 months after RAI: $r = 0.19$, $P = 0.021$). Using paired-sample t test, for HADS, except for difference between time points of 1 month before RAI and time of RAI, pairwise difference between scores of other time points were statistically significant after bonferroni correction. For SF-36, pairwise difference between scores of all three time points are statistically significant. Interaction of age, gender, RAI dose and TSH level at the time of RAI on HADS and SF-36 scores did not show statistical significance.

Conclusion: Lowest values of HADS and SF-36 scores were recorded at 6 months after RAI as compared to those at time of RAI. The latter may be consequences of levothyroxine withdrawal and side effects of RAI. Trend in scores over several-months' time discloses gradual improvement of QoL and merits close observation but limited psychiatric intervention.

p 011

Different dose strategies for radio-iodine therapy of patients with Graves' disease; A clinical trial

Susan Shafiei, Narjess Ayati, Atena Aghaei, Samira Zare Namdar, Hamideh Sadra, Seyed Rasoul Zakavi

Nuclear Medicine Department, Mashhad University of Medical Sciences, Mashhad, Iran

Background: Graves' disease (GD) is the most common cause of hyperthyroidism in iodine-sufficient areas. Although radioiodine therapy (RIT) has been confirmed as a standard method of treatment in patients with Graves' disease (GD) for several decades, the optimal dose of radioiodine has remained controversial.

Objective: In this study, we compared response to different doses of radioiodine and different strategies of calculating radioiodine dose in patients with Graves' disease.

Methods: 366 patients with GD, who were referred for RIT, were consecutively assigned to receive either fixed (FD) or calculated dose (CD) of I-131 after measurement of radioiodine uptake (RAIU) and thyroid volume. Patients in the FD group either received low dose (7mCi) or high dose (15mCi) of I-131 and patients in the CD groups further subdivided to receive 100, 150, 200 or 300 μ Ci/gram of thyroid weight. Follow up of patients was done for 6-78 months. Ultrasonography and laboratory tests were done 1, 3, 6 and 12 months after RIT, followed by yearly evaluation after that.

Results: We studied 366 patients (123men and 243women) with mean age of 39.09 ± 13.25 years. There was no significant difference in age, RAIU and thyroid volume between different groups ($p > 0.39$). Patients in the FD groups received 2.14 times more I-131 than patients in CD groups. We could not find any difference in response to treatment during follow up. Also, no significant difference was observed in the time of response to therapy between the subgroups ($p = 0.69$). Euthyroidism after RIT was more common in patients receiving calculated doses compared to fixed dose models.

Conclusion: RIT with CD strategy is the method of choice in Graves' disease. FD strategies give significantly higher doses of I-131 and is not associated with better long term response or earlier response to treatment.

p 012

Lymphoscintigraphic detection of sentinel lymph nodes using [^{99m}Tc- HMPAO] liposomes in colorectal cancers; an ex vivo study

Hamideh Abbasain, Kayvan Sadri, Abbas Abdollahi, Ramin Sadeghi

Nuclear Medicine Research Center, Ghaem Hospital, Mashhad University of Medical Science, Mashhad, Iran

Background: Nowadays colorectal cancers are one of the most widely diagnosed cancers worldwide that detection of sentinel lymph nodes (SLN) plays an important role in determining the best therapeutic protocol of the disease.

Objective: The aim of this study was to evaluate the efficacy of Sentinel Lymph Node Biopsy (SLNB) in colorectal cancers using [^{99m}Tc- HMPAO] Liposomes during an ex vivo study.

Methods: Immediately after tissue removal of the 40 patients with colorectal malignancies during a surgical procedure, the above mentioned radiopharmaceutical was injected around the tumoral tissue. Using the gamma probe, SLN(s) was detected after half an hour, and then the tissue was sent for pathological evaluation.

Results: Among the 40 cases that were included in the study, including 19 (47.5%) patients of colon cancer and 21 (52.5%) of the rectum, in six cases (15%), SLN was not found; but of the remaining 34 cases, according to pathological reports, 29 cases (85.3%) had no involvement of SLN and 5 cases (14.7%) had pathological involvement. Only in two cases without SLN involvement, other non-sentinel lymph nodes had pathologically involved. Knowing the 100% specificity of the Lymphoscintigraphic studies, our findings indicate a total detection rate of 85% with 80% and 50% sensitivity among colon and rectal cancers, respectively. False negative rate was calculated as 28%.

Conclusion: Lymphoscintigraphic mapping of SLNs in colorectal cancers using [^{99m}Tc- HMPAO] Liposomes, improves the accuracy of the pathologic staging, as well as a notable detection rate of SNLs, especially in colon cancers.

P 013

Effect of injection of mononuclear autologous cells during CABG on improvement of infarcted tissue in patients with ischemic cardiomyopathy

Farnaz Banezhad, Vahid Reaz Dabbagh, Mohammad Abbasi, Ramin Sadeghi, Farvah Vakilian

Nuclear Medicine Research Center, Mashhad University of Medical Sciences, Mashhad, Iran

Background: Ischemic cardiomyopathy means reduced ability of the heart to pump blood correctly due to the lesion following cardiac infarction, in which systolic function of the heart is deteriorated progressively.

Objective: One of the novel treatments that is used today and has drawn lots of attention to itself is using stem cells and evaluation of its effect on cardiac viability and function was the goal of this study.

Methods: This study was performed by randomized sampling on 18 patients with ischemic heart failure. Patients in two groups of case group (CABG with cellular therapy) and control group (only CABG) were evaluated with myocardial perfusion scan and echocardiography.

Results: In qualitative interpretation of viability, there was no significant difference between the two groups in initial and follow-up scans (p -value >0.05). In qualitative interpretation of the motions of the segments, there was no significant difference between the two groups in initial and 6-month scans, as well as during follow-up period (p -value >0.05). Also in quantitative evaluation, about ESV, EDV and EF the only significant difference was in 6-month scan (p -values were 0.017, 0.045 and 0.01 respectively), in which the results were better in the control group. In quantitative evaluation of motion, generally there was only significant difference on 6-month scan (p -value:0.017), in which the result was better in the control group and in segmental evaluation, there was no significant difference between the two groups (p -value >0.05). About thickness, in general and segmental evaluations, there was no significant difference between the two groups (p -value >0.05). About perfusion scores, in general and segmental evaluations, there was no significant difference between the two groups (p -value >0.05). In the evaluations of TPD parameter, summed Raws, summed Severities and summed of Extents of the infarcted segments, there was no significant difference between the two groups in initial and follow-up scans (p -value >0.05). In echocardiographic parameters, about EF, there were only significant differences between the two groups in initial and 3-month echocardiographies (p -values were 0.012 and 0.015 respectively), in which the results were better in the control group. There were no significant differences in ESV, LVEDD and RVEDD between the two groups in 3-month and 6-month echocardiographies (p -value >0.05).

Conclusion: Injection of mononuclear cells in patients with ischemic heart failure has no effect on viability, motion and thickness of myocardium, as well as functional factors like EF, ESV, EDV, RVEDD and LVEDD.

P 014

Prognostic significance of F18-FDG PET in renal cell carcinoma: a systematic review and meta-analysis

Farnaz Banezhad, Zahra Kiamanesh, Ramin Sadeghi

Nuclear Medicine Research Center, Mashhad University of Medical Sciences, Mashhad, Iran

Background: Prognostic significance of fluorine-18 fluorodeoxyglucose positron emission tomography (^{18}F -FDG-PET) in renal cell carcinoma (RCC) has been evaluated in multiple studies.

Objective: The current meta-analysis was carried out to comprehensively investigate the prognostic significance of ^{18}F -FDG-PET parameters in these patients.

Methods: A comprehensive literature search of PubMed/MEDLINE and Scopus was performed to retrieve all articles on the prognostic significance of ^{18}F -FDG-PET in RCC. No language restriction was used. Maximum standardized uptake value (SUVmax), metabolic tumor volume (MTV), total lesion glycolysis (TLG) and positivity of PET scan were used for prediction of progression-free survival (PFS) and overall survival (OS).

Results: Twelve studies were included. SUVmax (HR=1.98), MTL (HR=4.21), and TLG (HR=2.34) were associated with PFS. SUVmax (HR=2.5) and PET positivity (HR=1.15) were both associated with OS.

Conclusion: Our findings showed that ¹⁸F-FDG-PET could serve as prognostic indicator in RCC. Larger studies are needed to further validate our results for several PET parameters.

P 015

Longer time of excellent response to treatment in familial versus sporadic non-medullary differentiated thyroid cancer (DTC), a case-control study

Susan Shafiei, Narjess Ayati, Atena Aghaei, Mehrdokht Sadrolodabaei, Samira Zare Namdar, Zahra Kiamanesh, Seyed Rasoul Zakavi

Nuclear Medicine Department, Mashhad University of Medical Sciences, Mashhad, Iran

Background: Thyroid cancer, with recently fast increasing incidence rate, is the most common worldwide endocrine malignancy (1-3% of all cancers). Although most of thyroid cancers are sporadic, 3-9% of all non-medullary thyroid cancers have been reported to be familial. Some researchers suggest inherited feature for thyroid cancer and claim that familial NMTCs are more aggressive at first presentation and appear with more recurrences in long-term follow up. On the other hand, there are numerous published researches in which similar behavior and prognosis has been confirmed for sporadic and familial differentiated thyroid cancers. Regarding these controversies, the most appropriate approach to familial NMTCs has not been exactly identified and needs more investigation.

Objective: The aim of this retrospective study was to compare Familial and non-familial DTCs in terms of response to therapy and the first time of excellent response.

Methods: We reviewed medical records of 2944 thyroid cancer patients in our department and found 81 patients in 37 families with FDTC. Familial DTC was defined as having at least one another first degree relative with papillary or follicular thyroid carcinoma. Among them 66 patients with FDTC have been treated with surgery and radio-iodine therapy and followed up at least for 1 year. We compared them with 66 age, sex and TNM stage matched non-familial DTC as control group. Response to treatment was assessed 1 and 2 years after RIT, and time of excellent response was identified based on clinical exam, neck ultrasonography and thyroglobulin level.

Results: The incidence of FDTC in our patients was 2.75%, the mean age was 37.9±13.4 years and female to male ratio was 2.79. One family had 4 involved members and 5 families had 3 involved members. Other 29 families contained two DTC patients. There was no significant difference in the first thyroglobulin, radio-iodine dose and additional treatments (surgery or radiotherapy) as well as 1 and 2 years response to treatment between case and controls. Time to achieve excellent response was 26.7 ±24.9 versus 15.9±9.0 months in cases versus control(p=0.01). No significant difference in response to treatment was noted between FDTC with two or more than two involved relatives.

Conclusion: Our study showed that patients with FDTC had longer time to achieve excellent response than controls and may need more aggressive therapy, even when they have only one other involved relative.

P 016

Application of PET/CT in bone tumors

Esmail Gharepapagh

Nuclear Medicine Division, Radiology Department, Tabriz University of Medical Science, Tabriz, Iran

Malignant tumors are associated with increased glycolysis compared to normal tissues, likely related to increased number of GLUT transporters and a higher concentration of hexokinase within malignant cells. As a glucose analog, ¹⁸F-FDG is transported into cells by surface GLUT-1 transporters and then incorporated into the cell where it is phosphorylated and trapped. ¹⁸F-FDG PET/CT has high sensitivity and specificity in discriminating between sarcomas and benign tumors. More than 90% of bone tumors: Osteosarcoma (the most common), Chondrosarcoma, Ewing sarcoma, Chondroma, Malignant fibrous histiocytoma. ¹⁸F-NaF has been available for many years but has recently been rediscovered as the application of PET has grown. This radiotracer has a

similar distribution to the single-photon-emitting ^{99m}Tc -MDP used in general nuclear bone scan imaging but has the advantage of improved image resolution and faster image acquisition time afforded by PET. In the spectrum of primary bone tumors, one of the main indications for PET/CT with $^{18}\text{FNaF}$ is in the assessment of osteosarcoma. Usually, $^{18}\text{FNaF}$ has higher specificity compared to FDG in localizing sclerotic bone lesions, but has inferior performance in the assessment of lytic bone lesions. For this reason, the combined use of NaF and FDG has been studied with initial success. In hybrid PET-CT imaging, CT is used for two different purposes: 1- Attenuation Correction: Providing initial intensities of photon before attenuation by soft tissues with CT-derived attenuation coefficient maps. 2- Anatomical Localization: (after being assured no misregistration takes place). SUV is a semi-quantitative parameter to measure amount of uptake in a region SUV is defined as: $[\text{mCi/ml (decay corrected) in tissue}] / \text{mCi injected/body weight in grams}$. In dual phase PET/CT, malignant lesions continually increase their uptake of radiotracer, while benign conditions usually are characterized by increased uptake on the early-phase, but decreased or monotonic uptake on delayed-phase image. Most of malignant lesions have higher levels of SUV compared to the benign lesions. PET/CT is a hybrid imaging technique increasingly used in the diagnosis, staging, and follow-up of primary bone neoplasms. The use of PET/CT in some malignancies such as lymphoma and multiple myeloma has been steadily established. PET/CT can add valuable information in distinguishing benign from malignant lesions and in the staging of malignant bone tumors. PET/CT can play a role in biopsy planning, treatment planning, and response assessment.

P 017

Production of plaque $^{188}\text{W}/^{188}\text{Re}$ for the treatment of ocular melanoma tumors

Fateme Sadat Hasanzadeh, Mohammadreza Rezaie

Department of Nuclear Engineering, Faculty of Science and Technology, Kerman University of Technology and Advanced Studies, Kaerman, Iran

Background: Cancer cells are present in all parts of the body and produce tumors when they interfere with or spread irregularly. The vascular layer of melanoma is the most common cancer in the eye of the eye, which affects the iris, scrotum, and eyeball. A relatively small number of people around the world suffer from the disease, which has a standardized age classification. There are a number of therapies for controlling cancers in the eye of the eye, the most common being eye drain and radiation therapy (external radiation therapy and brachytherapy). Different plaques are used in radiation therapy. The three major plaques used to treat eye cancer using brachytherapy are the Ru-106, Pd-103, and I-125 plaque.

Objective: The main purpose of this study is to introduce new plaque that have a higher beta or half life than previous plaque.

Methods: Plaque production is carried out in different ways, one of which is the activation of neutrons in power and research reactors. In this study, their production has been studied using mcnp code based on this method.

Results: After investigations carried out on various radioisotopes, the W-188 isotope for use in plaque in terms of energy and half-life and vitality is used to treat eye cancer with an energy of 2.120 MeV and a half-life of 69.4 days.

Conclusion: The W-188 plaque is lower in terms of energy (2.42 MeV) and half-life (17 d) than pd-103, which is better than half-life than pd-103. The W-188 plaque is more energyefficient than 106-RU (1.51mev) and I-125 (0.354MeV). The yield of W-188 plaque production in Tehran and Bushehr Reactor is reported at 1.0345×10^{-8} and 1.04×10^{-3} , respectively.

P 018

Meningioma: A false positive finding of metastasis from prostate adenocarcinoma using a ^{68}Ga -PSMA PET/CT scan

Atena Aghaei, Kamran Aryana, Roham Salek, Rasoul Zakavi, Hojjat Ahmadzadefar

Nuclear Medicine Research Center, Mashhad University of Medical Sciences, Mashhad, Iran

A 73-year-old man with history of prostatic adenocarcinoma radical prostatectomy underwent ^{99m}Tc -MDP whole-body bone scan and subsequent ^{68}Ga -labeled prostate-specific membrane antigen

(PSMA) ligand PET/CT for restaging due to a gradual rise of prostate-specific antigen levels. Whole-body bone scan showed two focal zones of slightly increased uptake in the right fronto-parietal and temporal bones. ⁶⁸Ga-PSMA PET/CT scan showed local recurrence in the prostatic bed and two foci of slightly increased uptake in the right temporal and fronto-parietal lobes. A brain CT scan, with IV contrast confirmed that foci of increased uptake in the temporal and parietal lobes were consistent with typical meningiomas.

p 019

Assessment of myocardial viability

Vahid Reza Dabbagh Kakhki

Nuclear Medicine Research Center, Mashhad University of Medical Sciences, Mashhad, Iran

In many patients with CAD and heart failure, viable but dysfunctional myocardium has the ability to contract if perfusion improves. Determination of myocardial viability may be necessary in post-infarction patients receiving thrombolytic therapy, choosing the best therapy such as angioplasty and myocardial revascularization. In viability studies, while nuclear medicine techniques have high sensitivity, the techniques used to evaluate contractile reserve have higher specificity. Dobutamine stress echocardiography assesses regional left ventricular contractile reserve. Gated myocardial perfusion SPECT and PET examine myocardial perfusion, integrity of cellular membrane, sarcolemma, mitochondria, intracellular fatty acid, and glucose metabolism. In cardiac magnetic resonance (CMR), delayed gadolinium contrast enhancement identifies scarred myocardium. FDG-PET imaging + myocardial perfusion imaging and CMR are the current choice imaging modalities. Selection of any procedure depends on availability, local expertise and clinical conditions. Coronary revascularization was used for a patient with most likely to benefit from the procedure, indeed in a patient with substantial viable myocardium. In this situation, a test with high positive predictive accuracy is required. A test with high negative predictive accuracy (FDG PET, CMR) tells the clinician who will not benefit from revascularization but does not necessarily identify who will.

p 020

Effect of different I-131 dose strategies on ophthalmopathy in patients with Graves' disease

Shahrara Ariamanesh, Narjess Ayati, Zahra Mazloun khorasani, Zahra Kiamanesh, Seyed Rasoul Zakavi

Nuclear Medicine Research Center, Mashhad University of Medical Sciences, Mashhad, Iran
Metabolic Syndrome Research Center, Mashhad University of Medical Sciences, Mashhad, Iran
Ophthalmology Department, Mashhad University of Medical Sciences, Mashhad, Iran

Objectives: To define the effect of different dose strategies on ophthalmic complications in patients with Graves' disease (GD).

Methods: All patients with GD and no or mild ophthalmopathy (CAS<3) who referred for radio-iodine therapy (RIT) underwent Snellen chart examination, measurement of proptosis, thyroid volume determination and radioactive iodine uptake (RAIU) measurement and randomized into one of three groups. In group 1 (G1), all patients received fixed low dose of 259MBq of I-131 while in group 2 (G2), fixed high dose of 555MBq and in group 3 (G3), calculated dose were administered to deliver 5.55 MBq/gr of I-131. The examinations was repeated 6 months after treatment.

Results: We studied 58 female and 34 male patients with mean age of 38.2±12.0 years. Overall, 29, 32 and 31 patients were studied in Group 1, 2 and 3 respectively. Patients in G3 received a mean activity of 240.5MBq. The three groups were not significantly different regarding age, sex ratio, RAIU, smoking, visual acuity and proptosis. Response rate 12 months after RIT was 66.7%, 94.4% and 92.9% in group 1, 2 and 3 respectively (P=0.05). CAS were increased significantly after treatment. Delta proptosis and delta CAS was increased significantly, in G2 compared to other groups (P<0.05), while G1 and G3 had no significant difference in either variables.

Conclusion: Calculated dose strategy has fewer ophthalmic complications and is more effective than fixed dose models and may be considered as the preferred method of radio-iodine therapy.

Evaluating of vesicoureteral reflux incidence and grading by direct radionuclide cystography method in referred patients to N.M center of Imam Reza Hospital

P 021

Esmaeil Gharepapagh, Ashraf fakhari, Shahram Dabiri, F. Aryanpour

Division of Nuclear Medicine, Department of Radiology, Tabriz University of Medical Sciences, Tabriz, Iran

Background: urinary tract infections (UTI) are one of the most common infections in children. Vesico ureteral reflux(VUR) is a major risk factor for recurrent UTIs which can result in renal scarring.

Objective: The diagnostic tests that are being used to detect VUR include voiding cystoureterography(VCUG) and direct radionuclide cystography(DRNC). The sensitivity of each modality is controversial. The aim of this study was to evaluating of VUR incidence a grading by DRNC method in referred patients to N.M center of Imam Reza Hospital.

Methods: Patients referred to by their respective physicians underwent DRNC scan with ^{99m}Tc radiotracer. At the filling, post filling and voiding phases of the bladder, ureter and kidneys, dynamic imaging was performed and interpreted by a specialist physician regarding normal and abnormal study and also its grading in positive cases (presence of VUR).

Results: the prevalence of VUR was 29% among 300 patients. Most cases of VUR were one-sided (63.6%) and significantly (42%) were higher in left side (p=0.022). the most common type of engagement gradient in one-way cases was related to Grade B, and in bilateral cases related to Grade C. The highest number of VUR in the age group of under 1 year was observed with frequency of 30 (10%) and then 1 to 4 years and 5 to 8 years each with frequency of 26(8.67%), observed in the VUR outbreak (p=0.198).

Conclusion: It can be deduced that having repeated tests of DRNC or VCUG can detect missed VUR in patients with recurrent UTIs. Furthermore, DRNC study is most valuable than VCUG.

P 022

The Clinical utility of FDG-PET/CT in the evaluation of breast cancer patients

Nasim Norouzbeigi

Nuclear Medicine Department, Razavi Hospital, Imam Reza International University, Mashhad, Iran

Breast cancer is the most frequent tumor and the second leading cause of cancer mortality in women. The majority of women who develop breast cancer are postmenopausal; although breast cancer is not uncommon in premenopausal women and tends to be more aggressive, so it is an important cause of mortality in younger patients. Prevention and screening have become important health issues in the common belief that detection of breast cancer at an early stage may have an impact on survival or at least allows a less aggressive treatment. Most primary cancers are detected by physical examination or mammography during screening and it is the primary imaging modality for breast cancer screening, detection and diagnosis. Breast cancer stage at presentation which is accepted by (AJCC) system uses a TNM approach is an important factor in prognosis and treatment. Staging is typically divided into regional lymph nodes, especially axillary nodes, and distant or extra regional lymph nodes. Although breast cancer is one of the more responsive solid tumors, around 30% of breast cancer patients are likely to develop recurrence at some time within the course of their disease. FDG-PET/CT can provide both morphological and metabolic information by combining anatomical imaging from CT with functional imaging from PET. According to low sensitivity for small, well-differentiated and in situ cancers, it is not a proper method in order to considering for initial diagnosis of breast cancer, however, regarding to high sensitivity and accuracy of FDG-PET/CT for patient management, it is currently approved for women with stage III breast cancer, restaging of regional and distant metastatic disease where standard imaging results are equivocal or patients have high clinical suspicion of distant metastases and evaluation of tumor response to therapy. In this presentation, normal physiologic tracer uptake, staging, restaging, monitoring response to treatment and false positive lesions are discussed.

Accuracy of ¹⁸F-PSMA-11 PET/CT vs. ⁶⁸Ga-PSMA-11 in low and high grade of prostate cancer

P 023

Habibollah Dadgar, Zahra Pakdin Parizi, Samira Soltani, Rahim Jalinouszadeh, Arash Mohajerin, Majid Assadi

Cancer Research Center, Razavi Hospital, Imam Reza International University, Mashhad, Iran

Objective: PSMA PET has been presented as the most sensitive and specific modality for prostate cancer imaging in low and high-risk prostate cancer patients. Currently, ⁶⁸Ga labeled PSMA ligands, notably [⁶⁸Ga] Glu-urea-Lys (Ahx)-HBED-CC ([⁶⁸Ga]-PSMA-11) is commonly used in many centers. However, ⁶⁸Ga has several shortcomings including a short half-life and non-ideal energies. For overcome to this issue, ¹⁸F-labeled analogues was suggested for PET imaging of prostate cancer.

Methods: Here, we describe a simple synthesis and validation of a fluorine-18 labeled Glu-urea-Lys(Ahx)-HBED-CC ([¹⁸F]PSMA-11) for nuclear medicine applications. [¹⁸F]PSMA-11 was produced and validated (according to Pharm Eur) for routinely clinical applications. [¹⁸F]PSMA-11 was reproducibly obtained in radiochemical yields of 90±6% and >98% radiochemical purity using an improved one-step radiofluorination in aqueous solution.

Result: In addition, [¹⁸F]PSMA-11 exhibited higher uptake and retention in PMSA-expressing LNCap prostate cells as compared to its clinically established ⁶⁸Ga labeled analogues [⁶⁸Ga]PSMA-11. The simple and fast preparation of [¹⁸F]PSMA-11 combined with its favorable pharmacological properties warrant its translation to a clinical setting.

Conclusion: The facile and high-yielding radiosynthesis of [¹⁸F]PSMA-11 as well as its promising in vitro and in-vivo characteristics makes it worthy of clinical development for PET imaging of prostate cancer.

P 024

Height adjustment for pediatric bone densitometry: Comparison of three methods

Golnaz Gholami, Ramin sadeghi

Nuclear Medicine Research Center, Mashhad University of Medical Sciences, Mashhad, Iran

Background: In children, bone mineral content (BMC) and bone mineral density (BMD) measurements by dual-energy x-ray absorptiometry (DXA) are affected by height and age status. Choosing the best way to adjust BMC or BMD (BMC/BMD) measurements for short or tall statures is one of the most controversial issues.

Objective: The aim of this study was to compare three height adjustment methods for pediatric group of patients using an Iranian reference database.

Methods: 41 children aged 9–18 years were selected. We measured spine (L1-L4), whole body less head (WBLH) and femoral neck BMC Z-scores for age according to an Iranian database for age. Height adjustment was done using three different methods including height age, bone mineral apparent density (BMAD), and height-for-age BMC Z-score (HAZ). HAZ method is considered as the gold standard of height adjustment and the two other methods was compared with.

Results: BMD of 22 patients was considered abnormal according to our database. HAZ method changed the report of BMD in 10 patients (45%). Age height method changes the report of BMD in 8 patients (36%). BMAD method changed the report of BMD in 14 patients (63%). Height age adjustment was not possible in 18 patients. In 2 patients both HAZ and height age changed the report of BMD despite unchanged BMAD results. In 5 patients only BMAD and in 1 patient only height age changed the result of BMD.

Conclusion: Considering the HAZ method as the gold standard of height adjustment, BMAD and height age methods showed discrepancy in 59 % and 22 % of patients. Height age if possible can be used interchangeably with HAZ method. On the other hand, BMAD seems to either under correct or overcorrect for height in considerable number of patients and is not a reliable method for height adjustment.

Impact of ¹⁸F-FDG PET/CT comparing to MRI in primary staging and treatment approach of anal cancer

P 025

Mohsen Beheshti, Reyhaneh Manafi-Farid, A. Beheshti, H. Wundsam, F.M. Mottaghy, H. Geinitz, W. Langsteger

Nuclear Medicine, University Hospital, RWTH University, Aachen, Germany
Nuclear Medicine, Paracelsus Medical University, Salzburg, Austria
Research Center for Nuclear Medicine, Tehran University of Medical Sciences, Tehran, Iran

Background: Anal Carcinoma is rare cancer with increasing incidence and mortality rate in recent years. Accurate staging is imperative to preserve anal sphincter and enhance the quality-of-life.

Objective: We evaluated the additive value of ¹⁸F-FDG-PET/CT in initial staging and management of Anal Carcinoma. Also, we assessed the prognostic significance of pre-treatment intensity of ¹⁸F-FDG uptake.

Methods: Fifty-four patients with anal carcinoma underwent both ¹⁸F-FDG-PET/CT and pelvic MRI for primary staging and treatment planning were included. The interval between 2 imaging modalities had to be no longer than 4 weeks. Data regarding primary tumor, lymph-nodes (anorectal, iliac, and inguinal regions), and metastatic lesions were compared. The additional relevant information provided by ¹⁸F-FDG-PET/CT impacting the management was assessed. Also, patients were followed (mean of 41.5±29.3 months) to determine true/false findings, as well as find a correlation between SUVmax of the lesions and disease-free-survival.

Results: Discordant findings were found in 46.30% (25/54) of patients (5 in T; 1 in T and N; 18 in N; and 1 in M stage). T-stage appeared higher in 3.70% of patients and lower in 7.40% on ¹⁸F-FDG-PET/CT. Discordant findings regarding the region of involved lymph-nodes were observed in 35.18% of patients in a total number of 30 regions. There were 20 more involved regions on ¹⁸F-FDG-PET/CT and 7 more on MRI; three regions were positive on MRI and negative on ¹⁸F-FDG-PET/CT. N-stage was incongruent in 22.22% (higher in 14.82% on ¹⁸F-FDG-PET/CT and in 7.40% higher on MRI). ¹⁸F-FDG-PET/CT resulted in true up-staging in 9.26% and down-staging in 3.70% of patients. ¹⁸F-FDG-PET/CT was negative in 12.96% of patients with perirectal lymph-node involvement leading to erroneous down-staging in only 3.7%. Moreover, ¹⁸F-FDG-PET/CT resulted in management change in 24.08% of patients (18.52% received more radiation, 3.70% received less, and one patient (1.86%) underwent palliative therapy). Finally, an adverse relation was observed between metabolic lymph-node involvement and complete response to treatment (p=0.006). No significant correlation was demonstrated between disease-free-survival and metabolic activity of the primary tumor (p=0.127) or lymph-nodes (p=0.478) by means of SUVmax.

Conclusion: ¹⁸F-FDG-PET/CT provided more accurate staging in about 13% of patients and led to change in treatment management in 24% of cases. However, MRI was superior in the detection of anorectal lymph-nodes. No significant prognostic advantage was demonstrated using semi-quantitative parameters of ¹⁸F-FDG-PET/CT. Nevertheless, ¹⁸F-FDG-PET/CT seems to play a pivotal role in the treatment planning of Anal Carcinoma.

P 026

The Effect of simultaneous Wi-Fi and gamma rays irradiations on DNA double stranded breaks in rat peripheral blood lymphocyte: a radio protective note

Shima Afrashi, Karim Khoshgard, Ehsan Khodamoradi.

Student Research Committee, School of Medicine, Kermanshah University of Medical Sciences, Kermanshah, Iran

Background: The nuclear medicine centers, patients are isolated in room after injection of radiopharmaceutical and the number of nuclear medicine examinations is increasingly growing, and the principles of radiation protection are important in order to reduce the risk of radiation mobile phones connected to the internet through Wi-Fi have been increasingly used recently. On the other hand, with the increasing use of Wi-Fi waves, the study of the complication associated with this phenomenon is one of the most hazardous topics in radiation protection science e.g, to decreases human sperm motility etc. The hypothesis of this study predicts that the risk and biological damage

of the Wi-Fi waves on patients in the nuclear medicine sector can be more harmful than the risk of these waves for the community.

Objective: Investigating the effect of Simultaneous Wi-Fi and gamma-rays irradiations on DNA double stranded breaks in rat peripheral blood lymphocyte

Methods: Fifty male wistar rats (weighing 290 ± 20 grams) were divided to the control group and groups that for 2.24 and 72 hours in 3 categories were exposed only by Wi-Fi, only by Tc-99m and simultaneously by Wi-Fi and Tc-99m. The power density levels of Wi-Fi emitter 15cm was $4.2nW/cm^2$. The Tc-99m of per rate was injection $100\mu Ci$ intra peritoneally. Blood samples were taken by cardiac puncture following general anesthesia. Mononuclear cells are extraction using Ficoll Solution by density gradient centrifugation. The number of γ -H2AXfoci per nucleus were counted by flow cytometry. The statistical differences between experimental groups at 2, 24 and 72 h were determined with a repeated measure's analysis of variance. The significant difference between groups at the same time was analyzed with the Kruskal-Wallis Test.

Results: The number of γ -H2AX foci do not change for injected groups only Tc-99m and exposed groups simultaneous by Wi-Fi and Tc-99m in time. The number of γ -H2AX foci between two groups the simultaneously by Wi-Fi and Tc-99m and only Tc-99m groups was a significant difference after 72 hours.

Conclusion: Exposure of Wi-Fi and γ -Ray can interrupt the number of double strand break DNA relative to exposure of γ -Ray in peripheral blood lymphocytes of rat. As a result, patients should be away Wi-Fi waves for up to 72 hours after technetium injection in the nuclear medicine center.

p 027

Samarium-153 treatment of bone pain in patients with metastatic prostate and breast cancer

Mojtaba Rokni, Mehrangiz Amiri, Ali shabestani Monfared , Fatemeh Niksirat , Mohsen Vakili, Meysam Khosravi Farsani, Kouros Ebrahimnejad Gorji.

Department of Medical Physics Radiobiology and Radiation Protection, School of Medicine, Babol University of Medical Sciences, Babol, Iran

Background: Bone metastatic pain can be the result of different cancers and its symptoms have many influences on the quality of life in patients. Radiopharmaceuticals as a Systemic therapy are used instead of radiotherapy and sedative drugs, and have many advantages like reducing pain, minimizing side effects, higher survival rate and better quality of life.

Objective: The aim of this study is evaluating the effect of ^{153}Sm on bone pain palliation in bone metastatic patients.

Methods: This study conducted on 30 patients with generalized bone cancer, who did not show any positive response to conventional treatments, but the sufficient bone marrow function was observed in their full body scan. $1 mci/kg$ ^{153}Sm was prescribed to all patients using two Intravenous injections: before radiotherapy and one month after samarium injection. The level of pain palliation and quality of life were evaluated using a questionnaire based on "the Quality of Life Questionnaire for Cancer Patients", karnofsky index and visual analogue pain scale. The other information about patients' condition such as bone density, their BMD, and the number of metastatic foci involved in pre- and post-treatment were also examined.

Results: According to various diagnostic studies on the physical properties of ^{153}Sm , it is expected that this drug can completely relieve the pain in at least more than 50% of the samples within 2 to 7 days after receiving ^{153}Sm and this process can be continued several months after injection for more results.

Conclusion: It is anticipated that ^{153}Sm injection can decrease the pain level, increase the quality of life, decrease the mortality and create higher life expectancy in bone metastatic patients.

p 028

Role of nuclear FDG-PET in staging, treatment response and radiation planning in SCLC

Abbas Yousefi Koma

Masih Daneshvari Hospital, Shahid Behshti University, Tehran, Iran

Accurate staging is pivotal in the management of patients with small cell lung cancer (SCLC). The primary role for imaging is to accurately distinguish patients with limited disease (LD) from patients with extensive disease (ED). Treatment strategies in patients with LD are potentially curative, while local toxic treatment should be avoided in patients with distant metastases (i.e., ED). SCLC is a metabolic malignancy, leading to a sensitivity of 100% for PET detection of primary tumors. FDG-PET/CT is superior to conventional staging in the detection of all involved sites particularly in the assessment of mediastinal lymph nodes and bone metastases. PET influences stage in 29% of patients. Furthermore, there is preliminary evidence that PET/CT may be very useful for the planning of radiation treatment to cover all tumor tissue and lower normal tissue radiation dose including lung, heart and oesophagus. PET is useful as a prognostic biomarker, patient with high mean SUVmax are at higher risk of death both in LD and ED. The assessment of treatment response is another indication for FDG-PET. We performed FDG-PET mainly for staging and treatment response in Masih Hospital as a tertiary centre for lung disease in Tehran. Our valuable results by PET in more than 54 patients holds great promise to improve SCLC management.

p 029

Initial experience with ¹⁸F-NaF PET/CT in detection of bone metastasis

Nasim Norouzebeigi, H. Dadgar

Nuclear medicine Department, Razavi Hospital, Imam Reza International University, Mashhad, Iran

The aim of the study is to comparing the diagnostic value of ¹⁸F-NaF-PET/CT, ¹⁸F FDG PET/CT and PSMA-PET/CT for the detection of bone metastases in patient who is suspected for osseous metastasis and indeterminate result in other imaging modalities. This is the first experience of performing NaF-PET/CT in Iran in patients with breast and prostate cancer for evaluation of bone metastasis. NaF produced in cyclotron and higher accuracy for detecting both osteoblastic and osteolytic metastasis with the advantages of cross sectional anatomy for anatomic localization and there for higher sensitivity and specificity rather Tc-99m-MDP. Here by we presented 5 patients with history of breast and prostate cancer with rising tumor marker and negative F-FDG PET/CT and Ga-68- PSMA-PET/CT and there for audience will be aware of the most appropriate impression of F18- NaF-PET/CT in patients who is suspicious for bone metastasis.

p 030

The rule of nuclear medicine in tumor induced osteomalacia by phosphaturic mesenchymal tumor

B. Rashidi, I. Heydari

Department of Nuclear Medicine, Firouzgar Hospital, Iran University of Medical Sciences, Tehran, Iran

Tumor induced osteomalacia (TIO) or oncogenic osteomalacia is a rare condition associated with small tumor that secretes one of the phosphaturic hormones, i.e., fibroblast growth factor 23 (FGF23), resulting in abnormal phosphate metabolism. Patients may present with non-specific symptoms leading to delay in the diagnosis. Extensive skeletal involvement is frequently seen due to delay in the diagnosis and treatment. The small sized tumor and unexpected location make the identification of tumor difficult even after diagnosis of osteogenic osteomalacia. The bone scan done for the skeletal involvement may show the presence of metabolic features and the scan findings are a sensitive indicator of metabolic bone disorders. The diagnosis is established by the finding of acquired chronic hypophosphatemia due to isolated renal phosphate wasting with concomitant elevated or inappropriately normal blood levels of FGF23 and decreased or inappropriately normal 1,25-OH₂-Vitamin D. Locating the tumor is critical, as complete removal is curative. For this purpose, a step-wise approach is recommended, starting with a thorough medical history and physical examination, followed by functional imaging. Suspicious lesions should be confirmed by anatomical imaging, and if needed, selective venous sampling with measurement of FGF23. If the tumor is not localized, or surgical resection is not possible, medical therapy with phosphate and

active vitamin D is usually successful in healing the osteomalacia and reducing symptoms. If we can localize the tumor in the body that was approachable for surgery in this situation the nuclear medicine has great rule due to complete resection of tumor complete cure was seen. However, nuclear medicine can help for localization of very small tumors that causes hypophosphatemia & if surgical resection is possible a complete cure was seen. The first line in nuclear medicine is FDG/PET scan but due to the low availability of PET /CT & high cost, in our experience & other articles, the Octreotide scan (Pars HYNIC-TOC) is a valuable method for the localization of this small lesions.

p 031

The assessment of Stunning phenomenon in graves' hyperthyroidism patients following radioactive iodine uptake

Zahra Fazeli, Seyed Hossein Fatemizde, Ahmad yousefi, Hesam Alizadeh, Mohammadhadi Modarres

Department of Medical Genetics, Faculty of Medicine, Shahid Beheshti University of Medical Sciences, Tehran, Iran

Background: Low doses of radiation affect the response of cells to higher doses; this phenomenon is called radio-adaptive response, which leads to increased resistance to subsequent higher doses.

Methods: We have investigated the adaptive response using 0.37 MBq priming dose of I-131 followed by 296–444 MBq challenging dose in peripheral human lymphocyte cells. The study was performed on 42 patients with Graves' disease and 29 healthy adult persons as a control group. The patients were divided into two groups. In the first group, patients were referred for radioactive iodine therapy with a specific dose, and iodine was given to them on the day of referral. In the second group, patients were referred for radioactive iodine uptake and radioactive iodine therapy, and iodine uptake was initially performed, then 24 h later, iodine therapy was done. In both groups, Thyroid scan was performed after 48 hrs using gamma camera with high-energy collimators and ROI was drawn on thyroid to access the total count of thyroid.

Results: total count was 304529.751 ± 205198.1 and 246309.76 ± 133991.723 in the calculated dose and fixed-dose therapy groups, respectively Mean 24 hrs thyroid iodine uptake in calculated dose and fixed-dose groups were 45.5 ± 13.9 and 48.9 ± 16.9 , respectively. Evaluation of thyroid uptake was indicative of no significant difference between the groups ($t=0.72$, $P=0.47$).

Conclusion: According to the results, there was no significant difference between the total count and uptake percentage of study groups. However with 10 mci I131 as a small dose stunning will not occurred.

p 032

One-year prognosis of patients with normal myocardial perfusion imaging using technetium-^{99m}Tc-sestamibi in suspected coronary artery disease: a single-center experience of 1,047 patients

Ghasem Raziei, Alireza Tavakoli, Shahram Seifollahi Asl, Mahasti Amouei, Hamid Javadi, Majid Assadi

Department of Nuclear Medicine, Milad Hospital, Tehran, Iran

Background: The aim of the present study was to evaluate the clinical outcome of a normal technetium-99m (^{99m}Tc)-Sestamibi single photon emission computed tomography (SPECT) myocardial perfusion imaging (MPI) with different probabilities of coronary artery disease (CAD).

Methods: A total of 1,047 subjects with a normal ^{99m}Tc-MIBI SPECT were followed up for one year and hard and soft cardiac events were assessed. Hard cardiac events were defined as cardiac death or non-fatal myocardial infarction (MI). Soft cardiac events included the patient's development of recurrent chest pain requiring coronary revascularization or significant stenosis in coronary arteries on angiography.

Results: Overall, 1,047 patients (248 men and 799 women; mean age: 60.07 ± 12.31 , range 29-92) were enrolled. Three hard cardiac events occurred in the groups; two had cardiac arrest and one non-

fatal MI. As a result, the annualized hard cardiac event rate was 0.28%, the annualized cardiac mortality rate was 0.19%, and the rate of overall annualized cardiac events was 1.25%. Furthermore, there was a significant difference in cardiac events among patients with various pretest likelihoods of CAD (p value=0.04).

Conclusion: Our data confirmed that patients with a normal ^{99m}Tc-Sestamibi myocardial SPECT are associated with a very low incidence of cardiovascular events.

P 033

Bilateral breast metastasis from choroid melanoma: Application of photon emission tomography

Nasim Norouzbeigi

Nuclear Medicine Department, Razavi Hospital, Imam Reza International University, Mashhad, Iran

Ocular melanoma is a common type of primary eye tumor that is more frequently found between the age of 55 and 65 years. It is recognized during ophthalmic examination and needs a metastatic workup. When hematogenous spreading occurs, the liver is the most common site of metastasis. We describe an ocular melanoma with an unusual metastatic pattern. Melanoma can be either cutaneous, the most frequently occurring, or noncutaneous, which remains rare. Ocular melanoma is the most common kind of extracutaneous melanoma. Noncutaneous melanoma has the worse outcome and prognosis when compared to cutaneous melanoma. The most common primary eye tumor is ocular melanoma, and retinoblastoma is the second most common. The choroid layer of the uvea is the most frequent site of ocular melanoma, which occurs more frequently between the age of 55 and 65 years. Choroid melanoma is usually an accidental finding during a routine periodic ophthalmic examination. It appears as a pigmented, irregular, solid, sub retinal mass that commonly extends into the retina and vitreous, causing retinal detachment. Histopathological pattern, as offered by Callender's classification, indicates that those containing spindle cell melanomas carry the best prognosis and mixed-cell tumors were worse, with epithelioid cell tumors being the most likely to metastasize. They are characterized by vascular invasion and hematogenous spreading mainly to the liver and extrahepatic areas, including bone, lung, lymph node and skin. Involvement of extrahepatic sites occurs in association with liver metastasis. We report a case of a 33-year-old woman with primary choroid melanoma of the right eye. Abdominal imaging for preoperative staging and surveillance was found to be negative for metastasis. Histopathological pattern was mixed spindle and epithelioid cell type of 1.3*2 centimeters. Nine months after enucleation surgery, she was evaluated for right breast nodules. Biopsy indicated metastatic melanoma. Before performing a right mastectomy, whole body PET/CT was performed, and the imaging was observed in favor of metastatic involvement in the right breast. Eight months after right mastectomy, she was again evaluated for left breast nodules. Both biopsy and whole body PET/CT demonstrated metastasis disease in the left breast. Choroid melanoma is not as aggressive as cutaneous melanoma. The metastatic pattern of choroid melanoma also appears different as compared to cutaneous melanoma. The incidence rate of metastatic disease is highly related to histopathological pattern. So far, only two case reports are available in Medline for bilateral breast cancer from choroid melanoma. Demirci et al described a choroid melanoma in a 44-year-old woman and breast metastasis occurred 37 and 54 months after treatment. Another case report is of a 33-year-old woman without history of choroid melanoma but diagnosed with breast metastasis from an undetected choroid melanoma. Although it is not as aggressive as skin melanoma, Kujala et al reported mortality rates of 31 % by five years, 45 % by 10 years, 49 % by 25 years, and 52 % by 35 years. We concluded a better outcome for patients with choroid melanoma, particularly with a mixed histopathological pattern. In cases where the diameter of the tumor is more than 1 cm, a pre-operating PET/CT should be performed to find any occult metastasis, in addition to after surgery follow up.

P 034

Spurious lung perfusion ventilation defect on planar V/Q scan detected by SPECT imaging

Fatemeh Farahmandfar, Sara Shakeri, Toktam Masoudi, Soroush Zarehparvar Moghadam, Ramin Sadeghi

Nuclear Medicine Research Center, Mashhad University of Medical Sciences, Mashhad, Iran

We report a 32 y/o woman with history of rheumatologic disease and acute dyspnea, who was referred for V/Q scintigraphy. The V/Q planar images revealed multiple mismatched defects throughout both lungs. SPECT images showed that only one of the defects was real, the others were caused by patient's elevated right arm. Our case showed a pitfall with emphasis on importance of SPECT imaging in V/Q scintigraphy.

p 035

Primary skeletal muscle lymphoma with unusual soft tissue metastases in the stomach and pancreas detected by ¹⁸F-FDG PET/CT

Fatemeh Farahmandfar, Sara Shakeri, Sadegh Moradian, Shirin Shahlaei, Ramin Sadeghi

Nuclear Medicine Research Center, Mashhad University of Medical Sciences, Mashhad, Iran

A 69 y/o woman with history of primary diffuse large B cell lymphoma in the right thigh muscle was referred for recurrence evaluation with ¹⁸F-FDG PET/CT. After routine courses of chemoradiation, MRI was done in order to evaluate treatment response with inconclusive findings. ¹⁸F-FDG PET/CT revealed abnormal uptake in the primary site of the disease as well as secondary involvement of stomach, pancreas, pelvic lymph nodes and both tibiae. Our case showed the importance of ¹⁸F-FDG PET/CT in detection of unusual soft tissue extension of lymphoma.

p 036

Preliminary results of treating metastatic castration-resistant prostate cancer (mCRPC) patients using Lu-177-PSMA

Babak Fallahi, Emran Askari, Armaghan Fard-Esfahani, Mohammad Eftekhari, Alireza Emami-Ardekani, Najme Karamzade-Ziarati, Davood Beiki

Research Center for Nuclear Medicine, Tehran University of Medical Sciences, Tehran, Iran

Background: Prostate cancer is the second cancer of men over the world, and the third cancer in the Iranian men. Metastatic castration-resistant prostate cancer (mCRPC) is a late-stage form of the disease. Currently, patients with mCRPC merely receive palliative treatments. Targeted therapy with the radiolabeled peptide, Lu-177-PSMA, is a relatively new therapeutic method that could be used in mCRPC patients.

Objective: Here we provide preliminary experience in patients treated using Lu-177-PSMA.

Methods: Twelve patients with mCRPC were treated using standard protocol for Lu-177-PSMA therapy. The inclusion criteria was defined as rising prostate-specific antigen (PSA) during standard chemo/ anti-androgen therapy, concomitant with Ga-68-PSMA-avid metastatic lesions delineated on PET/CT imaging. Intravenous treatment with Lu-177-PSMA was given with an activity of 150-200 mCi per cycle in patients meeting the criteria. The degree of PSA decline, clinical response, and functional/anatomical response were evaluated.

Results: Median age of participants was 70.6 years (range 56-87). 1 and 2 cycles of Lu-177-PSMA therapy were applied in the patients till now. PSA decline of $\geq 50\%$ and $\geq 90\%$ was achieved in 50%, 15% of patients, respectively. In this evaluation liver metastases and neuroendocrine feature were associated with a worse prognosis despite PSA decline $>50\%$; while 5 out of 12 patients reveal partial response to treatment based upon biochemical and clinical criteria.

Conclusion: Radioligand therapy with Lu-177-PSMA might be considered in late-stage mCRPC with multiple skeletal and lymph node metastases, but may not be useful for hepatic metastasis.

p 037

Months of experience in ⁶⁸Ga-DOTATATE PET/CT imaging in SSTR positive malignancies

Armaghan Fard-Esfahani, Najme Karamzade-Ziarati, Babak Fallahi, Mohammad Eftekhari, Alireza Emami-Ardekani, Emran Askari, Davood Beiki

Research Center for Nuclear Medicine, Shariati Hospital, Tehran University of Medical Sciences, Tehran, Iran

Background: Ga-68 DOTATATE has a high affinity for somatostatin (SST) receptors, especially SSTR2. This receptor has been expressed predominantly in gastroenteropancreatic neuroendocrine tumors (NETs), sympathoadrenal system tumors (pheochromocytoma, paraganglioma, neuroblastoma, ganglioneuroma), medullary thyroid carcinoma (MTC), pituitary adenoma, medulloblastoma, Merkel cell carcinoma, small-cell lung cancer (mainly primary tumors), and meningioma. This relatively new modality is considered for localizing the primary site of tumor or metastases, patient follow up, evaluation of response to treatment, selecting candidates for SST receptor radio-ligand therapy.

Objective: We aim to offer 14 months of experience in performing Ga-68 DOTATATE PET/CT imaging to our colleagues.

Methods: We evaluate ninety four Ga-68 DOTATATE PET/CT scans were performed during 14 months. Among these, eight scans were excluded due to incomplete patient records. Patients had been underwent standard Ga-68 DOTATATE PET/CT imaging protocol including appropriate withdrawal duration for somatostatin analogs as patient preparation, 100 to 200 MBq Ga-68 DOTATATE IV injection and about 60 min injection-to- imaging duration. The acquisition was done using a 3-D mode PET/CT scanner with 4 min/bed position duration.

Results: Eighty six scans (48 female, 38 male) with patient mean age of 37.77 years were evaluated. Patients who underwent Ga-68 DOTATATE PET/CT included 7 cases of lung carcinoid, 13 pancreatic NET, 7 ectopic Cushing, 6 intestinal NET, 11 pheochromocytoma/paraganglioma, 16 neuroblastoma, 14 MTC, and 5 unknown origin NET. The 7 remaining cases include adrenocortical carcinoma, mediastinal NET, breast NET, primitive neuroectodermal tumor, and tuberosus sclerosis. In these patients the most common sites of metastasis were bone in lung carcinoid group, liver in pancreatic and intestinal NET, retroperitoneum in pheo/paraganglioma group, retroperitoneum and abdominal cavity in neuroblastoma, and neck and chest region in MTC.

Conclusion: In this descriptive study, we have shown the common sites of metastases in SSTR-positive malignancies using a specific modality, Ga-68 DOTATATE PET/CT, which could provide the basis for future studies in the field of diagnostic and therapeutic management of patients with same malignancies.

p 038

Breast metastasis from the pancreatic neuroendocrine tumor origin detected in Tc99m-HYNIC-octreotate scan

Atena Aghaei, Sousan Shafeie, Kamran Aryana, Seyed Rasoul Zakavi, Hasem Allahyari

Nuclear Medicine Research Center, Mashhad University of Medical Sciences, Mashhad, Iran

Background: A 50 years old woman with history of pancreatic neuroendocrine tumor dignosed 2 years ago, which has not been surgically removed, was referred to our department to perform Tc99m-octeroscan in order to evaluate the somatostatin receptor status. She was treated with regular sandostatin injections and chemotherapy.

Her CT scan which was previously performed confirmed lung, adrenal and hepatic metastases.

In her pancreatic mass biopsy performed at initial diagnosis, well differentiated neuroendocrine tumor of the pancreas with 3% rate of KI-67 positivity was reported.

Objective: performing Tc99m-HYNIC-octerotate scan to evaluate the functional status of metastasis and susceptibility of the patient for future somatostatin ligand therapies.

Methods: Whole body Tc99m-octerote scan was performed 4 hours after IV injection of 20 mCi of the radiotracer using a dual-head variable angle gamma camera.

Results: Whole body scan showed multiple areas of increased tracer uptake in the pancreas, left adrenal, both breasts and left axillary region. Single photon emission computed tomography also confirmed the metastatic sites.

Conclusion: Considering the fact that metastasis of the pancreatic NET to the breast is extremely rare, we recommended mammographic correlation and tissue biopsy. The mammography confirmed breast masses and the biopsy revealed metastatic NET from the pancreatic origin.

p 039

Ectopic submental thyroid tissue, with no evidence of orthotopic thyroid: A case report

Atena Aghaee, Farnaz Banezhad, Emran Askari, hamideh abbasian, keyvan sadri, Salman Soltani

Nuclear Medicine Research Center, Mashhad University of Medical Sciences, Mashhad, Iran

Background: Thyroid ectopia refers to a congenital disease with abnormal descending of thyroid gland. The most common subtype is lingual thyroid ectopia. Sublingual and submental thyroid ectopia is much less common. It may also found in other neck locations and distant positions. 70-90% of patients with ectopic thyroid do not have eutopic thyroid tissue. It is necessary to distinguish ectopic thyroid from other causes of neck masses.

Case presentation: A 18-year-old man was referred for evaluation of a palpable mass in the submental region. On biochemical examination, the thyroid function tests was normal while receiving levothyroxin therapy. Ultrasonography revealed a mass measuring $4.2 \times 2.7 \times 2.6$ cm in the submental region.

Methods: after IV administration of 4 mCi of Tc99m, thyroid scan was performed from the neck region, using dual head gamma camera, equipped with low energy high resolution collimator in anterior and lateral views.

Results: Thyroid scan didn't show any uptake in the thyroid region. A zone of tracer activity was noted in the central neck, compatible with the palpated mass in submental region. CT images showed a hyperdense soft tissue in submental region, too.

Conclusion: Thyroid ectopia is a rare condition and it is often accompanied by hypothyroidism. Ectopia often occurs in lingual and sublingual locations and submental one is less common. Thyroid scintigraphy is the best imaging modality for detection of thyroid ectopia. for precise localization, CT scan correlation may be needed.

p 040

Evaluation of liver enzymes and the rate of lymphocyte apoptosis following the iodine therapy of thyroid cancer

Zari Hamivand, Gholamhassan Haddadi, M. Alavi

Department of Radiology, Shiraz University of Medical Sciences, Shiraz, Iran

Background: Iodine-131 is one of the radioactive materials used in the nuclear medicine for treatment and diagnosis. Iodine therapy is done to destroy the remaining tissue or probable metastasis. In the patients under iodine therapy after thyroidectomy, the rate of iodine absorption is high in their liver. It may lead to disorder in the liver enzymes level, and accordingly dysfunction of the liver. In addition, ionizing radiation has been known as causing oxidative stress by generating active oxygen types and free radicals in the tissues and irradiated cells. These free radicals react with DNA, existing lipids in the nucleus and membrane. The considerable changes in the structure and action of DNA (DNA double-stranded break and) lead to the cell death by apoptosis. The lymphocytes, as the cells with high sensitivity in the patients treated with radioactive iodine, experience the apoptosis easily.

The aim of this study was to determine the liver enzymes changes and the rate of lymphocyte apoptosis in the patients with thyroid cancer following iodine treatment with different doses.

Methods: This study was conducted on 50 patients with thyroid cancer had undergone surgery and were under treatment with 100 and 150 millicurie doses. The blood samples were taken from the patients, one before iodine therapy and another 48 hours after the therapy. The level of liver enzymes (ALP, ALT and AST) was investigated before and after iodine therapy; also, the rate of apoptosis in the lymphocytes with the flow cytometer method using the PE Annexin V Apoptosis Detection kit.

Results: The significant increase in the apoptosis lymphocytes percentage was compared between the two groups of after iodine therapy and before therapy. The rate of apoptosis in the lymphocytes before and after therapy was compared with each other; a significant increase was seen in the rate of early and late apoptosis as well as total apoptosis in the peripheral blood lymphocytes of patients after therapy ($p < 0.05$). As to liver enzymes level, no any changes was observed in the ALP enzyme level before and after iodine therapy. There was a significant difference between the level of ALT and AST enzymes level before and after iodine therapy ($p < 0.05$).

Conclusion: Iodine therapy leads to an increase in apoptosis lymphocytes percentage and increase of liver enzymes level, as well. It can be mentioned that iodine therapy leads to apoptosis and disorder in the liver function level, as well.

P 041

Theragnostics with Lutetium-177 labelled peptides: Changes and challenges

Emran Askari, Babak Fallahi, Ghasemali Divband, Mohammad Eftekhari, Alireza Emami-Ardekani, Armaghan Fard-Esfahani, Davood Beiki

Nuclear Medicine Research Center, Mashhad University of Medical Sciences, Mashhad, Iran
Research Centre for Nuclear Medicine, Tehran University of Medical Sciences, Tehran, Iran

Background: In the past year, nuclear medicine guidelines have been developed for treatment of patients with Lutetium-177 labelled peptides, namely ¹⁷⁷Lu-Dotatate and ¹⁷⁷Lu-PSMA. The latter has not yet approved by FDA and therefore used as a compassionate treatment for patients who have exhausted all previous treatments.

Objective: We aimed to provide some pearls and pitfalls regarding the treatment of patients with Lutetium-177 labelled peptides.

Methods: We performed a literature review to seek the challenging cases of treatment with lutetium-177 labelled peptides. We also reviewed our educational cases from two centers in Iran. Finally, challenging cases were classified into different categories.

Results: General challenging topics in the field of treatment with Lutetium-177 labelled peptides were: (1) appropriate patient selection, and (2) the issues regarding pre-therapeutic and post-therapeutic dosimetry and the best time for image acquisition, and (3) patient hospitalization vs. outpatient management. The following specific challenging topics were considered of importance for ¹⁷⁷Lu-Dotatate therapy: (1) approach to patients in case of hormonal crisis, (2) the role of combination therapies, and (3) novel approaches for ¹⁷⁷Lu-Dotatate administration. Specific challenging topics for treatment with ¹⁷⁷Lu-PSMA were: (1) definition of adequate PSMA uptake for treatment considerations, (2) approach to patients with exceptional responses, (3) fixed doses vs. escalating doses of ¹⁷⁷Lu-PSMA, (4) approach to patients with single functioning kidney or renal insufficiency, (5) treatment strategies in patients with non-PSMA avid liver metastasis, and (6) prostate cancer with neuroendocrine differentiation.

Conclusion: There is an unmet need for continuous education and learning as well as prospective study designs to clarify the intricacies in the field of theragnostics.

P 042

Inguino-scrotal bladder hernia: an unexpected finding on ⁶⁸Ga-PSMA PET/CT

Shirin Shahlaei, Sara Shakeri, Fatemeh Farahmandfar, Farshad Emami, Ramin Sadeghi

Nuclear Medicine Research Center, Mashhad University of Medical Sciences, Mashhad, Iran
Nuclear Medicine & Molecular Imaging Department, Imam Reza International University, Mashhad, Iran

Bladder herniation is an uncommon condition mimicking suspicious metastasis on PET/CT imaging. We report a 67 y/o man with prostate cancer referred for recurrence evaluation with ⁶⁸Ga-PSMA PET/CT. The scan showed an asymmetric site of intense tracer accumulation in the left inguino-scrotal region with the same SUV_{max} to the pelvic bladder. Reviewing cross sectional CT images with PET confirmed the inguino-scrotal bladder herniation.

P 043

Nuclear medicine in bone metastases: molecular targeted diagnostic and therapeutic radiopharmaceuticals

Reyhaneh Manafi-Farid, Mohsen Beheshti, Bahar Ataeinia

Research Center for Nuclear Medicine, Tehran University of Medical Sciences, Tehran, Iran
Department of Nuclear Medicine, University Hospital, RWTH University, Aachen, Germany
Department of Nuclear Medicine & Endocrinology, Paracelsus Medical University, Salzburg, Austria
Non-Communicable Diseases Research Center, Endocrinology and Metabolism Population Sciences Institute, Tehran University of Medical Sciences, Tehran, Iran

Bone metastasis develops in a wide range of tumors with a wide spectrum of incidence. Not only the presence of bone metastasis indicates poorer prognosis and shorter survival, but it also leads to a multitude of complications. Precise assessment and localization of the bone metastases are imperative to predict the outcome and to go for the optimum treatment. Nuclear medicine plays a crucial role in the detection of bone metastases. ^{99m}Tc-methylene diphosphonate scintigraphy and, whenever feasible, F-18 sodium fluoride positron emission tomography are the mainstay in the detection of bone metastases although a host of other radiotracers, with F-18 fluorodeoxyglucose at the top, are employed. One of the disabling presentations of bone metastases is refractory bone pain which is managed using multidisciplinary approaches. Bone pain palliation with easy to administer radionuclides offers advantages including simultaneous treatment of multiple metastatic foci, the repeatability, and also the combination with other treatments. A multitude of radionuclides and pharmaceuticals-from the very first Strontium-89 chloride to recently introduced agents such as Radium-223 chloride-have been and still are investigating to find an optimum option. In this review, the indisputable role of nuclear medicine is briefly discussed in the detection of bone metastases, using the most reputable efficient radiotracers. Afterwards, a number of long-established and novel radiopharmaceuticals employed in bone pain palliation are remarked.

p 044

Practical flowchart for theragnostics: An experience from Shariati Hospital

Emran Askari, Babak Fallahi, Ghasemali Divband, Somayyeh Ghahremani, Mohammad Eftekhari, Alireza Emami-Ardekani, Armaghan Fard-Esfahani, Davood Beiki

Nuclear Medicine Research Center, Mashhad University of Medical Sciences, Mashhad, Iran
Research Centre for Nuclear Medicine, Tehran University of Medical Sciences, Tehran, Iran

Background: Rapid growth of theragnostics has led many nuclear medicine centers to initiate peptide receptor radionuclide therapy (PRRT) and peptide receptor radioligand therapy (PRLT) with Lutetium-177 labeled peptides. However, a logical stepwise protocol is necessary, especially in tertiary care centers dealing with education of nuclear medicine residents, to help in precise stratification and appropriate patient management.

Objective: We decided to develop an evidence-based practical flowchart for patient selection as well as for treatment planning and follow-up of the patients.

Methods: A review of the most recent valid information regarding PRRT and PRLT was gathered. The protocol was drafted and revised several times followed by a consensus meeting with the attending nuclear medicine board members discussing about the challenging topics. Then, we held educational sessions to enhance the knowledge and clinical reasoning of the nuclear medicine residents. Meanwhile, pilot study was carried out to by treating 15 cases in each group of PRLT and PRRT to evaluate the potential pitfalls in the logistics of our practical flowchart. Finally, the consolidated format was finalized in our nuclear medicine center.

Results: From the commencement of treatment with Lutetium-177, more than 50 cycles of treatment have been done in our department. Nuclear medicine residents have grasped the fundamental knowledge needed for patient selection as well as how to treat and follow-up the patients.

Conclusion: We believe that the information should be translated in an action plan and justified according to the local facilities. The practical flowchart developed in our center can be a guide for nuclear medicine physicians interested in the field of theragnostics.

¹⁷⁷Lu/¹⁵³Sm-EDTMP cocktail: a novel and effective palliative treatment for patients with bone metastases

P 045

Mehrosadat Alavi, Farnaz Khajeh-Rahimi, Hassan Yousefnia, Mohammad Mohammadianpanah, Samaneh Zolghadri, Ali Bahrami-Samani, Mohammad Ghannadi-Maragheh

Ionizing and Non-Ionizing Radiation Protection Research Center (INIRPRC), Shiraz University of Medical Sciences, Shiraz, Iran

Nuclear Medicine Department, Medical School, Shiraz University of Medical Science, Shiraz, Iran.

Background: Production of effective, low-cost, and efficient radiopharmaceuticals is an important task and requires further research and clinical studies.

Objective: In this clinical trial, safety and efficacy of Lu-177/Sm-153 ethylenediamine tetramethylene phosphonic acid (edtmp) cocktail has been evaluated for pain relief of bone metastases.

Methods: Twenty-five patients with the mean age of 55.5–15.8 years participated in this study. patients received a total dose of 37 mbq/kg. pain and performance assessments were followed using a brief pain inventory form. complete blood count and renal and liver function tests were also performed up to 12 weeks postadministration.

Results: Eighteen patients (72%) demonstrated complete pain relief (relief=100%) and approximately all patients (96%) experienced significant improvement in their quality of life. no grade iv hematological toxicity was observed during the 12-week follow-up period, and grade iii toxicity was seen in 1 patient only. in addition, no abnormalities were seen in renal and liver function during the follow-up period.

Conclusion: There were no considerable complications after administration of lu-177/sm-153 edtmp; this cocktail seems to be a safe and effective treatment for bone pain palliation in patients with skeletal metastases and improves the quality of life.

P 046

Detection of protein losing enteropathy by ^{99m}Tc-UBI scintigraphy in a patient with congenital heart disease

Farnaz Nesari Javan, Atena Aghaei, Ramin Sadeghi

Department of Nuclear Medicine, Faculty of Medicine, Ghaem Hospital, Mashhad University of Medical Sciences, Mashhad, Iran

Background: 18 year old female patient with a history of operated complex congenital heart disease, was referred for possible protein losing enteropathy by ^{99m}Tc- UBI scintigraphy. The patient suffered from abdominal ascites, pericardial effusion and unexplained decreased serum albumin since 1.5 years ago. Complex congenital heart disease was defined as single ventricle, common atrium and large ASD that reconstructed by Glenn and Fanton surgery.

Objective: Performing ^{99m}Tc- UBI scintigraphy to confirm the diagnosis and localizing the possible site of protein losing.

Methods: After IV administration of 740 MBq of ^{99m}Tc- UBI scanning was performed in 2 second intervals for 1 minute and then in 1 min/frame interval for 60 minutes from the abdominal region and then delayed static image of 24-hrs collected feces was performed.

Results: Dynamic images revealed an area of increased tracer uptake in the center of abdominal region, compatible with small intestine. Tracer activity in 24-hrs collected feces was noted.

Conclusion: PLE can be detected by increased alpha-1-antitrypsin concentration in a collected stool sample. However; the detection of alpha-1 antitrypsin does not show the site of protein loss in the intestine. Furthermore, it will not show a positive result when the stomach is the place of leakage .Our case represented that Tc-99m UBI is radiotracer which can be used for detection of protein leakage.

A case of noninvasive follicular thyroid neoplasm with papillary-like nuclear features (NIFTP) with bone metastasis

P 047

Yasaman Fakhar, Atena Aghaei, Hadis Mohammadzadeh Kosari, Seyed Rasoul Zakavi

Department of Nuclear Medicine, Faculty of Medicine, Ghaem Hospital, Mashhad University of Medical Sciences, Mashhad, Iran

Background: We describe a case of a 38-year-old woman with history of recent thyroidectomy for treatment of multinodular goiter. In her histopathology report, the final diagnosis was stated as NIFTP (noninvasive follicular thyroid neoplasm with papillary-like nuclear features). Considering the high level of serum thyroglobulin level, diagnostic ¹³¹I whole body scan was scheduled. Histopathological examination of the specimen was rechecked and confirmed the prior diagnosis of NIFTP. Therefore, considering the high serum level of thyroglobulin and the abnormal skeletal uptake on diagnostic iodine scan, the patient received 200 mCi of I131 orally.

Objective: To evaluate the possible sources for high level of serum thyroglobulin (Tg>300), which was disproportionate to the benign etiology.

Methods: Diagnostic and post ablation whole body iodine scan, using high energy parallel hole collimator in conjunction with SPECT/CT of the neck and pelvic regions were performed.

Results: On whole body images performed after administration of 1 mCi of I 131, a focus of abnormal uptake was noted in left hemipelvis. Subsequent SPECT/CT images of the pelvis revealed a lytic lesion in the left sacroiliac region, with intense iodine 131 uptake. Iliac bone metastasis was revealed more clearly on the post ablation scan.

Conclusion: The term non-invasive follicular thyroid neoplasm with papillary-like nuclear features (NIFTP) was recently proposed as non-malignant lesions with indolent behavior (1). However this is an unusual case with aggressive behavior showing distant metastasis.

P 048

Detecting aorto-ureteric fistula by ^{99m}Tc-labeled red blood cell SPECT

Hadis Mohammadzadeh Kosari, Atena Aghaei, Alireza Masoudifard, Mohammad Asle Are, Seyed Rasoul Zakavi

Department of Nuclear Medicine, Faculty of Medicine, Ghaem Hospital, Mashhad University of Medical Sciences, Mashhad, Iran

Background: A 68-year-old man was referred to our nuclear medicine department with gross hematuria and history of abdominal aortic dissection and endovascular stent-graft repair 5 years ago. The urologists had suspected aorto-ureteric fistula and open surgery (ureterolysis) had been performed last week. Considering the sustained gross hematuria Tc99m-RBC scintigraphy was ordered to confirm the diagnosis and localize the possible site of aorto-ureteric fistula.

Objective: Performing TC-99m labeled red blood cell scintigraphy to confirm the diagnosis and localizing the possible site of aorto-ureteric fistula.

Methods: In vitro labeling method of preparing Tc99m-RBC was performed to increase the labeling efficiency. Immediately after intravenous injection of 20mCi of Tc-99m-RBC, Dynamic imaging was performed from the abdominopelvic region using a dual-head variable angle gamma camera (30 second/frame intervals for 40 minutes).

Results: The scan revealed visualization of the liver, spleen and abdominal vessels indicating good labeling efficiency. Quality controlling of the prepared kit also showed 96% labeling efficiency. Also, the dynamic images showed an abnormal tracer activity in the left side of aorta. Therefore, Single-photon emission computed tomography (SPECT) was performed. The SPECT images revealed a left aorto-ureteric fistula approximately 8cm above the aortic bifurcation.

Conclusion: Because Tc99m-RBC scan relies on labeling of red blood cells, we can conclude that it would be helpful for detection of any site of RBC accumulation, such as hematoma, hemangioma, vascular aneurysms, etc. our case shows the utility of this scan in detection of aorto-ureteric fistula.

The role of Tc99m-HYNIC-PSMA 11 in metastatic castration resistant prostate cancer patients (mCRPC)

p 049

Kamran Aryana

Nuclear Medicine Research Center, Mashhad University of Medical Sciences, Mashhad, Iran

We used Tc99m-HYNIC-PSMA 11 kit produced by the Pars Isotope Company for the first time in IRAN in mCRPC patients with bone metastases. The quality of this kit is high for detection of PSMA positive bone metastases and we think it can replace 68Ga-PSMA PET/CT in centers that have no PET/CT facility for evaluation of mCRPC patients, before PRRT.

Oral (Physics)

ORAL PRESENTATIONS**Section A: Internal Dosimetry and Radiation Protection****OP 001**

Thursday, November 28, 2019

08:30-08:45, side hall (laleh)

Patient-specific dosimetry by using dose point kernel of ¹⁷⁷Lu/⁹⁰Y cocktail radionuclide

Milad Peer Firouzjaei, Mohammad Ali Tajik Mansoury, Parham Geramifar

Department of Medical Physics, Semnan University of Medical Sciences, Semnan, Iran
Research Center for Nuclear Medicine, Tehran University of Medical Sciences, Tehran, Iran

Background: An effective strategy in the treatment of neuroendocrine tumors is the treatment of Peptide Receptor Radionuclide Therapy (PRRT), along with peptides labeled with ¹⁷⁷Lu and ⁹⁰Y. One of the patient-specific dosimetry methods in this field is convolving Dose Point Kernel (DPK) function with the patient activity images. In clinical cases, it is highly likely that patients with clusters of different size of tumors could have been identified, and several studies have shown that the use of radionuclide cocktails is an effective way to treat tumors of different sizes.

Objective: Therefore, the aim of this work is to calculate DPK of cocktail point source of ¹⁷⁷Lu and ⁹⁰Y with various percentages of combination.

Methods: In this study, simulations and calculations of DPK were performed, using Monte Carlo GATE code (version 7.2). Simulations were performed for each of the ¹⁷⁷Lu and ⁹⁰Y point source radionuclides separately and in combination of percentages with a quarter step, Centered on homogeneous isotropic radiation of spheres of water. Besides, the spectrum of beta-radionuclides was used during the study.

Results and Conclusion: Differences in the DPK profile of single radionuclides and cocktails are observable, according to the results of this study. By using the DPK functions of the ¹⁷⁷Lu/⁹⁰Y cocktails, patient-specific dosimetry can be performed by convolving the DPK function with the activity map of patients in the combinational radionuclide therapy using cocktail of ¹⁷⁷Lu and ⁹⁰Y, which according to previous studies is effective for treating neuroendocrine tumors of various sizes.

op 002

Thursday, November 28, 2019

08:45-09:00, side hall (laleh)

An analytical modeling approach to dose quantification in targeted radionuclide therapy based on the Cerenkov light detection

Etesam Malekzadeh, Hossein Rajabi, Faraz Kalantari

Department of Medical Physics, Faculty of Medical Sciences, University of Tarbiat Modares, Tehran, Iran

Division of Medical Physics and Engineering, Department of Radiation Oncology, Southwestern Medical Center, University of Texas, USA

Background: Targeted Radionuclide Therapy (TRT) is one of the promising methods for the treatment of metastases. Basically in TRT, there is a need for methods to quantify the absorbed dose. Unfortunately, gamma camera devices cannot be used for imaging the beta emitter radioisotopes. More recently, Cerenkov radiation dosimetry has been proposed to determine the activity of the radionuclides. But, quantification of doses using this radiation is still a challenge.

Objective: In this work, a mathematical method is presented to examine the relationship between dose and Cerenkov light. In this regard, the doses and the number of emitted photons are calculated for 6 beta-emitter radionuclides, and their relationship is modeled.

Methods: The beta-emitter radionuclides Y-90, P-32, Sm-153, Re-186, Sr-89, Re-188, which have an energy of [0.808-2.3] MeV, with an activity of 0.1 MBq were considered. The photons generated by the Cerenkov mechanism were calculated using the Frank-Tamm equation. The environment was considered water. To calculate the range, the experimental relationship was used. The effect of the scattering and absorption of the photons were ignored. The average particle energy was used. For photon counting, an ideal detector with a surface area of 25 cm² was placed at a distance of 5 cm from the surface of the water. The doses for a sphere equivalent to the Y-90 range was calculated theoretically and with the MCNPX simulation. All calculations were performed using the MATLAB software.

Results: For energies higher than 1 MeV, the relationship between the doses and resulting photons from the Cerenkov radiation, was estimated linearly with a confidence of more than 95%. The

difference between the calculated photons, on average, were about 20% of the reported amounts in the references. The difference between dose values for analytical and simulation was less than 1%.

Conclusion: Quantification of the dose in certain conditions and assuming the use of the average beta energy was done. It was shown that for high-energy radionuclides, with a confidence level of 95%, it is possible to estimate the dose through the photons recorded.

op 003

Thursday, November 28, 2019
09:00-09:15, side hall (laleh)

The dose delivered to pediatrics from ³²P Synovectomy

Fatemeh Bahranizad, Mehrshad Abbasi, Ali Asghar Parach, Hamidreza Masjedi

Medical Physics Department, Shahid Sadoughi University of Medical Sciences and Health Services, Yazd, Iran

Department of Nuclear Medicine, Vali-Asr Hospital, Tehran University of Medical Sciences, Tehran, Iran

Background: Rheumatoid arthritis (RA) is a chronic autoimmune disease characterized by pain, swelling, as well as joint deformation and destruction. Radiation synovectomy (RSV) is a minimally invasive treatment for RA in which radionuclides are injected into the joint space. This procedure aims to destroy the diseased synovial membrane by the proper radionuclide. Considering the heterogeneous nature of the synovial membrane, patient-specific radiation dosimetry in RSV would be of major concern.

Objective: The goal of this study was to estimate the dose delivered to the organs (lung, spine, and brain) by the emission of injected Phosphorus-32 to the knee joint.

Methods: GATE version 8.0 was used to perform simulations. A 5 years old female XCAT phantom with a voxel size of 5 mm³ was implemented as the input. A disk source made of ³²P was simulated by the energy spectrum published by ICRP 107 and then, was located in the middle of one of the knee joints. The outputs were analyzed by MATLAB (2016a, Mathworks, Natick, MA), and hence, the dose absorbed by the spine, lung, and brain were extracted.

Results: In this procedure, the calculated 0.5 mCi of ³²P dose of the lung, Spine, and the Brain of the studied five years old female XCAT phantom were respectively as follows: 4.10, 3.9, 0.2 pGy.

Conclusion: The dose calculated with this amount of injectable activity of a five-year-old female XCAT phantom results from the safety of this treatment as a minimally invasive method.

op 004

Thursday, November 28, 2019
09:15-09:30, side hall (laleh)

Investigation of fetal dose in V/Q scan using Monte Carlo simulation

Shahabeddin Vakili, Daryoush Shahbazi-Gahrouei

Department of Medical Physics, School of Medicine, Isfahan University of Medical Sciences, Isfahan, Iran

Background: Pulmonary embolism (PE) is a blockage in one of the pulmonary arteries. A clinical suspicion of PE should always be confirmed by an imaging test. Ventilation/Perfusion (V/Q) scan is one of the diagnostic methods of PE in pregnant women. Estimating the amount of fetal dose received from a nuclear medical method performed on a mother is an essential factor in risk assessment. It is necessary to investigate fetal dose and compare it with recommended values.

Objective: The aim of this study was to determine the fetal dose in V/Q scan using Monte Carlo simulation.

Methods: An adult pregnant woman phantom and all her displaced organs were used for simulation. Source organs were defined for each of the radiopharmaceuticals used in two lung ventilation and perfusion scans, including lung and bladder for ¹³³Xe, ^{81m}Kr and technetium diethylene-triamine-pentaacetate aerosol (^{99m}Tc-DTPA-aerosol) for lung ventilation scan, and lung, bladder and liver for technetium macroaggregated albumin (^{99m}Tc-MAA) for lung perfusion scan. Fetal dose was determined and evaluated by the simulation output after calculations.

Results: For ^{99m}Tc-MAA at prescription dose of 200 MBq, fetal dose was found to be 1.01 mGy, maximum fetal dose was 1.97 mGy, and both of them were more than the values recommended by

International Commission on Radiological Protection (ICRP). For ^{99m}Tc-DTPA, fetal and maximum doses were below 1 mGy, and for ¹³³Xe and ^{81m}Kr, fetal dose was negligible.

Conclusion: It is concluded that considering higher dose to the fetus (200 MBq of ^{99m}Tc-MAA), if the pregnant woman scan is needed, her awareness must be done.

op 005

Thursday, November 28, 2019
09:30-09:45, side hall (laleh)

The investigation of ¹⁶⁶Ho and ¹⁷⁷Lu as theranostic radionuclides in radioembolization, a comparison with ⁹⁰Y

Asra Sadat Talebi, Abbas Emamyari, Hossein Rajabi

Department of Medical Physics, Tarbiat Modares University, Tehran, Iran

Background: Radioembolization with ⁹⁰Y is a palliative treatment of the primary and metastatic malignancies of the liver. The procedure requires post-treatment imaging to estimate the dose to the tumors and also follow up on the patients. Since ⁹⁰Y is a pure beta emitter, imaging is a big challenge. Recently ¹⁶⁶Ho and ¹⁷⁷Lu have been suggested as alternatives to improve the quality of images.

Objective: The aim of this study was to calculate the organ doses and comparison of gamma radiation spectra emitting from the patient's body due to administration of ¹⁶⁶Ho, ¹⁷⁷Lu and ⁹⁰Y. **METHODS:** Gate Monte Carlo toolkit and ICRP110 phantoms were used to carry out the required simulations. A tumor of 133 cm³ volume was considered inside the liver. The total activity of the tumor was calculated based on the body surface area of the phantoms, uniformly distributed in the tumor.

Results: The gamma radiation frounce that emitting from the phantoms was 3.3×10⁴, 3×10⁵ and 5.5×10⁵ for ⁹⁰Y, ¹⁶⁶Ho and ¹⁷⁷Lu respectively. The calculated tumor doses for the radionuclides tested as approximately 471 Gy. The normal tissue of liver dose was approximately 50% higher for ¹⁶⁶Ho and ¹⁷⁷Lu in compared with ⁹⁰Y.

Conclusion: Although ¹⁶⁶Ho and ¹⁷⁷Lu offer higher gamma frounce for post-procedure imaging, the absorbed dose to other organs was within the tolerance limits in radioembolization with ¹⁶⁶Ho and ¹⁷⁷Lu. The result showed, not potential advantages over as ⁹⁰Y.

op 006

Thursday, November 28, 2019
09:45-10:00, side hall (laleh)

¹⁸F-FET PET/CT in patients with suspicious recurrent low and high-grade glioma

Habibollah Dadgar, Majid Assadi

Cancer Research Center, Razavi Hospital, Imam Reza International University, Mashhad, Iran
The Persian Gulf Nuclear Medicine Research Center, Department of Molecular Imaging and Radionuclide Therapy (MIRT), Bushehr Medical University Hospital, Faculty of Medicine, Bushehr University of Medical Sciences, Bushehr, Iran

Objective: The precise definition margin of high and low-grade glioma is crucial for choosing best treatment approach after surgery and radio-chemotherapy. The aim of the current study was to assess the O-(2-¹⁸F-fluoroethyl)-L-tyrosine (¹⁸F-FET) positron emission tomography (PET)/computed tomography (CT) in patients with low (LGG) and high grade glioma (HGG).

Methods: We retrospectively analyzed ¹⁸F-FET PET/CT of 11 patients (age: 33±12 years) with suspicious recurrent of LGG and HGG. In these cases, final decision of recurrence was made by magnetic resonance imaging (MRI) and registered clinical data for PET-CT or PET-MR evaluation.

Result: While response to radio-chemotherapy by MRI is often complex and sophisticated due to the edema, necrosis and inflammation, emerging amino acid PET leading to the better interpretations with more specifically differentiate true tumor boundaries from equivocal lesions.

Conclusion: Therefore, integrating amino acid PET in the management of glioma to complement MRI will significantly improve early therapy response assessment, treatment planning, and clinical trial design.

op 007

Thursday, November 28, 2019

10:00-10:15, side hall (laleh)

Cellular dosimetry of Samarium-153 and Strontium-89 for palliative therapy of bone: A Monte Carlo simulation study

S. Dalvand, H. Rajabi, E. Malekzadeh

Department of Medical Physics, School of Medical Sciences, Tarbiat Modares University, Tehran, Iran

Background: Bone is one of the common metastatic sites of cancers. Systemic radiopharmaceutical therapy is an effective method for pain palliation of bone metastasis and several radionuclides have proposed. Metastron (Strontium-89 chloride) and Quadramet (¹⁵³Sm tetrakisphosphate chelator, ethylenediaminetetramethylenephosphonic acid) are approved by the FDA. The average energy of beta radiation from Strontium-89 and Samarium-153 is 585 keV and 224 keV, respectively. However, the mean energy of other radiations of Strontium-89 is much lower than that of the Samarium-153. This difference was neglected in most studies and reported a higher dose of Strontium-89 compared to dose of Samarium-153. But it is not true in microscale dose calculation due to short range of Auger electrons.

Objective: The aim of this study was comparing the absorbed dose of Strontium-89 and Samarium-153 using full spectrum of radiations in cellular level using Monte Carlo simulation.

Methods: Simulations were performed using GATE Monte Carlo toolkit. Two sizes were considered for osteoblasts, osteoclasts, and osteocytes based on published histological data. The radionuclides were assumed to be uniformly distributed in different subcomponents of the cell. Cellular S-values were calculated for five combinations of source-target organelles; cell-cell (C→C), cell surface-cell (CS→C), cell surface-nucleus (CS→N), cytoplasm-nucleus (Cy→N) and nucleus-nucleus (N→N).

Results: The Auger and internal conversion electrons S-values of Samarium-153 are much higher than those of Strontium-89. When radionuclides are in the cell nucleus, Auger electrons deposit the highest possible dose to the nucleus. In all source-target combinations, the nucleus dose is much higher when the source is inside the cell nucleus compared to the situations when the source is in cell surface, cytoplasm or entire of the cell.

Conclusion: Our results show that in the subcellular scale, the Auger and internal conversion electrons have a significant contribution to the deposited dose. Particularly in Osteoblastic metastases the Auger electron doses should be considered.

ORAL PRESENTATIONS**Section B: Nuclear Medicine Instrumentation**

op 008

Thursday, November 28, 2019

11:00-11:15, side hall (laleh)

Depth of interaction capable detectors for small PET system using dual-ended readout innovative method

I. Mohammadi, P.M.M. Correia, I.F.C. Castro, A.L.M. Silva and J.F.C.A. Veloso

Physics Department, University of Aveiro, 3810-193 Aveiro, Portugal
Department of Basic Sciences, Faculty of Medicine, Sari Branch, Islamic Azad University, Sari, Iran

Background: The spatial resolution of PET systems is often degraded due to the lack of information about the depth of interaction (DOI). Dual ended readout systems utilize photodetectors on both sides of a scintillation element. The drawbacks of general dual ended readout detectors are higher cost, photon attenuation and scatter by the front photo-sensors located at the inner detector ring.

Objective: This research work aims at developing a small PET scanner with improved spatial resolution using DOI information. Accurate DOI information is used to properly calculate the true lines of response helping to reduce parallax errors and provide a more uniform spatial resolution across the entire field of view. The system combines scintillator-photodetector cells with a new DOI determination method, based on light guides with silicon photomultiplier (SiPM) readout.

Methods: The foreseen system comprises rings of 128 $1.5 \times 1.5 \times 20$ mm³ LYSO crystals radially distributed. Each single LYSO crystal is read out on both ends by SiPMs, but using wavelength-shifting fibers and a reduced number of SiPMs on one end. GATE simulation of the system is carried out to evaluate the amount of light detected on each side of the crystal and the achievable DOI resolution with this method.

Results: Experimental results from dual-ended readout innovative method for PET (DRIM-PET) shown a DOI spatial resolution of up to 6 mm. Reconstructed images from simulations of the NEMA NU 4-2008 phantom were obtained using STIR software. The approach reduced the number of photodetectors needed, simplified the readout and allowed an increased sensitivity since there is less material in the inner side of the ring.

Conclusion: A novel dual-ended readout method was developed using individual SiPM readout in the outer detector ring and wavelength-shifting fibers in the inner ring, sharing the light output from several LYSO crystals. Simulation studies were performed in order to optimize the system's parameters with the aim of building and characterizing a proof-of-concept prototype of a new PET scanner for preclinical research.

op 009

Thursday, November 28, 2019

11:15-11:30, side hall (laleh)

Monte Carlo simulation of a PEM system (positron emission mammography) using GATE by considering the effect of time of flight (TOF)

Mehdi Rashidi, Niloufar Reshteban, Bahador Bahadorzadeh, Seyyed Abolfazl Hosseini

Department of Energy Engineering, Sharif University of Technology, Tehran, Iran
Department of Nuclear Engineering, Shiraz University, Shiraz, Iran

Background: Breast cancer is one of the most important causes of female mortality in the world. Diagnosing the disease in its early stage increases the chance of survival significantly. To this end, Positron Emission Mammography (PEM) as one of the complementary methods may be used. PEM imaging is a molecular imaging technique for diagnosing breast cancer.

Objective: In this work, we investigated the effect of TOF corrections in system's performance, sensitivity parameters, scattering fraction and NECR of PEM system.

Methods: In this work, we investigated the performance of a commercially-available clinical PEM scanner (Naviscan) using GATE software. This system consists of two non-rotating detector heads that are positioned in opposing fashion on each side of the body part. Each detector head contains 12 sensitive PMT with 6×2 array and each PMT is coupled by a light guide to 169 crystals with a 13×13 array of $2 \text{ mm} \times 2 \text{ mm} \times 13 \text{ mm}$ LYSO crystals. The sensitivity parameter and the scattering fraction test of the system are investigated according to the standard NEMA NU4-2008 manual.

Results: The sensitivity parameter and the scattering fraction test of the system suggest that the results of the simulation have an error less than 0.5% in comparison to reference papers. The simulated system was subsequently investigated in three coincidence windows (6, 8, and 10 ns). The constancy of the correct coincidence counts and the 59.7% decrease in random coincidence counts cause 32% increase in the NECR diagram's maximum in the 6 ns coincidence window. Considering the TOF in four coincidence resolutions (100, 350, 650, and 900 ps) causes an increase in the NECR diagram's maximum. The obtained results suggest that the NECR diagram's maximum occurs in the 6 ns coincidence window and the 100 ps resolution, which causes a 42.3% increase in the NECR diagram's maximum without considering the TOF.

Conclusion: Considering the TOF in the simulated system causes a 42.3% increase in the NECR diagram's maximum. Increase the sensitivity of the system may have a significant effect on the decreasing the patient's dose and improvement of the quality of the medical images.

op 010

Thursday, November 28, 2019

11:45-12:00, side hall (laleh)

Evaluation of LM-MLEM reconstruction method in the simulation of the Compton camera in GAMOS code

S.M.R. Hashemi, P. Taherparvar, M. Razzaghi

Faculty of Sciences, University of Guilan, Rasht, Iran

Background: In recent years, extensive studies have been carried out on the development of nuclear medicine imaging procedures. Beside of development some common imaging modality such as SPECT and PET systems, new imaging devices has been introduced such as Compton camera. The Compton camera is based on the reconstruction of recorded photons with Compton scattering, which is predominance interaction in photons energies used in nuclear medicine imaging.

Objective: The Compton camera is a new developed imaging system, which have some advantages in comparison with the common imaging systems, such as high sensitivity (due to the absence of mechanical collimator) and the possibility of imaging from wide energy spectrum sources. These advantages make it a promising candidate for application in hadrontherapy. Its applicability is currently under investigation either in hadron therapy. The methods of image reconstruction on Compton camera are more complex than conventional SPECT techniques.

Methods: Simulations were performed by the GAMOS software, which is a GEANT4 based architecture for Medicine-Oriented simulations, which allows performing GEANT4 simulations using a scripting language. At first, we simulated a standard gamma camera for Compton imaging, which consist of a silicon scatterer detector and an absorber detector of CZT (cadmium zinc telluride). A spherical source was simulated in the center of field of view and simulation time was performed to record 10,000,000 events at the output of the two detectors. We select proper events which undergo Compton scattering in the first detector and absorb in the second detector by examination of recorded energy and coincidence criteria. Image reconstruction was performed based on list-mode Maximum Likelihood Expectation Maximization (LM- MLEM) [4] algorithm with a code which was written in MATLAB code.

Results: The results were reconstructed by considering 5 iterations in the LM- MLEM algorithm. Our results show that the source could be estimated position and its size by our algorithm, with a percent error of less than 15%.

Conclusion: Our results show that the Compton camera could be produced 3-D images of source distribution without any camera rotation with acceptable resolution. It is noted that image reconstruction in Compton camera involve relatively complicated mathematics, which have a direct impact on the image resolution.

op 011

Thursday, November 28, 2019
12:00-12:15, side hall (laleh)

Design and development variable time bed position in whole-body PET/CT imaging

Maryam Pourghanad, Pardis Ghafarian, Parham Geramifar, and Mohammad Reza Ay

Department of Medical Physics and Biomedical Engineering, Tehran University of Medical Sciences, Tehran, Iran
Research Center for Molecular and Cellular Imaging, Tehran University of Medical Sciences, Tehran, Iran
PET/CT and Cyclotron Centre, Masih Daneshvari Hospital, Shahid Beheshti University of Medical Sciences, Tehran, Iran
Chronic Respiratory Diseases Research Center, National Research Institute of Tuberculosis and Lung Diseases (NRITLD), Shahid Beheshti University of Medical Sciences, Tehran, Iran
Research Center for Nuclear Medicine, Tehran University of Medical Sciences, Tehran, Iran

Background: In conventional whole-body PET protocols, a constant acquisition time per bed position (BP) is used, regardless of the size and characteristics of sections of the body. Since the amounts of attenuation vary in different sections of body, it may be possible to spend less acquisition time at less attenuating sections.

Objective: This study aims to investigate the possibility of using various acquisition time per bed position while keeping image quality constant. Using variable BP time could reduce total scan time during whole body PET/CT imaging.

Methods: PET images of a NEMA image quality phantom containing six cylindrical inserts filled with F-FDG solution in 2:1 radioactivity lesions to background ratio were investigated. The data acquired from phantom reconstructed for different acquisition times (60, 90, 120, 150, 180, 240, and 300 s) in GE Discovery 690 PET/CT scanner and reconstructed by HD+PSF, TOF and TOF+PSF methods. Image quality was evaluated by quantitative parameters such as signal to noise ratio (SNR), percent contrast (Q_H), recovery coefficient (RC) and standard uptake value (SUV).

Results: Considering the TBR of all spheres and images is the same, the detection spheres from the background depends on size and acquisition time. Results demonstrate that the largest hot sphere

(28mm) is the one with better SNR, particularly at 240s (SNR= 21.71) and for the 17mm varies between 7 and 12.74. The highest SNR for the 10mm sphere is 2.98 at 120s. Both noise and Q_H tend to decrease with time increase. The results for RC show that this parameter is higher for the largest sphere at 60s. Correlation of the SUVmax between different acquisition time is measured using the Pearson Correlation Coefficient and the t-test is used whether the correlation coefficient is significantly different from zero. The null hypothesis is rejected between 90 & 120s ($p=.06$), and 90 & 150s ($p=.07$).

Conclusion: Iterative reconstruction methods can compensate SNR in small lesions containing less tracer uptake. Generally, image quality demonstrates better results with higher time, although there were not significantly different between them. It is feasible to reduce the acquisition time to 2 min or less without compromising the detection of the lesions. In terms of SUVmax, decreasing time by 90s is still acceptable. Finally, it is possible to reduce total scan time by 50 % in comparison to the routine imaging method. This hypothesis is still under evaluation and needs more assessment.

Op 012

Thursday, November 28, 2019

12:15-12:30, side hall (laleh)

Performance assessment of LEHR collimators in comparison with HE for Lu-177 diagnostic imaging

Mahboobeh Asadi, Marzieh Ebrahimi, Mohammadreza Ramezanicharmineh, Ali Ebrahimi Fard, Maziar Khateri, Parham Geramifar

Research Center for Nuclear Medicine, Shariati Hospital, Tehran University of Medical Sciences, Tehran, Iran

Medical Physics Department, Faculty of Medicine, Iran University of Medical Sciences, Payam PET Scan Center, Mehrshahr, Alborz, Iran

Department of Medical Physics, Faculty of Medical Science, Tarbiat Modares University, Tehran, Iran

Background: Widespread interest in use of peptide receptor radionuclide therapy for neuroendocrine tumors such as ^{177}Lu -Dotatate, necessitate a need for patient specific dosimetry according to the diagnostic images which were acquired using SPECT/SPECT-CT modality. ^{177}Lu emits beta particles and low energy gamma photons [$E = 113 \text{ Kev}$ (6.6%), 208 Kev (11%)], therefore image acquisition criteria should be considered. Surprisingly, types of collimator have a substantial influence on subjective metrics as well as contrast and resolution of the images.

Objective: The aim of this study to assess the performance of low energy high resolution (LEHR) collimators in comparison with high energy (HE) for Lu-177 Diagnostic applications.

Methods: The research performed using a Symbia T (Siemens Medical, Germany) SPECT/CT camera to compare LEHR and HE collimators. Five cylinders with various diameters of 0.5, 0.9, 1.3, 1.6, 2.2 cm and same activity concentration of 1.22 MBq/ml of Lu-177 radionuclide were inserted in the Jaszczak phantom. To achieve the tumor- to -background ratio (TBR) of 12.2, the phantom was filled with water and represent the background with activity concentration of 0.1 MBq/ml. For each tomographic scan, one hundred and eighty projections were acquired with both LEHR and HE collimators with a circular orbit using 128×128 matrix size. As Lu-177 has two photopeak window (113 KeV and 208 KeV) different energy window configurations were used for HE and LEHR acquisitions; window widths of 15% and 20% were used separately and together, lower scatter windows (LSW) of 10% and 15%, besides upper scatter windows (USW) of 10% and 15% were applied.

Results: The highest CNR and consequently, the best detectability was belonged to images which were acquired by LEHR collimator with photopeak energy of 113 Kev, window width of 15% and LSW / USW of 10%. Considering full width at half maximum (FWHM) and full width at tenth maximum (FWTM), the smallest values of FWHM and FWTM for smaller syringes was revealed to be for images which were acquired using same collimator and parameters as before.

Conclusion: LEHR Collimator, photopeak energy of 113 KeV, window width of 15% and LSW/USW of 10% is recommended for Lu-177 diagnostic imaging and related dosimetry applications.

Techniques to improve GATE computational efficiency: an overview

Hojjat Mahani

Radiation Application Research School, Nuclear Science and Technology Research Institute, Tehran, Iran

Background: Although GATE simulations are widely used in tomographic scanners design and optimization, its flexibility comes at a price as it is highly CPU-intensive. Therefore, improving GATE simulation efficiency is of importance to keep the computing time at an acceptable level.

Objective: The principal aim of this study is to improve GATE simulation efficiency through a combination of efficient data analysis, dedicated variance reduction techniques, fast navigation algorithms, and parallelization.

Methods: In general, there are three main approaches to minimize the computational effort of a GATE simulation: (1) simplify the GATE model, (2) non-analog simulation, and (3) parallel computing. This work reviews available techniques to accelerate GATE simulations including physics process level discrimination, smart sampling, standard and convolution-based forced (CFD) detection, built-in variance reduction techniques, and GPU/cluster computing approach. As parallel computing is experiencing a supertrend during last years, more focuses are put on it in order to highlight recent advances and practical implementations.

Results: The non-analog simulation method offers an up to five orders of magnitude acceleration factor in GATE computations and renders realistic PET, SPECT, and CT simulations feasible within minutes on a single CPU. GATE also benefits from three easy-to-implement variance reduction techniques including splitting, Russian roulette, and track length estimator. Moreover, Monte Carlo simulations are excellently suited for parallelization. Hence, GATE provides tools for convenient use with clusters and benefits from two parallelization mechanisms: event splitting and time splitting. An interesting feature of GATE is GPU computing capability via NVIDIA hardware and CUDA tools for PET and CT imaging applications. However, the aforementioned methods usually trade the computational efficiency off against computational accuracy.

Conclusion: Acceleration techniques significantly shorten computation time while the applicability of the GATE platform is retained. A suitable acceleration technique can be chosen, depending on the required speed and accuracy.

ORAL PRESENTATIONS:**Section C: Quantitative Analysis and Image Correction in Nuclear Medicine****Impact of imaging context and duration as well as reconstruction algorithms on measured PET spatial resolutions**

Pardis Ghafarian, Sahar Rezaei, Mehrdad Bakhshayesh-Karam, Carlos F. Uribe, Arman Rahmim, Saeed Sarkar, Mohammad Reza Ay

Chronic Respiratory Diseases Research Center, National Research Institute of Tuberculosis and Lung Diseases (NRITLD), Shahid Beheshti University of Medical Sciences, Tehran, Iran
PET/CT and Cyclotron Center, Masih Daneshvari Hospital, Shahid Beheshti University of Medical Sciences, Tehran, Iran

Department of Medical Physics and Biomedical Engineering; Tehran University of Medical Sciences, Iran

Research Center for Molecular and Cellular Imaging, Tehran University of Medical Sciences, Iran

Department of Molecular Oncology, BC Cancer Research Centre, Vancouver, BC, Canada

Departments of Radiology and Physics, University of British Columbia, Vancouver, Canada

Department of Integrative Oncology, BC Cancer Research Center, Vancouver, Canada

Background: Spatial resolution in PET imaging is a major determinant of performance and image interpretation in oncology.

op 013

Thursday, November 28, 2019

12:30-12:45, side hall (Ialeh)

op 014

Thursday, November 28, 2019

13:30-13:45, side hall (Ialeh)

Objective: The present study aims to assess the impact of acquisition time, different iterative reconstruction protocols (PSF and/or TOF) as well as image context (including contrast levels and background activities) on the measured spatial resolution in PET images.

Methods: Discovery 690 PET/CT scanner was used to study spatial resolution measurement in terms of Full Width Half Maximum (FWHM) as derived (i) directly from capillary tubes embedded in air and (ii) indirectly from 10 mm diameter sphere of the NEMA phantom. To do this, 2 MBq of ¹⁸F-FDG was utilized for seven capillary tubes in different scanner FOV. The spheres with 10, 17 and 28 mm diameter of NEMA phantom were also filled with ¹⁸F-FDG solution. Different sphere-to-background ratios (2:1, 4:1 and 8:1), background activity levels (2.38 and 4.78 kBq/ml) and acquisition times were also applied. The emission data were reconstructed with iterative reconstruction protocols (PSF and/or TOF). Various combinations of iterations and subsets ($it \times sub$) and post smoothing filter was also evaluated. Relative differences (%) were calculated for assessment of measured FWHM in different protocols.

Results: For capillary tubes embedded in air, the higher $it \times sub$ yielded the smaller FWHM values with more impact for PSF algorithms (OSEM+PSF and OSEM+PSF+TOF) relative to non-PSF algorithms (OSEM and OSEM+TOF). Moreover, using post smoothing filter introduced degradations in spatial resolution with more impact for higher $it \times sub$ values. For the NEMA phantom, by increasing acquisition times from 1min to 5min, intrinsic FWHM for $it \times sub = 32(54)$ was improved by 15.3% (13.2%), 15.1% (13.8%), 14.5% (12.8%) and 13.7% (12.7%) for OSEM, OSEM+PSF, OSEM+TOF and OSEM+PSF+TOF, respectively. Furthermore, for all reconstruction protocols and both low and high background activities, the FWHM values improved with more impact for higher $it \times sub$.

Conclusion: Our results indicate that PET spatial resolution is greatly affected by SBR, background activity and the choice of the reconstruction protocols. In addition, PSF algorithms yielded more improved FWHM relative to non-SPF algorithms for higher $it \times sub$ and SBRs. For a given reconstruction protocol and $it \times sub$, acquisition times ≥ 3 min lead to approximately the same spatial resolution values.

op 015

Thursday, November 28, 2019

13:45-14:00, side hall (laleh)

Deep learning-based attenuation and scatter correction of brain ¹⁸F-FDG PET images in image domain

Reza Jahangir, Alireza Kamali-Asl, Hossein Arabi

Department of Medical Radiation Engineering, Shahid Beheshti University, Tehran, Iran.

Division of Nuclear Medicine and Molecular Imaging, Department of Medical Imaging, Geneva University Hospital, CH-1211 Geneva 4, Switzerland

Background: Accurate attenuation and scatter correction (ASC) is necessary for reliable quantitative Positron emission tomography (PET) imaging. However, in PET/MRI or standalone PET scanners, due to the lack of transmission imaging, there is no direct solution for accurate ASC.

Objective: Recently, deep convolutional neural networks (DCNNs) have been widely employed in medical image processing, in general, and in PET imaging, in particular. This work investigates the joint ASC in the image domain for brain ¹⁸F-FDG PET images based on a DCNN approach, wherein the PET corrected for scatter and attenuation is directly estimated from PET non-attenuation corrected (PET-nonAC) without using any anatomical or transmission scan.

Methods: In PET/MR imaging, normally, a synthetic CT image is produced from the MR image, thereby performing the ASC within the PET reconstruction. However, in this study, the ASC is directly performed on PET-nonAC using a DCNN to generate PET_{DCNN} . To this end, a dataset of 80 brain ¹⁸F-FDG PET/CT scan (60/20 training/test) was used to train a high-resolution, compact residual convolutional network, and the resulting PET_{DCNN} images were evaluated against the reference CT-based ASC PET (PET_{CTASC}) as well as two-class MR-guided ASC PET (PET_{MRASC}). Radiotracer uptake differences between PET_{DCNN} and PET_{MRASC} and the reference PET_{CTASC} were computed for the entire brain region and 70 individual brain regions obtained from automated anatomical labels (AALs) across 20 test subjects. The accuracy of standardized uptake value (SUV) estimation in PET_{DCNN} and PET_{MRASC} was evaluated against the reference PET_{CTASC} using mean absolute error (MAE) and root mean square error (RMSE).

Results: The mean SUV bias percentages were $0.35\% \pm 1.16\%$ and $-16.62 \pm 1.13\%$ for PET_{DCNN} and PET_{MRASC} images against the reference PET_{CTASC} for the entire brain region, respectively. DCNN ASC method also demonstrated lower MAE = 0.07 ± 0.03 (SUV) and RMSE = 0.05 ± 0.02

(SUV) compared to $MAE = 0.58 \pm 0.10$ (SUV) $RMSE = 0.4 \pm 0.07$ (SUV) observed in PET_{MRASC} . Moreover, the mean SUV bias in PET_{DCNN} and PET_{MRASC} images across the 70 brain regions in 20 test subjects were $0.56\% \pm 1.22\%$ and $-16.42 \pm 1.32\%$, respectively.

Conclusion: We have demonstrated the feasibility of directly applying the attenuation and scatter correction on PET-nonAC images using a DCNN without using any additional anatomical information. The DCNN-based method would be able to offer a possible alternative to MR-guided ASC for hybrid PET/MRI and standalone PET scanners.

op 016

Thursday, November 28, 2019
14:00-14:15, side hall (laleh)

Quantitative evaluation of the MR-guided attenuation correction in brain SPECT imaging

Faeze Gholamian Khah, Samaneh Mostafapour, Hossein Arabi, Seid Kazem Razavi-Ratki, Ali Asghar Parach

Department of Medical Physics, Shahid Sadoughi University of Medical Sciences, Yazd, Iran
Division of Nuclear Medicine and Molecular Imaging, Department of Medical Imaging, Geneva University Hospital, CH-1211 Geneva 4, Switzerland
Department of Radiology, Faculty of Medicine, Shahid Sadoughi University of Medical Sciences, Yazd, Iran

Background: Attenuation correction plays a key role in both visual interpretation and quantitative analysis of emission tomography. Although transmission or CT-based attenuation correction methods are considered as gold standards, these approaches impose additional radiation dose on the patients. Recent studies have evaluated the reliability of attenuation correction using MRI images as an alternative method.

Objective: The current study was aimed to assess the accuracy of MR-guided attenuation correction (MRAC) in brain SPECT imaging wherein CT-based attenuation correction (CTAC) was considered as the ground truth.

Methods: Six subjects who had undergone $99m\text{-Tc}$ Ethyl-Cysteinate-Dimer SPECT, MRI and CT scan included in this study. CT-based AC map was obtained through mapping Hounsfield units into the attenuation coefficients equivalent to the energy of SPECT gamma photon via employing a bilinear model. In order to generate the MRAC map, MR images were segmented into bone, soft-tissue, and air, and then the related attenuation coefficients at the energy of 140 keV were assigned to the corresponding classes. CT and MRAC maps were aligned to $99m\text{-Tc}$ SPECT images by applying a nonrigid image registration algorithm. For evaluation of MRAC method, activity concentration (ACC) values were compared in 24 volumes of interests (VOI) per subject through correlation analysis and calculation of relative difference.

Results: Correlation analysis resulted in a coefficient equal to 0.71 which revealed a strong correlation between the two data series. Calculation of relative difference percentages, by considering the ACC values acquired from the CTAC method as reference, represented underestimation in ACC values related to MRAC. The underestimation was up to 3.6% in central regions of the brain and 5.4% in cortical regions.

Conclusion: Although data analysis showed underestimation in ACC values resulted from the MRAC approach, a strong correlation was observed between the results obtained from the two AC methods. Therefore, in addition to taking advantage of excellent soft-tissue contrast in MR images for diagnostic purposes, it can be used for generating attenuation correction map in brain SPECT studies to reduce the patient dose.

op 017

Thursday, November 28, 2019
14:15-14:30, side hall (laleh)

Joint compensation of motion and partial volume effects in oncologic PET/CT imaging

Sahar Rezaei, Pardis Ghafarian, Mehrdad Bakhshayesh-Karam, Arman Rahmim, Saeed Sarkar and Mohammad Reza Ay

Department of Medical Physics and Biomedical Engineering; Tehran University of Medical Sciences, Tehran, Iran
Research Center for Molecular and Cellular Imaging, Tehran University of Medical Sciences, Tehran, Iran

Chronic Respiratory Diseases Research Center, National Research Institute of Tuberculosis and Lung Diseases (NRITLD), Shahid Beheshti University of Medical Sciences, Tehran, Iran
 PET/CT and Cyclotron Center, Masih Daneshvari Hospital, Shahid Beheshti University of Medical Sciences, Tehran, Iran

Departments of Radiology and Physics, University of British Columbia, Vancouver, Canada
 Department of Integrative Oncology, BC Cancer Research Center, Vancouver, Canada

Background: The use of maximum standardized uptake value (SUV_{max}) is commonplace in oncology positron emission tomography (PET). Respiratory motion and partial volume effects (PVEs) are two of the most important causes of image degradation in lung cancer imaging, significantly hampering PET quantification. Furthermore, reconstruction algorithms have a significant impact on SUV_{max} , presenting a challenge for centers with varied protocols for lesion classification based on SUV_{max} .

Objective: The present study aims to assess the application of image-based deconvolution method to jointly compensate respiratory motion and PVEs for quantitative non-small cell lung lesions (NSCLC), in conjunction with four different iterative reconstruction algorithms.

Methods: An image-based deconvolution method that incorporated wavelet-based denoising within the Lucy-Richardson algorithm was proposed. The method was evaluated using phantom studies with signal-to-background ratios (SBR) of 4 and 8, and clinical data of 10 patients with 62 lung lesions. In each study, PET images were reconstructed using four different methods: OSEM with time-of-flight (TOF) information, OSEM with point spread function modeling (PSF), OSEM with both TOF and PSF (TOFPSF), and OSEM without PSF or TOF (OSEM). Coefficient of variation (COV) and maximum standardized uptake values (SUV_{max}) were measured within the tumors, and compared to images that were not processed using the joint-compensation technique.

Results: In phantom images, for all reconstruction methods, SUV_{max} were higher in the images processed using the proposed compensation technique, particularly in small spheres. Overall, the incorporation of wavelet-based denoising within the Lucy Richardson algorithm gave the best compromise between intensity recovery, noise attenuation and qualitative aspect of the images in all cases. In patient data, the median values of the relative difference (%) of SUV_{max} for the compensated images in comparison to uncompensated images were 43.0%, 42.5%, 44.8% and 42.6% for OSEM, PSF, TOF, and TOFPSF, respectively, in small lesions (equivalent diameter <10 mm), and 35.8%, 33.5%, 37.2% and 35.1% in average-sized lesions (equivalent diameter <30 mm).

Conclusion: The proposed joint comparison method can improve the accuracy of PET quantification by simultaneously compensating for respiratory motion and PVEs in lung PET/CT imaging. Both PSF and TOF algorithms resulted in notable variations of SUV_{max} in non-small cell lung lesions. In compensated images, TOF algorithms provided higher SUV_{max} in low-uptake and small lesions relative to non-TOF algorithms, especially in lower lung lobes. For average-sized lesions, all reconstruction algorithms performed approximately equally. Thus, one should be aware that quantitative analyses of lesions with varying sizes and locations, e.g., in radiotherapy or follow-up studies, maybe mainly affected by either PSF or TOF algorithms, when applying any compensation methods.

OP 018

Thursday, November 28, 2019
 14:30-14:45, side hall (laleh)

Harmonization of PET/CT quantitative values between multiple scanners: a phantom study

Habibeh Vosoughi, Parham Geramifar, Mohsen Hajizade, Farshad Emami, Arman Rahmim, Mehdi Momenzadeh

Department of Medical Physics, Mashhad University of Medical Science, Mashhad, Iran
 Nuclear Medicine Department, Razavi Hospital, Imam Reza International University, Mashhad, Iran
 Research Center for Nuclear Medicine, Shariati Hospital, Tehran University of Medical Science, Tehran, Iran

Departments of Radiology and Physics, University of British Columbia, Vancouver, Canada

Background: New generation of PET/CT systems support resolution modeling (PSF) and time of flight (TOF), enabling improved image quality and detectability; at the same time, advanced reconstruction algorithms having varying effects on quantification of PET images. PSF is available on major PET/CT systems and increases SUV values in comparison to conventional reconstruction (OSEM). There are significant variations in PET quantification due to differences in scanner

hardware and developed reconstruction algorithms, and as such, measured SUVs vary significantly. Consequently, harmonization of quantitative values derived from PET images has to be considered in multicenter studies.

Objective: The aim of the present study is to investigate harmonization of PET/CT systems with different performances to reduce inter- and intra-scanner variability in SUV values.

Methods: NEMA IQ phantom data acquisition was performed for low and high signal-to-background ratios (SBRs of 4:1 and 10:1) on four different scanners in Iran (siemens Biograph 6-TrueV, Biograph 6, and Biograph mCT and Discovery 690 from GE). Reconstruction parameters sets consisting of 6 different sub-iterations, 5 FWHMs for the Gaussian post smoothing filter, and different reconstruction types were evaluated towards finding optimized reconstruction. Curves for RC_{max} , $RC_{50\%}$ and RC_{peak} vs. diameter of sphere, as generated for each reconstruction, that met EARL specification reference value curves were selected as satisfying harmonization for the given reconstruction protocol. Finally, RCs, MCR (mean RC of all spheres sizes), COV_{MCR} , curvature and absolute error were compared between proposed reconstruction protocols for harmonization and those used in routine clinical reconstruction from all scanners.

Results: In this study measured RCs in proposed reconstruction methods for each scanner were compared with average of EARL reference value, and each of them exhibiting minimal RMSE (below 10%) was selected as harmonized reconstruction. Comparison between harmonized and routine clinical reconstruction showed that using harmonized reconstructions are more reproducible than others, especially for SBR 10:1; although overall contrast recovery was a little reduced, COV_{MCR} was decreased about 50% using harmonized reconstruction protocols. No significant difference in curvature and absolute error between harmonized and clinical routine reconstruction was observed in SBR 10:1, whereas in SBR of 4:1, $RC_{50\%}$ and RC_{max} were 10% and 20% higher respectively in harmonized reconstructions.

Conclusion: Harmonization of PET/CT systems equipped with different hardware and reconstruction algorithms such as PSF and/or TOF is conceivable. Using harmonized image reconstruction increases reproducibility of PET images.

OP 019

Thursday, November 28, 2019
14:45-15:00, side hall (laleh)

Comparison of state-of-the-art atlas-based bone segmentation approaches from brain MR images for MR-only radiation planning and PET/MR attenuation correction

Samaneh Mostafapour, Hossein Arabi

Department of Radiology Technology, School of Paramedical Sciences, Mashhad University of Medical Sciences, Mashhad, Iran

Division of Nuclear Medicine and Molecular Imaging, Department of Medical Imaging, Geneva University Hospital, CH-1211 Geneva 4, Switzerland

Background: MR imaging has emerged as a valuable tool in radiation treatment (RT) planning owing to its capability to provide high resolution anatomical images for precise organ/lesion delineation. Moreover, due to the superior soft-tissue contrast and non-ionizing radiation compared to the CT images, hybrid PET/MR scanners are being extensively used in clinical practice. Unlike CT images, there is no direct transformation between voxel intensity in MRI images into electron density; as such MR image can't directly be used for dose estimation and attenuation correction (AC). Bone extraction from MR images is the major challenge in MR-only RT planning as well as in PET/MR AC. In this regard, atlas-based methods have been extensively employed and exhibited promising performance in bone segmentation from MR images.

Objective: Since bone delineation plays key role in PET/MR AC and MR-only RT planning, we investigate the performance of the two state-of-the-art atlas-based bone segmentation approaches from brain MR images.

Methods: Bone segmentation was performed on 43 brain CT/MR image pairs using atlas-based local weighting (Atlas-LW) and atlas registration combined with pattern recognition (AT-PR) techniques. The former approach utilizes voxel-wise atlas fusion scheme based on the similarity of target MR and atlas MR images. The latter technique employs Gaussian process regress to estimate bone tissue from aligned atlas images. The accuracy of bone extraction performed by these two approaches was investigated for the entire bony structures as well as cortical bone using standard segmentation metrics such as Dice similarity (DSC). Moreover, the accuracy of the CT value

estimation from MR images was evaluated using mean absolute error (MAE) and root mean square error (RMSE).

Results: Overall, Atlas-LW technique exhibited higher segmentation accuracy resulting in $DSC=0.79\pm0.61$ and 0.84 ± 0.03 , while AT-PR method led to $DSC=0.72\pm0.8$ and 0.77 ± 0.05 for cortical and total bone, respectively. Moreover, Atlas-LW approach estimated CT values for total bone tissue with $MAE=17.6\pm138.0$ HU and $RMSE=466.2\pm75.00$ HU compared to $MAE=10.9\pm147.0$ HU and $RMSE=522.5\pm89.7$ HU obtained from AT-PR approach.

Conclusion: Both of the methods evaluated in this study demonstrated promising performance in bone segmentation from MR brain scan. However, the Atlas-LW exhibited superior results demonstrating its potential to be used in PET/MR AC and MR-only RT planning.

op 020

Thursday, November 28, 2019
15:00-15:15, side hall (laleh)

Estimation of normal-dose SPECT myocardial perfusion images from the corresponding half-dose images using deep learning

Narges Aghakhan Olia, Sanaz Hariri Tabrizi, Alireza Kamali-Asl, Parham Geramifar, Peyman Sheikhzadeh, Saeed Farzanefer, Behnoosh Teimourian Fard

Department of Medical Radiation Engineering, Shahid Beheshti University, Tehran, Iran
Research Center for Nuclear Medicine, Shariati Hospital, Tehran University of Medical Sciences, Tehran, Iran

Department of Nuclear Medicine, Vali-Asr Hospital, Tehran University of Medical Sciences, Tehran, Iran
Research Center for Molecular and Cellular Imaging, Tehran University of Medical Sciences, Tehran, Iran

Background: Single photon emission computed tomography (SPECT) is an essential modality in myocardial perfusion imaging (MPI). In Practice, to obtain high-quality MPI images for an accurate diagnosis, a prescribed dose of radioactive tracer should be injected. Alongside SPECT-MPI widespread use, concerns have been raised about the risks associated with patients' exposure to radiation from this imaging modality.

Objective: In order to comply with as low as reasonably achievable (ALARA) doses simultaneous with not compromising the image quality, we proposed a deep neural network as a post-processing tool to denoise half-dose images and estimate normal-dose ones in SPECT-MPI.

Methods: We acquired list-mode clinical data from 130 patients (79 females and 51 males) by the ProSPECT scanner, a dedicated cardiac SPECT (Parto Negar Persia, Iran). Normal-dose and half-dose images were reconstructed from the list-mode files using filtered back projection (FBP) algorithm. We proposed a convolutional neural network with 40 filters in each hidden layer to map half-dose images to normal-dose ones like the only similar work. 75% of the data was randomly assigned to the training set and the remaining to testing set while 20% of the training set was used as the validation set to tune the network hyperparameters. The network was implemented using the Keras library over TensorFlow in python 3.7.

Results: Root mean square error (RMSE), structural similarity (SSIM) index, and peak signal-to-noise ratio (PSNR) between the estimated normal-dose or half-dose images and the actual normal-dose images were computed. The following table shows that CAE could increase the PSNR and SSIM values by 10 % and 3%, respectively and RMSE decreased 34%.

Conclusion: Based on the improvement observed using a simple deep learning structure to estimate the high-quality images from the corresponding low-dose ones, deep learning shows its promising role in achieving further dose reduction in SPECT-MPI.

op 021

Thursday, November 28, 2019
15:15-15:30, side hall (laleh)

Dual-energy CT-based energy mapping for attenuation correction of pre-clinical micro-PET/CT imaging: A simulation study

Hojjat Mamizadeh, Hossein Ghadiri

Department of Medical Physics and Biomedical Engineering, Tehran University of Medical Sciences, Tehran, Iran

Research Center for Molecular and Cellular Imaging, Tehran University of Medical Sciences, Tehran, Iran
Preclinical Core Facility, Tehran University of Medical Sciences, Tehran, Iran

Background: Small animal PET imaging is frequently used in biomedical research and has gained recognition as a transitional pathway to human molecular imaging. Micro-PET is a quantitative imaging technique, capable to provide accurate values of radiotracer concentration. Several physical factors, such as Attenuation Correction (AC), must be taken into account, in order to obtain it. One of the methods to utilize AC is to use micro-CT images to obtain an attenuation map (AM), which is scalable to the PET energy (511 keV).

Objective: Our main objective in this study is to evaluate the accuracy of attenuation images obtained by two methods of converting micro-CT images, bilinear transformation and subtraction dual-energy micro-CT (DE-mCT) method, to gain AM and their effect on attenuation recovery (AR) in micro-PET images.

Methods: A NEMA-PET phantom consists of a Lucite cylinder with three cylindrical inserts that were simulated. The materials used in the simulation include soft tissue, lung, and bone. The micro-CT has been simulated by the general-purpose Monte Carlo N-Particle code (MCNP). The phantom was imaged in two simulated spectra by MCNP (80,100 kVp). To obtain the emission images, the micro-PET was simulated by Gate software. To obtain the AMs, micro-CT images were converted to attenuation images by bilinear transformation and DE-mCT methods. These images were converted to AC factors and then applied to PET images for AR. Also, an image was simulated in 511 keV energy for evaluation of the accuracy of the AMs obtained from these methods.

Results: The linear attenuation coefficients (LAC) values calculated using the two methods agreed with the attenuation image from the simulation in 511 keV. The measured LACs of lung and soft tissue in bilinear and DE-mCT approaches (0.019 cm⁻¹, 0.091 cm⁻¹, 0.0205 cm⁻¹, 0.0935 cm⁻¹, respectively) agree with their simulated values (0.021 cm⁻¹ and 0.0939 cm⁻¹, respectively). The measured LAC of bone (0.135 cm⁻¹) overestimated the calculated value of 0.13 cm⁻¹ by 3.8% in the DE-mCT method.

Conclusion: AC is just one of the many problems currently hindering absolute quantification of micro-PET images and all require continued investigation and improvement. The AM obtained by the DE-mCT method has less error than the bilinear approach, so DE-mCT has the potential to improve the accuracy of AC in micro-PET images.

ORAL PRESENTATIONS:

Third Session: Quantitative Analysis and Image Correction in Nuclear Medicine

Comparison between quantitative analysis and visual assessment of brain ¹⁸F FDG-PET/CT in temporal lobe epilepsy

op 022

Thursday, November 28, 2019
15:45-16:00, side hall (laleh)

Maryam Fallahpoor, Mohammad R. Nazem-Zadeh, Pardis Ghafarian, Jafar Mehvari Habibabadi, Seyed Sohrab Hashemi-Fesharaki, Mehرداد Bakhshayesh Karam, Mohammad Reza Ay

Research Center for Molecular and Cellular Imaging (RCMCI), Tehran University of Medical Sciences

Chronic Respiratory Diseases Research Center, National Research Institute of Tuberculosis and Lung Diseases (NRITLD), Shahid Beheshti University of Medical Sciences, Tehran, Iran

PET/CT and cyclotron center, Masih Daneshvari hospital, Shahid Beheshti University of Medical Sciences, Tehran, Iran

Department of Neurology, Isfahan Neurosciences research center, neurology department, Isfahan University of Medical Science, Isfahan, Iran

Pars Advanced Medical Research Center, Pars Hospital, Tehran, Iran

Background: In patients suffering from temporal lobe epilepsy (TLE), resective surgical treatment can be performed only if the epileptogenic origin of the seizure can be demonstrated. Therefore, it is of special importance to accurately determine the focus of the seizure with the most possible confidence. ¹⁸F-FDG PET is one of complementary imaging methods usually prescribed for patients with TLE that can detect asymmetric hypo-activities in focal epileptogenic area which MRI may not detect.

Objective: The present investigation was designed to establish the potential value of quantitative analysis of brain PET in temporal lobe epilepsy and the difference between quantitative analysis and visual assessment.

Methods: Sixty one patients with TLE were involved in this study. All subjects underwent preoperative imaging in a 3.0T Prisma MRI system using standardized protocol for image acquisition. T1-weighted images were acquired using three-dimensional magnetization prepared rapid acquisition GRE-MPRAGE- protocol. ¹⁸F FDG-PET images for the same patients are acquired by a GE Healthcare Discovery 690 PET/CT scanner. The brain structures are derived from the MR image and applied to the ¹⁸F FDG-PET images for regional statistics. We exploited PMOD software and human atlas of the maximum probability atlas Hammers N30R83 to perform the analysis. The amounts of uptake in right and left temporals, z-scores, and Asymmetric Index are calculated and compared to visual assessment of PET imaging. To add more confidence, we compared the results with patients' MRI medical report.

Results: From 61 PET scans, 31 are reported to have TLE involvement and 30 as normal. According to the results of quantitative analysis, 12 patients are determined to have TLE and 49 patients are normal. Of these, 10 were jointly reported to have TLE involvement in both methods and 28 were normal. 21 false negative and 2 false positive were reported. Based on the analysis, there was a significant relationship between the results of PET assessment and quantitative analysis (P-value = 0.012). Also, in the present study, the hippocampus on average had a greater effect on asymmetry between the right and left temporal lobes.

Conclusion: Quantitative analysis, may add confidence to pre-decision about brain ¹⁸F FDG-PET for TLE patients. Using PMOD software is user-friendly for analyses of the amount of activity in different region of the brain, and hence, is useful for finding the epileptogenic focus for in TLE. However, there is still a demand for performing this study for a larger number of patients.

op 023

Thursday, November 28, 2019
16:00-16:15, side hall (laleh)

Optimization of image reconstruction parameters in TOF/PSF-modeling of PET data due to different lesion sizes in NEMA phantom

Samira Rezvani, Pardis Ghafarian, Mohammad Reza Ay

Research Center for Molecular and Cellular Imaging/Tehran University of Medical Sciences, Tehran, Iran

Department of Medical Physics and Biomedical Engineering/ Tehran University of Medical Sciences, Tehran, Iran

Chronic Respiratory Diseases Research Center/ National Research Institute of Tuberculosis and Lung Disease (NRITLD)/ Shahid Beheshti University of Medical Sciences, Tehran, Iran

PET/CT and Cyclotron Center/Masih Daneshvari Hospital, Shahid Beheshti University of Medical Sciences, Tehran, Iran

Background: 18F-FDG PET/CT is an imaging method for tumor detection, treatment planning and patient follow up. PSF modeling and TOF technology help to improve image quality and precise quantitative analysis but if they are used in a correct way.

Objective: The aim of this study is evaluating the effect of different reconstruction parameters on image quality and quantification of tumors with different sizes.

Methods: In this study, we filled NEMA IQ phantom, which consists of different lesion size, with 18F-FDG in three-level background activity. Reconstructions were performed with HD (OSEM), HDS (OSEM+PSF), T (OSEM+TOF) and TS (OSEM+TOF) protocol, two iterations, different subsets (18, 24, 32 and 36) and Gaussian filter (with FWHM of 4.5, 5.5 and 6.4 mm). Image quality factors (noise, SNR, Contrast) and Quantitative parameters were calculated for all reconstructed images and lesion. Man Whitney and Kruskal Wallis tests were performed for the statistical test.

Results: When PSF-modeling added on reconstruction method, noise decreases 20-30% for OSEM protocol and 17-20% for OSEM+TOF protocol. However, Time of flight increases the noise, 5-10% when applied on OSEM and 7-20% for OSEM+PSF-modeling. SNR of the small lesion in high background activity were 2.5 ± 0.9 , 1.9 ± 1.3 , 1.4 ± 0.7 and 1.1 ± 0.8 in HD, HDS, T and TS respectively. SNR of the big lesion were 13 ± 1.5 , 16.8 ± 1.7 , 13.8 ± 2.1 and 17.7 ± 2.9 respectively for the mentioned protocols. When PSF-modeling or TOF or even both of them added to OSEM, the contrast of small lesions were decreased 5-10% but the contrast of big lesion when PSF-modeling added to OSEM 4.5% decreased, and when TOF added 8-10% contrast increased.

Conclusion: OSEM+PSF-modeling and OSEM+PSF+TOF protocol had more acceptable image quality and lesion detectability than OSEM and OSEM+TOF. TOF increase the noise when increasing the number of iterations, but depends on lesion size, it increases SNR for big lesion and decreases SNR for the small lesion. When PSF-modeling added to OSEM or OSEM+TOF protocol, the noise of images and SNR of the big lesions decreased but SNR of small lesions increased. SUV_{max}, SUV_{mean} behave the same as SNR for TOF and PSF-modeling according to lesion size in different protocols.

op 024

Thursday, November 28, 2019

16:15-16:30, side hall (laleh)

A new approach for attenuation correction of SPECT data in the dedicated cardiac ProSPECT scanner using emission data only

Getu F. Tadesse, Parham Geramifar, Mehrshad Abbasi, Behnoosh Teymourian, Mohammad Amin Izadi, Ali Salimi, Mohammad Reza Ay

Department of Medical Physics and Biomedical engineering, School of Medicine, Tehran University of Medical Sciences, Tehran, Iran

Research Center for Molecular and Cellular Imaging, Tehran University of Medical Sciences, Tehran, Iran

Research Center for Nuclear Medicine, Tehran University of Medical Sciences, Tehran, Iran

Department of Nuclear Medicine, Vali-Asr Hospital, Tehran University of Medical Sciences, Tehran, Iran

Department of Computer Science, Faculty of Science, Shahed University, Tehran, Iran

Department of Computer Engineering, Faculty of Information and Communication Technology, Imam Hossein Comprehensive University, Tehran, Iran

Background: It is well known that the ability to correct the effect of attenuation for cardiac emission data has tremendous importance to improve the clinical utility of the resulting reconstructed images. There are a few studies investigate the feasibility of attenuation correction using emission data only.

Objective: The purpose of this study is to develop a new way of generating attenuation coefficient map for cardiac SPECT images and generate attenuation corrected (AC) images.

Methods: The raw data of the dedicated cardiac ProSPECT scanner is reconstructed by in-house developed MLEM algorithm. The reconstructed images were coregistered with the anatomical digital XCAT phantom to determine the contour of the thorax region like soft-tissue, lung and bones. An attenuation coefficient map was generated to apply attenuation coefficient values for bone, soft tissue and lung in the energy window of 140 keV. This attenuation map used during image reconstruction for AC. Segmental myocardial counts in a 17-segment model were compared on the basis of paired T test. The attenuation corrected image by the new method was compared with the AC by CT scan (CTAC).

Results: We found insignificant difference between AC image by new method and CTAC ($p < 0.08$). Average myocardial perfusion count was significantly higher in AC images in comparison to non_AC in the septal and inferior regions ($p < 0.03$). However, average count was decreased in the anterolateral and apical regions in the AC images.

Conclusion: These results indicate that proposed method for AC using emission data only is a promising choice of AC and may be applied for ProSPECT scanner, without the need for separate transmission scan.

op 025

Thursday, November 28, 2019

16:30-16:45, side hall (laleh)

Evaluation of the effect of random coincidence rates on PET image quality

Mahak Osouli Alamdari, Pardis Ghafarian, Mehrdad Bakhshayesh Karam, Mohammad Reza Ay

Research Center for Molecular and Cellular Imaging, Tehran University of Medical Sciences, Tehran, Iran

Department of Medical Physics and Biomedical Engineering, Tehran University of Medical Sciences, Tehran, Iran

Chronic Respiratory Diseases Research Center, National Research Institute of Tuberculosis and Lung Diseases (NRITLD), Shahid Beheshti University of Medical Sciences, Tehran, Iran

PET/CT and Cyclotron Center, Masih Daneshvari Hospital, Shahid Beheshti University of Medical Sciences, Tehran, Iran

Background: PET-CT imaging is a subset of nuclear medicine devices. This device provides the functions of two separate PET and CT units in one set. The PET system provides high-quality images of the human body's metabolism. The emission of positrons is a Poisson distributed random process. Therefore, PET is a statistical imaging technique, where the presence of noise is inevitable. The PET coincidence events are categorized into the real and background coincidences. The latter are distinguished as either accidental (or random) coincidences where the two photons did not arise from the same annihilation event. It is not feasible to compute accurate estimates of activity distributions within a patient using PET unless the effects of accidental coincidences are quantitatively taken into account.

Objective: In this study, we investigated the effect of random coincidence rates on image quality parameters, including contrast, signal to noise ratio (SNR), and standard uptake value (SUV) in the phantom study.

Methods: Discovery-690 PET/CT scanner was used in this study. We used two different lesions to background ratios, 4:1 and 2: 1 with the activity of 3.96 and 2.86 mCi, respectively. In both cases, the phantom was placed in the center of the FOV and scanned in a single bed position for 3 minutes. This imaging was repeated 22 times, with 10–20 minutes' intervals between each imaging. The purpose of repeated imaging was to investigate image quality parameters at different random coincidence rates. In each imaging, we recorded the random and true coincidence rates, image quality parameters, including contrast and SNR and SUV, then they were calculated at each imaging. Finally, the changes in image quality parameters were evaluated in terms of random coincidence rates in both lesions to background ratio.

Results: The results of this study indicated that SNR, SUV, and contrast were almost constant with the change of random coincidence rates in activities up to about 4 mCi. The results also show that with the change of the lesion to background ratio, there is no change in the effect of random coincidences on the image quality parameters.

Conclusion: From this study, we concluded that up to the activity of 16.2 kBq/cc in the phantom study, the image quality parameters do not change significantly with the change of random coincidence rates. Changes in image quality parameters in the higher activity range must also be evaluated.

PET/CT radiomics-based machine learning model for survival prediction of non-small cell lung cancer patients

Ghasem Hajianfar, Isaac Shiri, Hossein Arabi, Parham Geramifar, Mehrdad Oveisi, Habib Zaidi

Rajaie Cardiovascular Medical and Research Center, Iran University of Medical Science, Tehran, Iran

Department of Nuclear Medicine, Vali-Asr Hospital, Tehran University of Medical Sciences, Tehran, Iran.

Division of Nuclear Medicine and Molecular Imaging, Geneva University Hospital, CH-1211 Geneva 4, Switzerland

Research Center for Nuclear Medicine, Tehran University of Medical Sciences, Tehran, Iran

Department of Computer Science, University of British Columbia, Vancouver BC, Canada

Geneva University Neurocenter, Geneva University, Geneva, Switzerland

Department of Nuclear Medicine and Molecular Imaging, University of Groningen, University Medical Center Groningen, Groningen, Netherlands

Department of Nuclear Medicine, University of Southern Denmark, Odense, Denmark

Background: Lung cancer is one the most prevalent cancers worldwide. Non-small cell lung cancer (NSCLC) accounts for 85% of lung cancers with varying disease stages. Different biomarkers, such as genomic, proteomic are available for prognostic assessment; however, they are invasive. Radiomics analysis enables prediction of survival of NSCLC patients.

Objective: The main aim of the current study was to investigate radiomics efficiency in survival prediction of NSCLC patients using PET/CT images.

Methods: We used data of 138 NSCLC patients (114 patients in training dataset and 24 patients as external validation dataset) consisting of PET and low-dose CT images. Tumors were segmented on

op 026

Thursday, November 28, 2019
16:45-17:00, side hall (laleh)

PET images (with the aid of CT images). Three image pre-processing procedures, including bin discretization, Laplacian of Gaussian (LOG) and Wavelet transform were applied to PET and CT images. Three thousand and five hundred radiomic features were extracted from the different images. Features with correlation over 90% were removed. Subsequently, Least Absolute Shrinkage and Selection Operator (LASSO) feature selector was applied on the extracted features. Random Survival Forest (RSF) as a survival predictor was used. Performance of RSF model was evaluated using the Concordance index.

Results: Among radiomic features, the LASSO feature selector narrowed down to 12 features extracted from PET and CT images. The concordance index of the RSF model in the training dataset with 100 bootstraps was 0.76 (95% confidence interval: 0.75 - 0.77) whereas it was 0.65 in the test dataset.

Conclusion: These findings suggested that machine learning-based PET/CT radiomics model enables effective prediction of survival rate in NSCLC patients which can aid in monitoring the treatment of patients with early-stage NSCLC.

op 027

Thursday, November 28, 2019
17:00-17:15, side hall (laleh)

The impact of different reconstruction protocols on ⁶⁸Ga-PSMA PET-CT image quality

Zohreh Shahpouri, Pardis Ghafarian, Mehrdad Bakhshayesh-Karam, Mohammadreza Ay

Research Center for Molecular and Cellular Imaging, Tehran University of Medical Sciences, Tehran, Iran

Chronic Respiratory Diseases Research Center, National Research Institute of Tuberculosis and Lung Diseases (NRITLD), Shahid Beheshti University of Medical Sciences, Tehran, Iran
PET/CT and Cyclotron Center, Masih Daneshvari Hospital, Shahid Beheshti University of Medical Sciences, Tehran, Iran

Department of Medical Physics and Biomedical Engineering, Tehran University of Medical Sciences, Tehran, Iran

Background: Prostate cancer is one of the most frequent malignancy and main cause of cancer deaths in men. Nowadays, ⁶⁸Ga-PSMA PET-CT has made a tremendous evolution for the radiotherapy management of metastases and standard imaging in prostate cancer

Objective: The aim of this study is to evaluate the influence of different image reconstruction method in ⁶⁸Ga-PSMA PET/CT image quality.

Methods: The study consisted of retrospective reconstruction and analysis of 10 PET/CT examinations acquired 60±9 min uptake time and 2 MBq/kg administrated with ⁶⁸Ga-PSMA. OSEM+PSF, OSEM+PSF+TOF and OSEM+TOF methods were applied. 2 iterations (TOF) and 3 iterations (non TOF) with 18 subsets, 6.4 and 5mm Gaussian post-processing filter were also used for data reconstruction. The image quality was evaluated in terms of signal-to-noise ratio (SNR) and signal-to-background ratio (SBR) and SUV_{max} for all lesions. The image noise level was calculated in gluteal muscle by placing 10 spherical volume of interest (approximately 3 cm in diameter) in the gluteal tissue and defined as the mean standardized uptake value (SUV_{mean}) divided by the standard deviation. All data normalized to our routine method (OSEM+PSF, 6.4 mm Gaussian filter).

Results: SUV_{max} was 5.58 ± 0.86 (Range, 1.1-38.6) for OSEM+PSF and increased to 5.65 ± 6.63 (Rang, 1.3-40.0) for OSEM+PSF+TOF, but decreased to 5.11 ± 0.94 (Range, 1.2-35.1) for OSEM+TOF method. In compared with the routine method, the mean SNR decreased to 0.88±0.15 by OSEM+TOF and improved 1.04±0.16 by OSEM+PSF+TOF, whereas the mean SBR increased to 1.16±0.16 and 1.08±0.18 for mentioned protocol, respectively. Also, in the 5 mm Gaussian filter versus to 6.4 mm, the mean SBR increased to 1.20±0.03 by non TOF method and improved 1.18±0.05 and 1.28±0.04 by OSEM+TOF and OSEM+PSF+TOF methods. It was interesting that noise level was level 2.77%, 2.71% and 2.92% for OSEM+PSF and OSEM+TOF and OSEM+PSF+TOF respectively.

Conclusion: In comparison to our routine method, higher SUV_{max} was seen for OSEM+PSF+TOF that was in contrast to OSEM+TOF. Even though OSEM+PSF+TOF method makes little more noise versus to OSEM+TOF and OSEM+PSF methods, higher signal to background ratio illustrated in TOF methods in Ga-PSMA PET/CT imaging. Lesion detectability was increased by applying Gaussian filter 5 mm vs. 6.4 mm. Signal to background ratio was improved by TOF methods with the highest SBR was obtained by OSEM+PSF+TOF.

Physics (Posters)

p 001 **Monte-Carlo based assessment of ^{99m}Tc (DMSA, MAG3 and DTPA) dosimetry in renal pediatric SPECT imaging.**

Zeynab Khoshyari Morad, Hashem Miri Hakimabad, Najmeh Mohammadi, Reza Jahangir

Faculty of Science, Ferdowsi University of Mashhad, Mashhad, Iran
Department of Medical Radiation Engineering, Shahid Beheshti University, Tehran, Iran

Background: Nuclear medicine has played an important role in the management of various renal diseases in children. A wide variety of nephron-urological conditions can be diagnosed and evaluated using renal SPECT imaging methods. Children are generally at greater risk of radiation exposure due to their greater sensitivity to the radiation and the longer time frame after exposure during which effects can manifest themselves. Therefore, evaluating the absorbed dose on them has great importance to avoid secondary failure.

Objective: Assessment of the patient's risk for either acute effects or secondary cancer induction begins with detailed knowledge of the radiation absorbed dose on individual tissues and organs. Therefore, in this work organ radiation doses were calculated for common radiopharmaceuticals which were used in children with kidney disease including ^{99m}Tc dimercaptosuccinic acid (^{99m}Tc-DMSA), ^{99m}Tc mercaptoacetyltriglycine (^{99m}Tc-MAG3) and ^{99m}Tc diethylenetriaminepentaacetic acid (^{99m}Tc-DTPA).

Methods: The absorbed dose in patients experiencing diagnostic examinations in nuclear medicine is obtained through calculations which are based on models of the human body and the radiopharmaceutical behavior in the body. Accordingly, in this work, we employed three pediatric tomographic voxel phantoms of different ages in normal renal function, for use in the Monte Carlo radiation transport simulations. All simulations were carried out using Monte Carlo n-particle (MCNP) transport code. The accuracy of dosimetric results was evaluated against the data, reported by the international commission on radiological protection (ICRP).

Results: The highest and lowest dose to the kidney was 0.43 mGy/MBq and 0.0042 mGy/MBq obtained for 4-years old and 14-years old children when ^{99m}Tc-DMSA and ^{99m}Tc-MAG3 were used as a radiopharmaceutical, respectively. Moreover, in such cases, the relative errors of simulation results against the reference ICRP data were 12.1% and 0.95%, respectively.

Conclusion: The results of our study demonstrated that absorbed dose on kidneys is highly dependent on the age of the children. Moreover, the dose absorbed by kidney is larger when ^{99m}Tc-DMSA is used. On the other hand, the smaller dose is obtained when ^{99m}Tc-MAG3 is used during the normal renal function study. In addition, the simulation results showed a good agreement with ICRP data.

p 002 **Selection of optimized energy for ¹⁷⁷Lu in radionuclide therapy of neuroendocrine Tumors: A simulation study**

Milad Peer Firouzjaei, Mohammad Ali Tajik Mansoury

Department of Medical Physics, Semnan University of Medical Sciences, Semnan, Iran

Background: The use of ¹⁷⁷Lu-labeled peptides is an effective method for the treatment of neuroendocrine tumors. Simulation studies performed for tumor dosimetry are used to evaluate the doses reached to tumors of different sizes from different ¹⁷⁷Lu energy modes, such as complete spectrum, beta particle spectrum and average energy of beta particles, i.e. monoenergetic.

Objective: This study aims to make a comparison for each of these energy modes for treatment of tumors of different sizes to investigate the average dose, uniformity of dose reached to tumors, and simulation time by using the Monte Carlo GATE code.

Methods: In this study, simulations were performed using the GATE Monte Carlo code (version 7.2). During this work, tumors modeled as spheres of different sizes (radius 0.5 to 20 mm) and the ¹⁷⁷Lu radionuclide was uniformly distributed in the tumor with complete and beta particle spectrum and average energy of beta particles (monoenergetic). Results have been reported as the average dose, simulation time and the uniformity of the dose reached to tumors and plotted over sizes and modes of radiation energy.

Results: The average dose of all tumor sizes in the monoenergetic modes is greater than the beta spectrum and the beta spectrum is greater than the full spectrum of ^{177}Lu . simulation time for tumor radius smaller than 2 mm in monoenergetic mode, complete spectrum and beta particle spectrum, is respectively from more to less; but for radius larger than 2 mm simulation time for complete spectrum, monoenergetic and beta particle spectrum are respectively from more to less. Flatness in tumor radius smaller than 10 mm in complete spectrum, beta particles spectrum and monoenergetic radiation are respectively from more to less; but in tumor radius larger than 10 mm, it's the opposite.

Conclusion: Since simulation for tumor dosimetry in complete spectrum mode takes the most time, we can perform simulations using beta spectrum or monoenergetic mode, which takes less time and apply the error coefficient to the uniformity and average dose to obtain the real data of the complete spectrum of ^{177}Lu .

p 003

MRI-based pet attenuation-correction on PET/MR brain prototype

Alireza Sadre Momtaz, Mohammad Babee Ghane

Department of Physics, Faculty of Science, University of Guilan, Rasht, Iran

Background: While the combination of PET and CT was relatively straight-forward in that the two components were merged in a sequential design, the combination of PET and MRI proved more challenging due to the mutual interferences.

Objective: In this work, the challenges and requirements for implementing an MRI-based AC method for the Siemens MR- PET brain prototype were investigated. In particular, the need for identifying the bone for accurate PET data quantification in brain structures was studied in simulations using segmented MR and CT images.

Methods: A prototype MRI-compatible PET scanner designed to fit inside the MAGNETOM Trio, a total-imaging-matrix system 3-T human MRI scanner. This PET scanner—called Brain PET—uses magnetic field-insensitive avalanche photodiodes as scintillation photon detectors.

Results: The air–bone tissue segmentation problem is approached differently in the 2 approximate MRI-based AC methods. In the MRI first model, the bone tissue is misclassified as air, whereas in the MRI second model the voxels corresponding to bone tissue and some thin air cavities are misclassified as water. The MRI first method leads to moderate overall underestimation of the activity and large underestimation in structures adjacent to bone. The MRI second method leads to a moderate overall underestimation in most brain structures but also to a severe overestimation in structures adjacent to real air cavities filled by the morphologic filter. The CT segmented model estimates accurately (within 5%, compared with the CT scaled model) the activity concentrations in most of the brain structures.

Conclusion: Attenuation correction is a mandatory step not only for obtaining quantitative data but also for performing meaningful qualitative image interpretation in PET studies. In this work, segmented CT was proposed as the silver standard for segmented MRI-based AC. For accurate AC in neurologic studies performed using the integrated MR- PET scanner, 3 compartments must be identified: water- based structures, bone tissue, and air-filled cavities. The most challenging task—the discrimination of bone tissue from air cavities—can be achieved using the proposed DUTE sequence. In addition, the attenuation of the radiofrequency coil has to be accounted for. An MRI DUTE-based AC method that considers all these aspects could, in principle, provide an estimation of the radiotracer concentration in a particular voxel as accurately as could the silver standard. Implementing an accurate MRI-based AC method is essential for the wide acceptance of this new imaging modality and will allow us to take advantage of the augmented quantitative capabilities of the combined MR-PET scanner.

p 004

Calculation of organ S-value for targeted radionuclide therapy (TRT) of head and neck cancer: Simulation Study

Amine Rajabi, Hossein Rajaie, Mohammad Ali Tajik-mansoury, Maryam Rezaei

Faculty of Medical Sciences, Department of Medical Physics, Tarbiat Modares University, Tehran, Iran

Faculty of Medical Sciences, Department of Medical Physics, Semnan University, Semnan, Iran

Department of Radiation Sciences, Faculty of Paramedicine, Yasuj University of Medical Sciences, Yasuj, Iran

Background: in targeted radionuclide therapy (TRT) of head and neck cancer calculation of organ s-value is an essential parameter for treatment planning and we need to assess the organ doses in sub-regions of brain to understand associated risks and optimize the clinical procedures.

Objective: the aim of this work is estimation of head phantom s-values for radionuclides.

Methods: in this study we used gate monte carlo code and zupal head phantom (based mr images that contains 63 segmented sub- regions) for simulation. the activity was assumed uniformly distributed in the source organs and simulation was performed for i-131, re -188, re-186,y-90. the results report as s-value's and compared with the mird published data.

Results: we tabulated a set of s-values calculated for the computational zupal head phantom and compare it with the mird (1999) and proportional error reported. results of comparison demonstrated 100% difference in maximum value, in many cases the zupal phantom resulted in smaller s-values and statistical analysis demonstrated significant differences of s-value(as much as 100%).

Conclusion: since we can conclude for targeted radionuclide therapy (trt) of head and neck cancer, patient specific dosimetry is an essential role for administered activity in treatment planning and mird published data must be revised for general application.

p 005

Multi-energy x-ray beam generation through selective filtering mechanism for accurate tissue decomposition and dosimetry in small animal CT and PET/CT imaging

Vahid Lohrabian, Alireza Kamali-Asl, Hossein Ghadiri, Hossein Arabi, Habib Zaidi

Department of Medical Radiation Engineering, Shahid Beheshti University, Tehran, Iran

Medical Physics and Biomedical Engineering Department, and Research Center for Molecular and Cellular Imaging, Tehran University of Medical Sciences, Tehran, Iran

Division of Nuclear Medicine and Molecular Imaging, Department of Medical Imaging, Geneva University Hospital, CH-1211 Geneva 4, Switzerland

Background: The alteration of the energy spectrum of the x-ray beam when photons pass through the absorbing medium carries beneficial information about the materials with different elemental compositions. Therefore, the differentiation between multiple materials would be possible provided that energy-dependent absorption characteristics of the materials can be individually measured. In this regard, dual- or multi-energy CT imaging enables accurate tissue/material decomposition by energy-dependent analysis of photon interactions within the absorbing medium. This allows accurate absorbed dose estimation in PET/CT imaging through accurate quantification of the mass density of the materials.

Objective: The purpose of this work is to upgrade the existing pre-clinical mono-energy micro-CT scanner [1] to a hybrid multi-energy x-ray and PET imaging system through applying a selective filtering mechanism to channelize the energy spectrum of the x-ray beam.

Methods: To this end, the preclinical micro-CT system with variable resolution capability was simulated using Monte Carlo (MC) techniques to determine the optimum properties of x-ray filters to generate the desirable x-ray energy spectrum. The results obtained from MC simulations were empirically validated via measurement of the resulting x-ray spectra after passage through the designed x-ray filters by using a high energy-resolution HPGe detector. Empirical measurement was also performed on the micro-CT scanner to assess the accuracy of the MC simulation results.

Results: Through MC simulations and empirical measurements, two different x-ray filters were designed to generate three different x-ray spectra with tube potentials of 40 kVp, 80 kVp and 120 kVp. The spectra obtained from MC simulations and experimental measurement exhibited close agreement with less than 6% relative difference.

Conclusion: MC simulations and empirical measurements demonstrated the feasibility of the x-ray beam alteration into desirable energy spectra. As such, the micro-CT scanner would be able to effectively discriminate different tissue types through joint material- and energy-dependent analysis. This allows accurate material specific imaging and accurate dosimetry in PET/CT imaging.

p 006

Investigating effective parameters of pinhole collimator in SPECT imaging system for small FOV objects

Alireza Sadremomtaz, Maryam Saed

Department of Physics, Faculty of Science, University of Guilan, Rasht, Iran

Background: In the SPECT Scanners, the relationship between sensitivity and resolution has always been challenging. In recent years, pinhole collimator has been used in small animals imaging. The spatial resolution in this model of collimator has been improved and it is in millimeters range, but its small FOV is the big problem of pinhole collimator, which is used to increase the sensitivity and maintain the desired resolution of multi pinhole collimators.

Objective: The aim of paper is the creation of a balance between resolution and sensitivity in the SPECT system by optimization of geometric parameters in the multi-pinhole collimator.

Methods: In this paper, we investigated the parameters that are effective in pinhole collimator in order to capture an image of small targets in such a way that there is a balance between resolution and sensitivity. Pinhole collimator geometry is an important factor in image quality and plays a key role in SPECT imaging. The important variables to be considered in pinhole collimator are as follows: 1) magnification 2) pinhole diameter 3) Acceptance angle aperture 4) collimator thickness 5) pinhole position and tilted angle.

Results: According to our studies, it is understood that the desirable number of pinholes may vary for different pinhole structures due to differences in sampling and overlapping of projections.

Results show that the maximum sensitivity value is obtained at a large pinhole acceptance angle (α) and with a large pinhole physical diameter (d). The effect of increasing pinhole diameter also applies to increasing resolution, but increasing the pinhole angle results in a weakening of the resolution.

Conclusion: Therefore, an interaction can be established between the resolution and the sensitivity in the SPECT system with the multi pinhole collimator by optimizing these geometric parameters, and the multi pinhole collimator can be a very suitable option for the SPECT scanning system when we have a small field of view.

p 007

Accuracy evaluation of ICRP's radiation protection guidelines in Semnan's Raaheeseman nuclear medicine center (2018-2019)

Nader Asadian, Mohammad Ali Tajik Mansoury, Fatemeh Pazooki, Elham Kashian

Department of Medical Physics, Semnan University of Medical Sciences, Semnan, Iran
Raaheeseman Center of Nuclear Medicine, Semnan University of Medical Sciences, Semnan, Iran

Background: By the expansion of clinical nuclear medicine and its significance in the procedure of therapeutics and diagnostics of disease, presence of the unsealed radionuclide leading to the importance of radiation protection in nuclear medicine centers. So need for more control and survey of the environment in different parts of the nuclear medicine centers seems to be necessary more than before.

Objective: Therefore, the aim of this study was to investigation and observation of the principles of radiation protection in the nuclear medicine center of Semnan city and its compliance with reference guidelines.

Methods: Dose rate in different rooms was measured using DGM 1500 Turva dosimeter over a 1 year period (2018-2019). Mean dose rate was calculated with SPSS 2016 and compared with International Commission on Radiological Protection (ICRP) guidelines.

Results: Using the statistical methods, it was determined that the highest and lowest mean dose rate, is related to the Hot-Lab room (0.40 $\mu\text{Sv/h}$) and Scan room (0.12 $\mu\text{Sv/h}$, respectively).

Conclusion: Measurement and analysis of data showed that the principles of radiation protection in the nuclear medicine center of Semnan was in agreement with ICRP guidelines.

Comparative evaluation of novel multi-atlas based segmentation methods for MRI-guided radiotherapy treatment planning and PET-MRI attenuation correction in pelvic region

p 008

Reza Jahangir, Alireza Kamali-Asl, Hossein Arabi

Department of Medical Radiation Engineering, Shahid Beheshti University, Tehran, Iran
Division of Nuclear Medicine and Molecular Imaging, Department of Medical Imaging, Geneva University Hospital, CH-1211 Geneva 4, Switzerland

Background: Magnetic resonance imaging (MRI)-guided attenuation correction (AC) of positron emission tomography (PET) data and/or radiation therapy (RT) treatment planning is challenged by the lack of a direct link between MRI voxel intensities and electron density. Therefore, a pseudo-computed tomography (CT) image generation from MRI is highly crucial for PET/MRI AC as well as MRI-guided RT planning.

Objective: Bone extraction from MR images is the major challenge in MRI-guided RT planning as well as PET/MRI AC [2]. As such, to extract bone in pelvic region, we quantitatively investigate five novel multi-atlas based MRI-guided pseudo-CT generation methods showing promising performance in literature.

Methods: In the atlas-based methods, an atlas dataset was registered to a target MR image by calculating the deformation field between the atlas MR images and a target MRI. Then, given the transformation matrices, the corresponding atlas CT images were warped to the target MR image. Lastly, the transformed atlas CT images were fused to generate a pseudo CT pertinent to the target MR image. In the CT fusion step five different schemes were evaluated: the voxel-wise weighted method, top 10 atlases and overall average, MaxProb method (voxel-wise maximum probability intensity averaging approach) [and bone-enhanced method. A database of 39 MRI/CT image pairs was used in this work. The resulting bone segmentations were compared with manual reference segmentations using Dice similarity coefficient (DSC). Moreover, the accuracy of CT value estimation for bone tissue was evaluated using mean absolute error (MAE) and root mean square error (RMSE).

Results: The MaxProb showed higher segmentation accuracy resulting in DSC of 0.75 ± 0.06 and 0.85 ± 0.03 for cortical and total bones respectively. On the other hand, Overall average and top 10 showed the lowest accuracy with $DSC=0.67 \pm 0.08$ and 0.79 ± 0.04 respectively. Bone-enhanced method scored the best performance in terms of accurate estimation of CT values with a $MAE=150.44 \pm 67.49$ HU and 118.44 ± 30.89 HU and RMSE of 313.44 ± 111.54 HU and 187.37 ± 48.55 HU for cortical and total bones respectively. Overall average and MaxProb methods led to the highest error with $MAE=322.03 \pm 149.66$ HU and 181.29 ± 74.21 HU and $RMSE=590.04 \pm 196.40$ HU and 353.71 ± 100.49 HU, respectively.

Conclusion: Except overall average and top 10 approaches, the rest of methods evaluated in this work showed promising results for both cortical and total bone segmentation in pelvic region. Nevertheless, altogether, the bone-enhanced approach exhibited superior performance in terms of both bone segmentation and CT value estimation with tolerable error in the context of PET/MR AC and MR-guided RT planning.

p 009

Simulation of long-lived activation products in nuclear reactor biological shield by MCNP and ORIGEN-S codes

Alireza Sadrmomt, Mohammadreza Kazemiyan haghghat, Aryan Nikrah

Medical Physics Department, Faculty of Science, University of Guilan, Rasht, Iran

Background: Radiation protection issue has high importance from beginning of nuclear technology the term bio-protection refers to an absorbent mass or substance that is placed around a reactor or radionuclide source in order to reduce radiation to a safe level for humans.

Objective: The purpose of this paper is to investigate the shielding properties and calculate the neutron attenuation coefficient of concrete with additive polyethylene, serpentine and magnetite iron using MCNP code. The time required for each of these compounds to reach the purity level determined by the Agency is then examined by the ORIGEN-S code

Methods: MCNP code was used to perform the simulation, in this study, the concrete bio-shield was cylindrical with a radius of 5cm and a thickness of 30 cm. The shield was divided into 2cm thick sections to calculate the neutron flux at any given depth. The source is 1MeV, 10KeV, 1KeV, 100eV, 10eV. Six compounds were used as the structure for the concrete, consisting of 1-ordinary concrete, 2-concrete with 1% by weight of boron B1, 3-concrete with 2% by weight of boron B2, 4-concrete with 1% by weight of boron and 4% by weight of polyethylene B1P4, 5- concrete with 1 wt% boron and 10 wt% polyethylene, 6- concrete with serpentine additive and concrete with magnetite iron additive.

Results: the neutron attenuation coefficient of each concrete was obtained. The value obtained for ordinary concrete is in good agreement with the experimental value obtained in the sources and in this respect the accuracy of the simulation is confirmed. From the second part of the study, the output of ORIGEN-S code was calculated as the activity of different concrete compounds after 60 years of irradiation and then after 6 and 25 years of cooling at 10, 20 and 30 cm depth of shield. Responses to common questions is very good for determining the accuracy of the study.

Conclusion: Of the three most important parameters in bio-shielding design, namely 1- protection (neutron attenuation coefficient) 2- low activity and 3- rapid purity, this study shows that B1P4 concrete can be better than other types of concrete and as suitable bio-shield in Reactors and nuclear power plants.

p 010

Dose calculation of lu-177 & Ra-223 for treatment of bone metastases using MCNPX code

Alireza Sadremomtaz, Maryam Tajadod

Department of Physics, Faculty of Science, University of Guilan, Rasht, Iran

Background: In treating cancer by means of radiotherapy, determining the dose of tissues involved is one of the most vital steps in the treatment protocol using radiopharmaceuticals that are absorbed by bone is crucial in treating treatment of bone metastases.

Objective: The aim of this work is to find the radial dose distribution and cumulative dose and differential dose for Lu-177 and Ra-223 at the involved tissues metastases

Methods: By the use of mcnp computer code, a model for bone phantom was designed and dose values were measured in this phantom

Results: The results showed that the Ra-223 that is an alpha emitter radiopharmaceutical with shorter range than Lu-177 which is beta emitter, has very little effect on bone marrow and soft tissue and leaves the highest absorbed dose in the bone where the source is located. But, the behavior of the two radiopharmaceuticals in gamma irradiation is different. Ra-223 produces the highest absorbed dose in bone marrow and soft tissue due to higher amounts of gamma energy.

Conclusion: Therefore, it is recommended that Ra-223 is a better choice than Lu-177 in the treatment of bone metastases causes by prostate and breast cancers because it leaves a large volume of dose solely in the bone.

p 011

Evaluation of microsphere brachytherapy dosimetry in liver lobular structure for ³²P and ⁹⁰Y microsphere with use of mcnp2.6 code

Mohadeseh Zadnorouzi, Alireza Sadremomtaz

Faculty of Basic Science, University of Guilan, Rasht, Iran

Background: Microsphere brachytherapy is one of the proper methods for liver cancer treatment in which the optimum value of dose is obtained by damaged tissue. Because of the non-uniform distribution of microspheres in the liver structure, there is a need to study the absorbed dose values in small structures. Evaluation of liver lobular model helps to evaluate the details of dose distribution in small structures and their relationship to dose effects.

Objective: The aim of the present study was to evaluate and compare the absorbed dose values of ³²P and ⁹⁰Y microspheres in liver lobular structure using MCNPX2.6 code.

Methods: In order to investigate the absorbed dose in the structure of the liver, the liver was simulated as a 3- dimensional hexagonal structure with a portal tract with specific dimensions at each corner of the lobule and a vein in the center of the lobule. Also, the structure of several lobules was simulated together to investigate the dose changes. Absorbed dose values were evaluated in the areas of the portal tract, central vein and lobular tissue. F6 tally was used to calculate absorbed dose values in the present work.

Results: The investigation in the present work showed a rapid decrease in the absorbed dose around each portal tract in which the source was located. Comparison of absorbed dose values for one lobule and several adjacent lobules showed a significant difference.

Conclusion: Investigation in this work have shown that a large fraction of the emission energy from microsphere sources is deposited into the portal tract area. Also, because of localization of microspheres in the corner of hexagonal structure, absorbed dose rate was increased in central vein and lobular tissue. Absorbed dose values were significantly increased when several adjacent lobules were considered relative to one lobule, due to the penetration of the emission particles of adjacent lobules into each other due to the multiplicity of beta particles range compared to width of one lobule that results in higher energy deposition per lobule.

p 012

Calculation absorbed dose for some radiopharmaceuticals in digital human phantoms with Monte Carlo code

Ali Farmahini Farahani, Alireza Sadremomtaz

Department of Physics, University of Guilan, Rasht, Iran

Background: In recent years, one of the most common diseases, which increased mortality in human societies, is cancer. With the advancement of nuclear medicine, there were several ways to diagnose and treat various types of cancers. In this area, the radiolabeled drugs and the dose received by the patient for diagnostic and therapeutic purposes is important therefore, individual dosimeters are very important.

Objective: The purpose of this work is determine absorbed doses from four radiopharmaceuticals in digital human phantoms .This is an introduction to calculating individual patient dosimetry and increasing treatment accuracy.

Methods: We use Monte Carlo code (GATE) and digital phantoms (Zubal and Xcat) to calculate internal dose for some radiopharmaceuticals in some critical organs.

Results: The results of the simulations were in good agreement with the published values of the MIRDCOMMITTEE, but the main problem with these methods is the high computational time that if we reduce the computational time by other methods, these techniques and experimental studies can help to improve accuracy in individual therapy.

Conclusion: In this study, we used the Monte Carlo code to measure the dose received in some organs for some radiopharmaceuticals. By completing these studies using experimental results we can provide a solution to increase the accuracy of treatment. We are conducting empirical studies to provide new solutions.

p 013

Fatal cancer risks associated with myocardial perfusion imaging in Yazd province, Iran

Mohammad Hosein Zare, Hamed Zamani, Reza Omid, Ghazale Perota, Hamidreza Masjedi

Medical Physics Department, Shahid Sadoughi University of Medical Sciences and Health Services, Yazd, Iran

Background: Myocardial perfusion imaging (MPI) is a non-invasive nuclear medicine (NM) procedure for diagnosis and risk evaluation of coronary artery disease. Patient dose from an MPI is comparable to or higher than that of a typical computed tomography scan. This, combined with the fact that these scans are among the most common nuclear medicine exams conducted in Iran, raise concerns regarding public health protection against ionization radiation.

Objective: This study aimed to estimate the excess risk of fatal cancer incidence triggered by MPIs and hence to put it in a more tangible context for the general population.

Objective: Data were collected cross-sectionally for more than 10 consecutive patients 18 years and older who had undergone myocardial perfusion scan with ^{99m}Tc-MIBI at all the two active nuclear medicine institutions affiliated to Shahid Sadoughi University of Medical Sciences and Health Services in Yazd, Iran. The patients' data and net administered activity were abstracted for each. For all the participants, organ and effective doses were estimated by the conversion coefficients published by ICRP in publication 128, and subsequently, the risk of exposure-induced death (REID) was calculated using PCXMC (v. 2, STUK, Helsinki, Finland). To make the risks more tangible for physicians, technologists, and even patients, a comparison with the most top ten causes of death in Iran was made. In order to assess the annual number of excess fatal cancers, the frequency of performed scans in 2018 was obtained from the hospital information system's (HIS) data at each institution.

Results: Of 79 patients with the mean age of 59 years, 73% were female, and the mean BMI was 26 kg/m². In a rest/stress scan, the administered activity and estimated effective dose were, on average, 21.6 mCi and 6.71mSv, respectively. Approximately, 190±66 excess fatal cancers were predicted per million scans; around 150 of such scans might thus induce an equivalent risk of dying from stroke. On balance, the 6508 MPIs (exceeding three fourth of total NM scans) performed in Yazd in 2018 can cause 1 excess cancer death in the future.

Conclusion: Much as the benefits from myocardial perfusion scans far outweigh the risks concerning the patient exposure to ionization radiation, yet, on a large scale, they may threaten public health. The risk could be lowered either by decreasing the number of scans or reducing the radiation dose per scan.

p 014

Optimum mode of inpatient room shielding design for patients treated by ¹³¹I

Ali Ebrahimi fard, Hossein Rajabi, Parham Geramifar

Department of Medical Physics, Faculty of Medical sciences, Tarbiat Modares University, Tehran, Iran

Research Center for Nuclear Medicine, Tehran University of Medical Sciences, Tehran, Iran

Background: Isolation rooms must be shielded to minimize the dose rate inside and outside the room. Backscattered radiation from walls increases the patient dose without benefit for the patients. At the same time, shielding efficiency must high enough to protect the staff.

Objective: The objective of this study was evaluating the shielding design of isolation for the patients receiving ¹³¹I. Different combinations of lead and concrete were investigated to find the optimal combination of lead and concrete layers.

Methods: We used the Gate Monte Carlo toolkit to evaluate the protection efficiency of adding a lead shield of 1, 2, and 3 mm into the building material of the isolation room. The lead shields were considered in three positions, in front, middle and outside of the concrete walls of different thicknesses. Two cylindrical sources containing 200 mCi of ¹³¹I were placed inside the room and the dose rate (μSv/h) at certain distances from the external surface of the room was estimated. Also, to determine the absorbed dose to the patients, a cylindrical water phantom was also considered inside the room.

Results: The results showed that dose rate reduction was considerably different depending on the position of the lead shield in concrete walls. Also, there was significant increase in the absorbed dose to water phantom with increasing thickness of concrete and lead shield in all three designs. The minimum dose rate in the water phantom was for the lead shield in the outside of concrete walls.

Conclusion: Placing the lead on the back of the concrete shield is the best possible way to reduce the dose rate outside the room. But the increasing the dose rate in the water phantom indicated that the scattered beams from walls must be considered in the shield designing. So, the optimum mode for shield designing with lead and concrete must be taken for reducing the radiation absorbed doses to the patients.

A Comparison of the results of Monte Carlo GATE and MCNP codes on dosimetry of neuroendocrine tumors in treatment with ¹⁷⁷Lu

P 015

Milad Peer Firouzjaei, Mohammad Ali Tajik Mansoury, Parham Geramifar, Rasoul Shamohammadi

Department of Medical Physics, Semnan University of Medical Sciences, Semnan, Iran
Research Center for Nuclear Medicine, Tehran University of Medical Sciences, Tehran, Iran

Background: The use of radioactive sources such as ¹⁷⁷Lu has been considered for the treatment of disseminated tumors, especially neuroendocrine tumors for a long time. One of the methods used for tumor dosimetry is computational methods such as Monte Carlo simulation. Numerous studies have been conducted using Monte Carlo codes in this field, which utilize various energy modes including full energy spectrum, beta particle spectrum and average energy of beta particles, i.e. monoenergetic.

Objective: The purpose of this study is to compare the doses of different sizes tumors with different energy modes using two Monte Carlo GATE and MCNP codes and comparing them together.

Methods: In this study, simulations were performed using the two Monte Carlo MCNP (x2.6) and GATE (version 7.2) codes. Spheres of water were modeled with different sizes, and the ¹⁷⁷Lu radionuclide was uniformly distributed in the tumor with each of the complete spectrum, the beta particle spectrum, and the average energy of the beta particles. The sizes of the voxels and the energies corresponding to the decay spectra were assumed to be identical in both simulation codes. The number of primary particles in the simulations was considered to be such that the statistical error is less than 0.05%. The results are reported in average dose and simulation time for tumors of different sizes at different radiation energy modes for both Monte Carlo GATE and MCNP codes.

Results: According to the outputs of this work, there was no significant difference between the mean doses of tumors of different sizes in the respective energy modes, but the MCNP simulation times are less than the GATE code.

Conclusion: Based on the results of this work, it can be concluded that the use of two GATE and MCNP codes is the same in tumor dosimetry. Because of the disadvantages of the Monte Carlo method are that its time consuming, the two codes can be used interchangeably.

P 016

A comparative study on positron emitter productions at PET monitoring hadron therapy using proton, carbon and oxygen beams

Siamak Hooshmand Koochi, Ahmad Esmaili Torshabi

Faculty of Sciences and Modern Technologies, Graduate University of Advanced Technology, Kerman, Iran

Background: Nowadays, hadron therapy has been strongly preferred mainly for deep-seated tumors to yield a conformal irradiation of a tumor volume while sparing surrounding normal tissues versus conventional radiotherapy. However, therapeutic hadron beams are particularly of concern due to their non-negligible uncertainties in treatment planning and dose delivery. Currently, the only practical way is the use of Positron Emission Tomography (PET) imaging to monitor the delivered dose of hadron beams for understanding the uncertainties. This measurement enables one to realize the difference among planned and delivered dose distributions of therapeutic beam on tumor and normal tissues.

Objective: In this work, we investigate quantitatively the presence of positrons produced by three common therapeutic beams as proton, carbon and oxygen ions as a comparative study. The physical properties of different ion species are taken into account at interacting with a tissue like material.

Methods: In this work, the production and distribution of positron emitters are calculated with Monte Carlo simulations using FLUKA code. FLUKA is a general purpose Monte Carlo code for simulating the interaction and transport of various particles. A cubic water phantom with 10 cm dimension of each side was considered to mimic real soft tissues of patient body located at 1 cm far away from therapeutic beam. Three therapeutic beam of proton, carbon and oxygen were simulated at Gaussian shape in 80, 146 and 175 MeV energies, respectively. The produced positrons were considered inside water phantom, therefore, the results can be implemented for all three PET monitoring modalities.

Results: Total energies deposited by produced positrons inside water phantom for carbon and oxygen beams is related to proton beam with 2.30 and 4.39 ratio. Furthermore, the total number of paired photons due to annihilation events are 0.52 for proton, and 2.48 for carbon and 3.65 for oxygen beam per unit area cm^2 .

Conclusion: In this work, nuclear reactions induced by proton, carbon and oxygen in water as tissue-like material was considered to assess the production of positrons for PET monitoring cancer therapy. The results help one to understand actual treatment by comparing dose distribution obtained from PET to reference dataset. The main focus of this work is to assess the role Proton, Carbon and Oxygen as therapeutic beams on positron emitter nuclei production due to physical properties of each beam, uniquely.

p 017

The role of various scintillation detectors of positron emission tomography at PET monitoring particle therapy: A simulation study

Ahmad Esmaili Torshabi, Siamak Hooshmand Koochi

Faculty of Sciences and Modern Technologies, Graduate University of Advanced Technology, Kerman, Iran

Background: Compared to the conventional radiotherapy, hadron therapy is increasingly important due to lower entrance dose and fall of dose sharply beyond the target volume. A part from the advantages, hadron therapy is limited while there is no direct monitoring of delivered dose to the tumor and normal surrounding tissues, experimentally. There are many investigations of using Positron Emission Tomography system to monitor hadron therapy delivered dose along with beams trajectory as promising strategy. During therapeutic irradiation, positron emitters are produced on the beam path length through nuclear reactions and the spatial distribution of positrons can be measured.

Objective: In this work, an investigation was performed on the effect of various type of scintillation detectors of PET imaging system to result better accuracy of obtained images. Final results may help one to better realize the performance of each detecting system of PET implemented at Particle therapy for dose monitoring.

Methods: The effect of five common available detectors of PET system were taken into account as: LSO, Stilbene, Anthracene, NaI and CsI using FLUKA Monte Carlo simulation code. In FLUKA code, our simulated PET system is Siemens Biograph mCT with 41.2 cm radius. Our geometry is a spherical water phantom with 10 cm radius located at center of PET system and is bombarded by proton, carbon and oxygen as therapeutic beam at various energies. The calculations were done from 5 to 15 cm of depth of water with 2.5 cm increasing at each step for all three beams.

Results: final analyzed results represent that Anthracene detectors has the best performance versus other detectors at PET system in dose distribution depiction. The worst case belongs to LSO detecting system of our PET. Moreover, the performance accuracy of CsI is almost same as LSO. It should be noted that the number of gamma rays that reach to detectors are as 0.65, 1.30, 1.35, 1.57 and 1.96 per unit area for 70, 90, 110, 125 and 140 MeV of proton beam, respectively.

Conclusion: The role of five different detectors were considered at PET imager utilized for hadron therapy dose monitoring. To do this, nuclear reactions induced by therapeutic proton, carbon and oxygen in water phantom was simulated to investigate the interaction of paired photons with each detector type. The results show that Anthracene and Stilbene has the best performance mainly due to its high light output in comparison with other detecting system.

p 018

Dosimetry calculations of liver and adjacent organs in brachytherapy of liver cancer using FLUKA code

Arezou Karimian, Asghar Haddadi, Elham Saeedzadeh

Department of Nuclear Engineering, Science and Research branch, Islamic Azad University, Tehran, Iran

Background: Hepatocellular carcinoma is the fifth common cancer worldwide and second reason of cancer death rates. One of the best method for treatment of liver cancer is brachytherapy by ^{90}Y . ^{90}Y emits beta particles and because of low half life is suitable for brachytherapy. This radionuclide delivers maximum dose to the tumor tissue and the lowest dose to the adjacent tissue. Although this radionuclide suitable for treating and no need special shield for personnel and patient, the image that obtained using this radionuclide is not suitable for dose distribution in adjacent organs and tumors but that is possible using other gamma emitter radionuclide such as ^{153}Sm , ^{177}Lu , ^{166}Ho with ^{90}Y .

Objective: The aim of this study is calculation cumulative dose for adjacent organs and tumors in liver cancer brachytherapy by ^{90}Y .

Methods: In this study, dosimetry calculations for ^{90}Y , $^{90}\text{Y}+^{153}\text{Sm}$, $^{90}\text{Y}+^{177}\text{Lu}$, $^{90}\text{Y}+^{166}\text{Ho}$ in normal liver, right and left lungs, gallbladder, stomach, heart, thymus, pancreas, breast adipose right and left, breast glandular right and left and two tumors, by FLUKA code and using ICRP-110Famle voxel phantom. Tumors were considered as sphere with 5.6 cm diameter in right lobe and in 4 and 5 segments. Radionuclide sources are homogeneous in normal liver and lungs according to the shunt is intended. Also, particulate emissions are considered as isotropic. Lung shunt was got from average of other tasks % 6.7 and uptake ratio or T/N was considered 4.8. The ratio of gamma emitter radionuclides to ^{90}Y %10 and activity was 1.158GBq. Flair program and USRBIN card were used for describing NaI(Tl) crystal plate with size $40\times 1\times 50$ to imaging.

Results: Cumulative dose normal liver was found the highest 22.14384 Gy in radionuclide ^{90}Y and Cumulative dose breast left glandular was found the least $2.54227\text{E}-4$ in radionuclides $^{90}\text{Y}+^{153}\text{Sm}$. Radionuclide ^{90}Y delivered the highest dose to organs and tumors after that radionuclides, $^{90}\text{Y}+^{177}\text{Lu}$, $^{90}\text{Y}+^{166}\text{Ho}$, $^{90}\text{Y}+^{153}\text{Sm}$ respectively delivered dose to organs and tumors. After we added radionuclides ^{177}Lu , ^{166}Ho , ^{153}Sm dose were decreased.

Conclusion: Normal liver 's Cumulative dose should be less than 50Gy and lung's Cumulative dose should be less than 20Gy and our data results were under them $^{90}\text{Y}+^{166}\text{Ho}$ and $^{90}\text{Y}+^{153}\text{Sm}$ respectively because of high γ energy had better image. We selected $^{90}\text{Y}+^{166}\text{Ho}$ and $^{90}\text{Y}+^{153}\text{Sm}$ for studying.

p 019

Standardization and optimization of reconstruction parameters that impact image quality and quantification of PET/CT images

Habibeh Vosoughi, Parham Geramifar, Mohsen Hajizade, Farshad Emami, Arman Rahmim, Mehdi Momenzad

Department of Medical Physics, Mashhad University of Medical Science, Mashhad, Iran
Nuclear Medicine Department, Razavi Hospital, Imam Reza International University, Mashhad, Iran
Research Center for Nuclear Medicine, Tehran University of Medical Science, Tehran, Iran
Departments of Radiology and Physics, University of British Columbia, Vancouver, Canada

Background: PET/CT imaging is an essential tool in diagnosis, staging, restaging, treatment response evaluation and recurrence in oncology. Image reconstruction methods produce significant variations in quantification and uptake in small lesions especially for low tumor-to-background ratio. Clinical protocols should aim to optimize image quality and detectability with accurate quantification, and as such, reconstruction protocols should be standardized and optimized.

Objective: The overall goal of this study is assessment of the impact of reconstruction protocols on image quality and quantitative values as obtained from PET/CT images.

Methods: Data acquisition was performed for the IQ-NEMA phantom with signal-to-ground (SBR) ratios of 4:1, 6:1, 8:1 and 10:1 on a Siemens Biograph 6 TrueV PET/CT scanner. Raw PET data was reconstructed using different values of sub-iterations and various Gaussian post-smoothing filters. In addition, image reconstruction was performed using attenuation and scatter correction with and without resolution recovery (PSF modeling). CNR, contrast and noise were measured in order to assess image quality. RC_{max} , $\text{RC}_{50\%}$ and RC_{peak} were calculated to enable standardization and optimization of quantitative values, and were compared with the EARL specification reference values.

Results: Though contrast improved by utilizing less smoothing and increasing sub-iterations, CNR and COV were improved using smoother filters and fewer sub-iterations. COV was less than cutoff (15%) for all reconstructions beyond 180sec. Setting the number of iterations to a range between 30 to 60 with post-smoothing of 6 mm FWHM Gaussian filter harmonized quantitative PET data. There

were no differences in RC curves between OSEM and PSF in SBR 4:1, but when using PSF, RCmax and RCA50% were overestimated for higher SBRs and for higher iterations. PSF based reconstruction introduced positive bias in RCmax and RCA50% for 13, 17, 22mm spheres in addition to edge artifacts. Applying suitable FWHM Gaussian filters or using RCpeak may reduce the aforementioned bias.

Conclusion: Among the parameters that affect SUV accuracy, reconstruction algorithms play an important role especially in high tumor-to-background ratios. Image quality and detectability in PET images strongly depend on reconstruction parameters and post-smoothing filter. An optimized post-reconstruction filter was found to minimize variations of RC in comparison to EARL references.

p 020

Cyclotron production of ^{139}Pr : A Monte Carlo prediction

Marzie Yektaee, Tayeb Kakavand, Mohammad Mirzaii, Mohammad Rahimi

Department of Physics, Faculty of Science, Imam Khomeini International University, Qazvin, Iran
Agricultural and Health Research School, Nuclear Science and Technology Research Institute, Tehran, Iran

Background: The ^{139}Pr ($T_{1/2} = 4.41$ h, $EC = 92\%$, $\beta^+ = 8\%$) is one of the promising isotopes of the praseodymium. The main interest in ^{139}Pr arises from the fact that the lanthanides can be readily bound to conjugate biomolecules of human serum albumin. It is a potential PET diagnostic agent. Although β^+ emission occurs only in 8% of the decays, the relatively long half-life of the ^{139}Pr (more than twice that of ^{18}F) makes it a suitable candidate to study metabolic processes with an uptake of several hours. It may also be a proper candidate as the diagnostic partner of the therapeutic ^{142}Pr .

Objective: Because of the difficulty of production, it seems to be important to have a theoretical/imaginary background regarding the production route to warrant the precision of laboratory procedures. Two cross section measurements for $^{140}\text{Ce} (p,2n)^{139}\text{Pr}$ have been reported, Zeisler and Tarkany.

Methods: In this work, the production of ^{139}Pr through different projectiles and targets has been analyzed by using TALYS-1.8 code. From this results, the reaction $^{140}\text{Ce} (p,2n)^{139}\text{Pr}$ is identified as the best route for ^{139}Pr production. The proton energy range for this route is optimized using the excitation function to achieve a maximum cross section and minimum impurity due to the other reaction channels. The production reaction has been simulated with MCNPX code.

Results: The production yield of ^{139}Pr has been calculated via proton induced reaction on ^{140}Ce target at the optimal energy 16-21 MeV with MCNPX and SRIM codes results and TALYS-1.8 code. In addition, the experimental production yield has been obtained. The simulation production yield: 37/0, the theoretical production yield: 37/1, the production yield obtained by Steyn et al: 32/6 and the production yield obtained by Dimitriev et al: 24/8.

Conclusion: The agreement between our results and the experimental values is good. Due to ideality of simulation and theory, the theoretical and simulation-based data are higher. It is possible to use the simulation for optimizing objects and locaters in the place of experimental recipes. It is crystal clear that by this method we can avoid laboratory errors and overabundance of costs.

p 021

Estimation of positron range using GATE simulation

Milad Fard Balaskale, Alireza Sadremomtaz

University of Guilan, Rasht, Iran

Background: An important challenge in PET imaging is spatial resolution. Image resolution in PET is limited by a variety of factors including the spatial resolution of the detectors, noncollinearity and positron range. This last limitation causes a blurring effect during imaging which constrains a limit on the accessible spatial resolution .

Objective: This study surveys the positron annihilation distributions in body, rib bone and lung for ^{18}F , ^{11}C , and ^{68}Ga using GATE simulation. Getting information about the positron range in a range

of tissues would assist us to optimize the PET images. To a large extent, it can be remedied during image reconstruction if accurate estimates of positron range are available.

Methods: GATE is a Monte Carlo simulation platform based on GEANT4 core libraries, specifically designed to provide realistic models of some medical imaging systems such as PET and SPECT. In this study, GATE7.2 was utilized to simulate a point source of each above-mentioned radioisotope with 0.01 mm diameter, which was positioned at the center of a cube that was 30 cm wide on all sides. This cube was simulated in homogeneous medium of body, rib bone or lung. Approximately, 5×10^6 events were simulated for each radioisotope and medium combination. Mean positron range (r_{mean}) for each simulation was calculated and also, annihilation points spread function (aPSF) is obtained from histograms of the 3D annihilation coordinate for each axis to visualize the contribution of range blurring for the 1D distribution. To describe the annihilation distribution at the center and extensive tails further from the emission location, the FWTM is used.

Results: Positron range is proportionally dependent on the maximum energy of radioisotope, and inversely proportional to the density of the surrounding material. Moreover, high FWTM causes drastic blurring effect to the images. ^{68}Ga gives blur up to 4 times higher than ^{18}F in rib bone, body and lung respectively. Also, when the radionuclide with higher energy is used, the blurring effect increases. In addition, since the density of lung is lower than body and bone, the FWTM is the highest in the lung. The contribution of image blur was up to 4 times larger in the lung than in body and 10 times larger than rib bone.

Conclusion: The impact of positron range is a crucial factor in image degradation when using high-energy positron emitters like ^{68}Ga , particularly in the lung. Therefore, it must be accounted during and after reconstruction of PET images.

p 022

Evaluation of dose point kernel around gold nanoparticles using Monte Carlo simulations

Hossein khosravi

Department of Radiology, Faculty of Paramedical, Hamadan University of Medical Sciences, Hamadan, Iran

Background: investigate the dose-enhancing properties of gold nanoparticles (GNPs) interacting with radiation has prompted the development of various Monte Carlo (MC)-based nanodosimetry techniques that generally require considerable computational knowledge, time and specific tools/platforms.

Objective: The aim of this study investigated a hybrid computational framework, based on the electron dose point kernel (DPK) method, by combining MC simulations with an analytical approach.

Methods: This hybrid framework was applied to estimate the dose distributions around GNPs due to the secondary electrons emitted from GNPs irradiated by various photon sources. Specifically, the equivalent path length approximation was used to rescale the homogeneous DPKs for heterogeneous GNPs embedded in water/tissue.

Results: Compared with simulations, the hybrid framework halved calculation time while utilizing fewer computer resources, and also resulted in mean discrepancies less than 21% for Yb-169 irradiation. Its appropriateness and computational efficiency in handling more complex cases were also demonstrated using an example derived from a transmission electron microscopy image of a cancer cell containing internalized GNPs.

Conclusion: Overall, the currently proposed hybrid computational framework can be a practical alternative to full-fledged MC simulations, benefiting a wide range of GNP- and radiation-related applications.

p 023

Cellular dosimetry of Samarium-153 and Strontium-89 for palliative therapy of bone metastases: A Monte Carlo simulation study

Saman Dalvand, Hossein Rajabi, Etesam Malekzadeh

Department of Medical Physics, School of Medical Sciences, Tarbiat Modares University, Tehran, Iran

Background: Bone is one of the common metastatic sites of cancers. Systemic radiopharmaceutical therapy is an effective method for pain palliation of bone metastasis and several radionuclides have proposed. Metastron (Strontium-89 chloride) and Quadramet (¹⁵³Sm tetraphosphonate chelator, ethylenediaminetetramethylenephosphonic acid) are approved by the FDA. The average energy of beta radiation from Strontium-89 and Samarium-153 is 585 keV and 224 keV, respectively. However, the mean energy of other radiations of Strontium-89 is much lower than that of the Samarium-153. This difference was neglected in most studies and reported a higher dose of Strontium-89 compared to dose of Samarium-153. But it is not true in microscale dose calculation due to short range of Auger electrons.

Objective: The aim of this study was comparing the absorbed dose of Strontium-89 and Samarium-153 using full spectrum of radiations in cellular level using Monte Carlo simulation.

Methods: Simulations were performed using GATE Monte Carlo toolkit. Two sizes were considered for osteoblasts, osteoclasts, and osteocytes based on published histological data. The radionuclides were assumed to be uniformly distributed in different subcomponents of the cell. Cellular S-values were calculated for five combinations of source-target organelles; cell-cell (C→C), cell surface-cell (CS→C), cell surface-nucleus (CS→N), cytoplasm-nucleus (Cy→N) and nucleus-nucleus (N→N).

Results: The Auger and internal conversion electrons S-values of Samarium-153 are much higher than those of Strontium-89. When radionuclides are in the cell nucleus, Auger electrons deposit the highest possible dose to the nucleus. In all source-target combinations, the nucleus dose is much higher when the source is inside the cell nucleus compared to the situations when the source is in cell surface, cytoplasm or entire of the cell.

Conclusion: Our results show that in the subcellular scale, the Auger and internal conversion electrons have a significant contribution to the deposited dose. Particularly in Osteoblastic metastases the Auger electron doses should be considered.

p 024

Optimization of radioactive iodine dose in hyperthyroid patients based on dosimetry

Fatemeh Niksirat, yousof fatahpour, Ali shabestani Monfared, Mehrangiz Amiri, Kourosh Ebrahimnejad Gorji, Mohammadali Bayani, Amir Gholami

Departments of Medical Physics Radiobiology and Radiation Protection, School of Medicine, Babol University of Medical Sciences, Babol, Iran

Cancer Research Center, Health Research Institute, Babol University of Medical Sciences, Babol, Iran

Department of Radiology and Radiotherapy, School of Medicine, Babol University of Medical Sciences, Babol, Iran

Department of Internal Medicine, Babol University of Medical Sciences, Babol, Iran

Background: One common treatment for hyperthyroidism is using the I-131. Due to the radioactivity property of I-131, high doses cannot be prescribed for the treatment. On the other hand, prescribing inadequate doses may reduce the chance of improvement. Also, a specific dose cannot be generally prescribed to all patients due to individual physiological differences of different patients in radioiodine uptake.

Objective: This study aimed to find the appropriate dose of I-131 for each specific patient according to his/her physiological conditions.

Methods: 30 hyperthyroid patients (case group) were selected from the Nuclear Medicine Department introduced by the Endocrinologist and received a dose of 1 mCi of I-131 under the supervision of a Nuclear Medicine Specialist. After 1 hour, a thyroid scan was taken using a gamma camera. Two other scans were taken 2 and 6 days after and the scans were analyzed by Imagej software and the information was obtained by counting. The data resulted from the counting was drawn based on time for each of the three steps in a graph of changes in radioactive substance in the body, and the effective half-life (T_{eff}) was calculated in the software using count changes. The dose

of iodine-131 absorbed in the thyroid can be calculated using the T_{eff} , based on which the specialist can decide exactly how much iodine-131 should be prescribed for each particular patient. Then, the patients' response to treatment will be evaluated by Endocrinologist considering the changes in thyroid hormone levels.

Results: It is expected to calculate the dose of radioactive iodine for each hyperthyroid patient and this method will increase the therapeutic efficacy and decrease the complications of prescribing higher dose of ^{131}I .

Conclusion: Based on the results of the duration of the biological presence of the radioactive substance in each patient's body, the dose of radioactive iodine needed for the treatment of hyperthyroidism can be calculated.

p 025

Absorbed dose calculation from beta ray of ^{188}Re , ^{186}Re and ^{90}Y in follicle thyroid models

Alireza Sadremomtaz, Parvaneh Fekri, Mohammad Reza Kazemiyanhaghighat

Department of Physics, University of Guilan, Rasht, Iran

Background: The use of beta and gamma emitting radionuclides is one of the ways to treat cancer. Radionuclides ^{188}Re , ^{186}Re and ^{90}Y are commonly used for diagnostic and therapeutic purposes.

Objective: The aim of this study was to calculate the beta absorbed dose of ^{188}Re , ^{186}Re and ^{90}Y radiopharmaceuticals in previously developed thyroid follicle models for man, rat and mouse, using the Mont Carlo Mncp4c code.

Methods: Initially the input file for the Mncp4c code was prepared for calculating of tally *f8. Then the beta absorbed energy radiopharmaceuticals ^{188}Re , ^{186}Re and ^{90}Y was obtained from output file, to calculate the absorbed dose, the absorption energy of each organ was divided by mass of that organ. In this simulation single follicle thyroid model containing a thyroid follicle duct, a layer of follicle cell and six spherical nuclei alternating with same distance from the center of follicle duct to each other was used.

Results: The results of this research show that for constant activity in follicle thyroid with increasing diameter for follicle cell (6-10) μm , follicle lumen (50-150) μm and follicle cell nucleus (4-8) μm , absorbed dose of beta in the thyroid follicle models decreases. The highest absorbed dose was obtained respectively for ^{186}Re , ^{90}Y and ^{188}Re in the follicle cell division.

Conclusion: For constant activity in follicle thyroid by increasing follicle thyroid size absorbed dose of beta decreased. Therefore, with increasing cell size (for example lumen diameter), the ionizing radiation loses some of its energy along the path. that is, that is. In this case, for different age ranges, a higher dose should be given to an adult than the infant.

p 026

Optimization of subset and filter size for TOF and PSF-modeling protocol in PET/CT image in IQ NEMA phantom

Pardis Ghafarian, Samira Rezvani, Mohammad Reza Ay

Chronic Respiratory Diseases Research Center, National Research Institute of Tuberculosis and Lung Disease (NRITLD), Shahid Beheshti University of Medical Sciences, Tehran, Iran
PET/CT and Cyclotron Center, Masih Daneshvari Hospital, Shahid Beheshti University of Medical Sciences, Tehran, Iran.

Research Center for Molecular and Cellular Imaging, Tehran University of Medical Sciences, Tehran, Iran

Department of Medical Physics and Biomedical Engineering, Tehran University of Medical Sciences, Tehran, Iran

Background: PET/CT imaging is used for the aim of tumor detection and quantitative analyzing of tumors for patient follow up and response to therapy. With better image quality the mentioned procedure would be more precise and accurate.

Objective: The aim of this study is the optimization of subset and filter for proper protocol considering lesion size and its background activity.

Methods: data acquisition from IQ NEMA phantom has been done with Discovery 690 PET/CT scanner with 2:1 SBR in 4.95, 3.95 and 2.85 KBq/cc background with three different - lesion size of 10, 17 and 28 ml. The list-mode data reconstructed with HDS (OSEM+PSF), HD (OSEM), T (OSEM+TOF) and TS (OSEM+PSF+TOF). Subsets were 18, 24, 32 and 36 and iteration was two. We applied the Gaussian filter with 4.5, 5.5 and 6.4 mm FWHM. 48-images were reconstructed for each list-mode data. The Image quality and quantitative parameters were calculated, then physicians scored to image quality visually. Kruskal Wallis and Man Whitney test were used as statistical tests.

Results: optimized protocol decreased the noise 25.2%, 23.6% and 21.6% in high, medium and low background respectively. In small lesions, mean of the SNR were 13.8 ± 3.7 , 10.9 ± 3.1 and 9.1 ± 2.2 , while in the optimized protocol they were 16.5 ± 3.4 , 13.2 ± 2.6 and 10.8 ± 1.8 in high, medium and low background activity respectively, also In big lesions, SNR were 21.4 ± 5.5 , 15.4 ± 3.6 and 14.2 ± 3.0 while in the optimized protocol were 25.8 ± 4.5 , 18.3 ± 2.8 and 16.6 ± 2.4 . CNR improved 28%, 23% and 20% in small lesions, and 18.5%, 11.5% and 9% in big lesions in high, medium and low background activity respectively.

Conclusion: Proper protocol for the aim of small lesion detection is OSEM+PSF modeling and its optimized subset is 18 or 24 with a 5.5 mm FWHM filter. OSEM protocol with 18 or 24 with a 5.5 mm filter size also can be a good choice. When the aim is big lesion quantitative analyzing, OSEM+PSF modeling+ TOF is more proper and its optimized subset is 18 or 24 with 5.5 mm filter size. If in reconstruction we have time limitation, OSEM+PSF modeling with 24 or 32 Subset with 5.5 mm filter size can be as optimized protocols.

p 027

Assessment of effective doses received by caregivers taking care of non-cancerous thyroid patients treated with I-131 therapy

Ali Abdulhasan Kadhim, Peyman Sheikhzadeh, Shima Yavari, Saeed Farzanehfar, Mohammad Reza Ay

Department of Medical Physics, Tehran University of Medical Sciences, Tehran, Iran
Department of Nuclear Medicine, Yas Hospital, Tehran University of Medical sciences, Tehran, Iran
Department of Nuclear Medicine, Vali-asr Hospital, Tehran university of Medical sciences, Tehran, Iran

Background: In radioiodine therapy, undesired radiation exposure to caregivers is almost inevitable. Safety of caregivers is necessary to ensure that patients get adequate support. Thus, it is important that caregivers be well-informed about adequate protective measures to ensure that their radiation doses received from patients are kept within the barest minimum according to international recommendations.

Objective: This study aims to determine the radiation dose received by caregivers taking care of non-cancerous thyroid patients treated with I-131. Furthermore, we will assess their levels of compliance to radiation protection measures according to international recommendations.

Methods: Ten caregivers of 10 patients as a prototype study receiving radioiodine therapy for non-cancerous thyroid diseases were given specific instructions with regards to radiation safety. Afterwards, each caregiver was provided with a Thermo Luminescent Dosimeter (GR-200(LiF: Mg, Cu, P)) badge. They were asked to wear the badges for 14 days when taking care of the patients. At the end of this period, the radiation dose received by each caregiver was measured from the TLD and compared with the recommendations of the International Commission on Radiological Protection (ICRP).

Results: The treatment doses administered to the patients of average age 39.7 ± 10.8 years ranged between 8 - 30 mCi. The effective doses received by the caregivers after 2 weeks were between 0.02 - 0.26 mSv, with an average of 0.11 ± 0.088 mSv. Comparison of these results with ICRP recommendations showed that the doses to caregivers of the patients are well under the safety limit of 5 mSv given by ICRP (1).

Conclusion: The radiation doses to caregivers were well within the limits of ICRP, thereby indicating good compliance by the caregivers to radiation protection and safety instructions. These encouraging results would comfort caregivers, as their safety is not compromised as long as they abide by radiation safety instructions.

Radiation exposure hazard in nuclear medicine department of hospitals

Seyed Ali Shafiei

p 028

Department of Medical physics, School of Medicine, Qom University of Medical Sciences, Qom, Iran

Background: A considerable number of staff in nuclear medicine departments do not routinely use lead aprons (LA) and thyroid shields. They believe that entrance surface dose (ESD) and radiation dose under LA are very great in high energy radiation because of Compton scattering. These technicians imagine that the extra radiation absorbed by not using LA can be dramatically decreased by reducing the preparation time of radiopharmaceutical and its injection.

Objective: In this study, radiation dose and skin dose due to using the radioactive element of Technetium-99m (^{99m}Tc) has been investigated by computer simulation using Monte Carlo N-Particle (MCNP) Transport Code.

Methods: A ^{99m}Tc (140keV) source with 5mCi activity was placed 30cm from a water phantom (WP) with 50.5kg mass. A lead layer 0.5mm thick was situated in front of one surface WP (6400cm²) that had been placed in the direction of the radioactive source (RS). A dosimeter with sensitive volume 0.6cm³ was placed behind the lead shield and very near the RS. Closest and farthest distances of WP surface in back of the shield to the RS were 30cm and 50cm, respectively. A layer with 3mm thick of phantom was considered the skin. All of this structure was simulated and run in MCNP code. After removing the lead shield, this simulation was rerun and the results of these two simulations were evaluated.

Results: Evaluation of the simulations' results showed that dose rate measured by dosimeter, skin dose rate, and WP dose rate was much less than the ambient dose rate ($\ll 0.2\mu\text{sv/h}$) when the LA (0.5 mm) was used. In the absence of LA, the dose rate measured by dosimeter was 48.4 $\mu\text{sv/h}$ and the skin dose rate and WP dose rate were 27.6 $\mu\text{sv/h}$ and 18.5 $\mu\text{sv/h}$, respectively.

Conclusion: According to the recommendations of the Atomic Energy Organization of Iran, the maximum dose rate in the staff room must be less than 7.5 $\mu\text{sv/h}$. The present study showed that failure to use LA creates severe risk to staff. According to the values obtained, even if the performance speed of personnel is reduced by the use of LA and gloves, they do reduce the level of exposure to below the permissible level and even the background exposure level. As a result, the need for quick staff functioning can in no way substitute for the utilization of LA. Consequently, the use of LA, thyroid shields, and other radiation protection in nuclear medicine departments is highly recommended.

p 029

Embryonic and fetal dosimetry during pregnancy in ^{131}I radionuclide therapy

Ali Ebrahimi Fard, Parham Geramifar, Hossein Rajabi

Department of Medical Physics, Faculty of Medical sciences, Tarbiat Modares University, Iran
Research Center for Nuclear Medicine, Shariati Hospital, Tehran University of Medical Sciences, Tehran, Iran

Background: Radioiodine therapy is the main treatment in patients with differentiated thyroid cancer. Lack of awareness in the first few weeks of pregnancy and failure of pregnancy tests taken before treatment makes the treatment of female patients a big challenge as the embryo will be under the high risk of radiation damage. Moreover, the embryo/fetus absorbed dose estimation is very complicated.

Objective: The objective of this study was the evaluation of biokinetic parameters and physical models used for dose estimation of embryo and fetus at different weeks of pregnancy. Absorbed dose to embryos/fetuses can be estimated using the absorbed dose assessments in mother tissues.

Methods: This study was mainly based on the ICRP reports concerning the estimation of absorbed dose to embryo and fetus during the radioiodine treatment of pregnant females. The simulation studies were performed using MCNP Monte-carlo package.

Results: Rapid changes in the biokinetic and fetal mass are parameters that are not taken into account in different models of dose estimation. Currently, the absorbed dose to embryos is estimated using the average absorbed dose in the mother's uterus in which the shielding effect of uterus is not

considered. Also, due to the lack of information on the dimensions of the fetal bones, no correction is made for the different absorption coefficient of fetal bone. In other words, it is assumed that all primary energy is transferred to the bone. The absorbed changes of liver, in the second trimester of pregnancy, and bone marrow in the third trimester of pregnancy can be considered as the primary targets for the radiation.

Conclusion: Based on the ICRP approach, bone marrow is considered as the target of biological damages during the second and third trimesters. At the treatment dose of 100-200 mGy, the probability of CNS damage, growth retardation, and even fetal death can be considered for an embryo or fetus whose mother is under ¹³¹I therapy. The intensity of these effects is quite variable for different stages of pregnancy. At fetal doses of less than 100 mGy, termination of pregnancy is not medically justified. At higher fetal doses, the extent and type of fetal damages depend on the dose and stage of pregnancy, and decisions of termination pregnancy should be made on the basis of consultation sessions and individual decisions. Recent studies showed that microdosimetry using high-resolution voxelized phantom and Monte Carlo simulation provides a better assessment during early pregnancy.

p 030

Harmonization based on multicenter analysis of PET/CT standardized uptake value (SUV) measurement variation

Abbas Monsef, Pardis Ghafarian, Peyman Sheikh Zadeh, Parham Geramifar, Mohammad Reza Ay

Department of Medical Physics and Biomedical Engineering, Tehran University of Medical Sciences, Tehran, Iran

Research Center for Molecular and Cellular Imaging, Tehran University of Medical Sciences, Tehran, Iran

Chronic Respiratory Diseases Research Center, National Research Institute of Tuberculosis and Lung Diseases (NRITLD), Shahid Beheshti University of Medical Sciences, Iran

PET/CT and Cyclotron Center, Masih Daneshvari Hospital, Shahid Beheshti University of Medical Sciences, Tehran, Iran

Department of Nuclear Medicine, Vali-Asr Hospital, Tehran University of Medical Sciences, Tehran, Iran

Research Center for Nuclear Medicine, Tehran University of Medical Sciences, Tehran, Iran

Background: The standardized uptake value (SUV) is common parameter is used to quantify radiotracer uptake in PET/CT which plays essential role in detection, staging and response to therapy assessment in oncology. The main concern is here SUV is associated with multiple source of variation and varies among different centers and also in a center in different times at the same conditions. Since, variability disturbs its reliability, a solution for its bias challenges is the Harmonization which includes set of process that are applied into quantitative content of images so as to minimize SUV variability.

Objective: This study measures inter-site and intra-site SUV variability in PET images, minimizes SUV inconsistency and enables comparison of SUV directly across different scanners and facilitates multicenter oncology study.

Methods: A NEMA phantom including 6 cylindrical lesions is used for data acquisition at the same conditions. Images are acquired based on optimized routine imaging protocol in each PET/CT center. Phantom is prepared at different lesion to background ratio(LBR) for 2,4 and 8, then is scanned at different background activity concentration. Test retest study is also performed for each of above. At first, SUVs are calculated to measure inter-site and intra-site variability. Then harmonization process is applied to align each center recovery coefficient plot within the reference range which is characterized by EANM. The procedure schematic is shown in figure1.

Results: The recovery coefficient plots for SUV_{mean} of 4 and 8 have been illustrated in figure 2(a) and 2(b) respectively which both scans were done in Shariati hospital so far. In small lesions, deviance is more obvious. Albeit the SUV_{max} is frequently used, but its variability was more than SUV_{mean} . the intra-site variability at $SUV=4$ and $SUV=8$ was $SD=0.16 \pm 0.07$ and $SD=0.33 \pm 0.25$ respectively. The SUV variability was significant when was evaluated in various background activity concentration. (P value < 0.05, Friedman test)

Conclusion: Inter-site and intra-site SUV variability can significantly affect on its accuracy and reliability. Harmonizing SUVs among different PET-CT systems can improve the SUV reproducibility and repeatability and facilitates comparability of SUVs directly across centers.

p 031

Hand dose assessment in nuclear medicine practices by use of active survey meter

Shima Yavari, Peyman Sheikhzadeh, Mansour Jafarizadeh, Nahid Ghomi-Molkar

Department of Nuclear Medicine, Yas Hospital, Tehran University of Medical sciences, Tehran, Iran

Department of Nuclear Medicine, Vali-Asr Hospital, Tehran University of Medical Sciences, Tehran, Iran

Background: Radiation protection of workers in nuclear medicine is a matter of concern since high activities are used. Hands are exposed to high dose rate. So care must be taken on hand dose assessment in order to implement extremities dose limit. In spite of high dose limit recommended by ICRP for quantity $H_p(0.07)$ to be implemented for extremities, with the value of 500 mSv, several methods active/passive such as TLD and electronic finger dosimeters have been used for hand dose assessment. But in practice finger dosimeters have some difficulties such as wearing them under or over the gloves, being contaminated with the radioisotopes and so on. So based on the ALARA principles, seeking methods to be practical and reliable for hand dose reduction is necessary.

Objective: The objective of this method is reducing of received hands doses during dispensing of radiopharmaceuticals

Methods: In this study we have evaluated the hand absorbed dose rate during radiopharmaceuticals dispensing in two different situations using a survey meter in units of $\mu\text{Sv/hr}$. once when all the vials containing radioisotopes inside the lead shield not covered with the lead cap. And once more when the vials with the same amount in the shield covered with the lead caps. Measurements were made above the vials at the point where the workers hand encounter with the radiation. We have carried out this procedure during 10 days with different amount of activities of ^{99m}Tc radioisotope in the vials.

Results: The results obtained for different activities of ^{99m}Tc ranged between 14 to 235 mci, show that the mean hand dose rate of workers can be considered to be 3381 $\mu\text{sv/hr}$ and 4408 $\mu\text{sv/hr}$ with and without using lead caps respectively. So depending on the total time being spent during dispensing of radiopharmaceuticals the total hand dose can be calculated. and the ratio of mean measured dose rate with lead caps to measured dose rate without lead cap in 10 different days are 0.83, 0.78, 0.58, 0.70, 0.80, 0.73, 0.75, 0.60, 0.74, 0.77.

Conclusion: Our results showed that during the time of preparation of one radiopharmaceutical, with using lead caps for the other vials, which is a simple, practical and helpful method, the amount of hand received dose, decreased about 24%.

p 032

Quantitative analysis of non-small cell lung cancer using radiomics features to differentiate benign and malignant

Seyyed Ali Hosseini, Pardis Ghafarian, Mohammad Reza Ay

Departement of Medical physics and biomedical engineering, Tehran University of Medical Sciences, Tehran, Iran

Research Center for Science and Technology in Medicine, Tehran University of Medical Sciences, Chronic Respiratory Diseases Research Center, National Research Institute of Tuberculosis and Lung Diseases (NRITLD), Shahid Beheshti University of Medical Sciences, Tehran, Iran
PET/CT and cyclotron center, Masih Daneshvari hospital, Shahid Beheshti University of Medical Sciences, Tehran, Iran

Background: Scientists understood medical images had more useful information that cannot be extracted with bare eyes. So the term "Radiomic" introduced to extract this Additional information by applying a large number of quantitative image features. Radiomics is a field in quantitative

imaging that uses advanced image processing, and extracts features to quantitatively describe tumor phenotypes.

Objective: The term “heterogeneity” carries various meanings relevant to the imaging modality: in FDG-PET it refers to the variability in the distribution of body cells uptake. Lesion “heterogeneity” can be illustrated by a multitude of mathematical image processing methods that, taken together, create the “texture analysis” which provides numerous quantitative and semi-quantitative marks and in the end; it helps to improve diagnosis specifically in patients with NoN-small cell lung cancer (NSCLC).

Methods: 10 PET and CT image datasets from patients who underwent FDG-PET/CT for the staging of NSCLC were extracted from the PACS and transferred to MATLAB that allows for manual tumor segmentation. Tumor segmentation was controlled by an experienced nuclear medicine physician. Then, radiomics features were extracted for each patient, In total, 75 radiomics features (tumor shape and size, intensity statistics, and texture) were extracted from each segmented tumor volume. Statistical analysis was performed to assess the association of each feature with the histological condition. feature selection using independent sample t-test to discriminate the benign and malignant lesions in lung cancer with SPSS software.

Results: The data were analyzed using Independent two-tailed Student t-tests were used to compare the radiomic features of benign and malignant tumors at the baseline and final time points. The p-value of 0.041 with a 90% confidence interval was considered significant.

Univariate and multivariate logistic regression analyses were performed to determine significant differences between the radiomic features of benign and malignant tumors.

Conclusion: Radiomics features can be a useful and promising non-invasive method for the differentiation of benign and malignant lesions in NoN-small cell lung cancer.

p 033

Compensation of missing data in XTRIM preclinical PET sinograms via gantry wobbling

Bahador Bahadorzadeh, Reza Faghihi, Alireza Aghaz, Arman Rahmim, Mohammad Reza Ay

Nuclear Engineering Department, Shiraz University, Shiraz, Iran

Research Center for Molecular and Cellular Imaging, Tehran University of Medical Sciences, Tehran, Iran

Radiation Research Center, Shiraz University, Shiraz, Iran

Nuclear Science and Technology Research Institute, Tehran, Iran

Departments of Radiology and Physics, University of British Columbia, Vancouver, BC, Canada

Department of Medical Physics and Biomedical Engineering, Tehran University of Medical Sciences, Tehran, Iran

Background: The Xtrim preclinical PET scanner was designed for small animal PET imaging. The system consists of ten detector blocks that are separated by 4mm gaps, resulting in gaps in the sinogram. Furthermore, detector-block failures may occur, causing gaps in the acquired projection data. Filling such data gaps can mitigate artifacts and other degradations in the reconstructed images.

Objective: The purpose of our study is to compensate the sinograms for missing data by utilizing partial rotation of the gantry during data acquisition.

Methods: We implemented continuous wobble motion during data collection by partial rotation of the gantry around the center of the field of view (CFOV) in the transaxial plane. To simulate partial rotation of the gantry to compensate for missing data in sinograms, we used the Gate Monte Carlo code. The rotation angle changed from 0 to 360° for optimizing wobble angle motion. For performance evaluation of the proposed correction method, we collected data for from IQ phantom NEMA-NU4 and preclinical PET HotRod phantom QRM during gantry wobbling. In addition, we compared images obtained using our method to those reconstructed from data without gap-filling. Data acquisition and image reconstruction were implemented using in-house developed software using MATLAB.

Results: The simulation results showed that gap-compensation by partial rotation of the gantry could control gap artifacts, as well as Poisson random noise. When the wobble motion was implemented during data collection by partial rotation, the quantitative results showed that the proposed method producing %MSE values lower than 5%. Images from data gap-filled using the proposed method were artifacts free, and image quality was slightly improved.

Conclusion: We observed that gantry wobbling improved the reconstructed images, both quantitatively and visually. The proposed technique can be used to compensate for missing data in

the projection-space, and with detector failure artifacts in high-resolution preclinical PET scanners. Overall, the proposed gap-filling method utilizing partial rotation of gantry during data acquisition is an effective method of repairing missed data in preclinical PET sinograms.

p 034

Determining optimum criteria for discharging patients treated with radioiodine-131 treatment with regard to the Iran nuclear regulatory authority (INRA)

Marzieh Ebrahimi, Mohammad Reza Kardan, Vahid Changizi, Seyed Mahdi Hosseini Pooya, Parham Geramifar

Department of Medical Physics, Faculty of Medicine, Iran University of Medical Sciences, Tehran, Iran

Reactor and Nuclear Safety Research School, Nuclear Science and Technology Research Institute, Tehran, Iran

Department of Technology of Radiology and Radiotherapy, Allied Medical Sciences School, Tehran University of Medical Sciences, Tehran, Iran

Radiation Application Research School, Nuclear Science and Technology Research Institute, Tehran, Iran

Research Center for Nuclear Medicine, Tehran University of Medical Sciences, Tehran, Iran

Background: Radioiodine-131 treatment associated with quarantine after thyroidectomy has been commonly used for thyroid cancer patients. Hence, quarantine period for managing exposure for relatives (less than 5 and 1 mSv in each treatment phase, for adults and children respectively) is still a challenge.

Objective: In this study, the optimum discharge criterion for patients treated with radioiodine-131 is determined to obtain the minimum duration of quarantine in accordance with INRA.

Methods: 220 patients were enrolled in the study that the range of prescription activity for patients was 3700 to 7400 MBq. External dose rate at 2, 4, 24 and 40 hours after radioiodine-131 administration and effective half-life were measured to apply for estimation of received effective dose to family members of patients. Moreover, the received effective dose to 99 family members of 52 patients after discharging were measured using thermoluminescence dosimeter (TLD) in order to verification of estimation.

Results: The mean external dose rate of patients at discharge moment was 40.6 μ Sv/h. The mean received effective dose to family members was measured 0.4 ± 0.46 mSv. The mean effective half-life of I-131 of patients who was treated with 3700 MBq, was calculated 15.52 ± 13.24 hour.

Conclusion: Determining quarantine period based on relative's effective dose is in accordance with radiation protection criteria and may decrease the quarantine period from 48h to 24 h which is very helpful considering the limited number of radioiodine-131 treatment centers in our country.

p 035

Evaluation of dosimetry calculation of Yb-175 radiopharmacy for nuclear medicine applications

Ali Moghadasi, Omid Afra

Department of Nuclear Engineering, Science and Research Branch, Islamic Azad University, Tehran, Iran

Department of Basic Science, Technical and Vocational University, Karaj, Iran

Background: Radionuclide ytterbium-175 is one of the newest radiopharmaceuticals used for imaging bone marrow that comprises a reticular of connective tissue, due to its favorable property, such as a half-life of 185 days and a 0.47MeV beta beam of radiation. radiopharmacies are pharmacologically ineffective and prescribe in small quantities. However, the necessity of evaluating the risks of dose to the target tissue and other tissues is very important. In this study, MCNPX2.6 code was used to evaluate ¹⁷⁵Yb radiopharmacy dosimetry in spine containing reticuloendothelial cells and other sensitive tissues. The results showed that the highest absorbed dose was ¹⁷⁵Yb in and around the spine and other tissues received less absorbed dose.

Objective: In nuclear medicine, compounds labeled with radioactive substances (radiopharmaceuticals) enter the body and, therefore, reach radiation doses to all tissues and organs of the body; therefore, evaluation of the absorbed dose in organs to optimally use methods Different diagnostic and therapeutic approaches to assessing patient benefit are the basis for the use radiopharmacy in nuclear medicine, so the object of this study is to utilize the MIRD-ORNL phantom and MCNPX code absorbed dose in different organs and tissues.

Methods: In this study, MCNPX code and the MIRD-ORNL phantom were used to estimate the dose induced by ¹⁷⁵Yb injections into target tissues and other sensitive tissue. The source used (¹⁷⁵Yb) in this study was a generic source defined in the middle part of the spine. The output type in the phantom in question is Tally *F8.

Results and Conclusion: Estimation of ¹⁷⁵Yb dose in different organs of human body using MIRD-ORNL phantom and MCNPX2.6 code with 2.67% computational error in this study and comparing with permissible values, according to Table 1 showed that other organs dose dose They receive little compared to the target body. As a result, the benefits of using ¹⁷⁵Yb radio medicine in nuclear medicine outweigh the risks.

p 036

PET radiomics features reproducibility: A novel heterogeneous wall-less lesion in lung phantom

Ghasem Hajianfar, Isaac Shiri, Maziar Khateri, Hossein Arabi, Parham Geramifar, Mehrdad Oveisi, Ahmad Bitarafan, Habib Zaidi

Rajaie Cardiovascular Medical and Research Center, Iran University of Medical Science, Tehran, Iran

Department of Nuclear Medicine, Vali-Asr Hospital, Tehran University of Medical Sciences, Tehran, Iran

Division of Nuclear Medicine and Molecular Imaging, Geneva University Hospital, CH-1211 Geneva 4, Switzerland

Research Center for Nuclear Medicine, Tehran University of Medical Sciences, Tehran, Iran

Department of Computer Science, University of British Columbia, Vancouver BC, Canada

Geneva University Neurocenter, Geneva University, Geneva, Switzerland

Department of Nuclear Medicine and Molecular Imaging, University of Groningen, University Medical Center Groningen, Groningen, Netherlands

Department of Nuclear Medicine, University of Southern Denmark, Odense, Denmark

Background: Quantification of malignant lesions using radiomic analysis could be performed through extraction of a number of image features. Radiomic features commonly exhibit noticeable sensitivity to different imaging settings. Hence, the robustness and reproducibility are key issues for reliability of radiomics-based studies.

Objective: The aim of this study was to investigate of variability and robustness of radiomic features to a wide range of reconstruction parameters using a novel lung phantom with heterogeneous wall-less lesion inserts.

Methods: A lung phantom with six heterogeneous wall-less lesions, filled with ¹⁸F-FDG, underwent PET/CT scanning. Two reconstruction algorithms (OSEM with and without resolution modeling) with different parameters including number of iterations, number of subsets, full width at half maximum (FWHM) of Gaussian filter, and matrix size were considered. Lesions were segmented on CT images and mapped on PET images. For each lesion 107 features were extracted, including SUV statistics, Gray Level Co-occurrence Matrix (GLCM), Normalized GLCM (NGLCM), Gray Level Size Zone Matrix (GLSZM), Gray Level Run Length Matrix (GLRLM), Neighborhood Intensity-Difference (NID), Neighboring Gray Level Dependence (NGLD). Coefficient of variation (COV) was calculated for each feature and categorized into 4 levels, namely very high (COV<5%), high (5%<COV<10%), medium(10%<COV<20%) and low (20%<COV) reproducible features.

Results: Based on COV, 35%,45% ,31%, 36% and 17% of the features were reproducible for different reconstruction algorithms, number of iterations, number of subsets, FWHM of Gaussian filter and matrix size, respectively. Moreover, 12%, 16%, 7% ,25%,16% and 35% of the features were non-reproducible for reconstruction algorithms, number of iterations, number of subsets, FWHM of Gaussian filter and matrix size, respectively. Low-intensity run emphasis from GLRLM, Contrast from NGCLM, Entropy and Surface entropy of SUV were highly reproducible (COV<5%)

in different imaging settings. Low-intensity large-zone emphasis from GLSZM were non-reproducible in all reconstruction settings.

Conclusion: This study demonstrated the reproducibility of radiomic features with respect to different reconstruction parameters. Radiomic features exhibiting low COV could be considered as reproducible biomarkers for tumor characterization.

p 037

Joint ¹⁸F-FDG PET and CT texture features for survival prediction in NSCLC patients: A machine learning study based on radiomic textures

Mehdi Amini, Isaac Shiri, Ghasem Hajianfar, Hossein Arabi, Mehrdad Oveisi, Mohammad Reza Debvand, Habib Zaidi

Department of Medical Physics, School of Medicine, Shahid Beheshti University of Medical Sciences, Tehran, Iran

Division of Nuclear Medicine and Molecular Imaging, Geneva University Hospital, CH-1211 Geneva 4, Switzerland

Rajaie Cardiovascular Medical and Research Center, Iran University of Medical Science, Tehran, Iran

Department of Nuclear Medicine, Vali-Asr Hospital, Tehran University of Medical Sciences, Tehran, Iran.

Department of Computer Science, University of British Columbia, Vancouver BC, Canada

Geneva University Neurocenter, Geneva University, Geneva, Switzerland

Department of Nuclear Medicine and Molecular Imaging, University of Groningen, University Medical Center Groningen, Groningen, Netherlands

Department of Nuclear Medicine, University of Southern Denmark, Odense, Denmark

Background: NSCLC (non-small cell lung cancer) has a wide spectrum of characteristics with a variety of genotypes and phenotypes. Some are aggressive demanding a prompt treatment and others are clinically indolent. Therefore, identifying patients at high risk can be precious for adopting an enhanced therapy. Radiomics is an emerging technique which has shown promising results in identifying intra-tumor heterogeneities by employing high dimensional quantitative features from medical images.

Objective: The purpose of this work was to investigate survival prediction based on machine learning algorithms using joint ¹⁸F-FDG PET and CT images through Gray Level Co-occurrence Matrix (GLCM) texture features in NSCLC patients.

Methods: This is a retrospective study including 119 NSCLC patients (101 patients in the training dataset and 18 patients in the test dataset) who underwent ¹⁸F-FDG PET/CT studies. PET and CT volumes were delineated manually using 3D-Slicer software. Tumor volumes delineated on PET and CT were fused using sym8 3D-wavelet function. The fused volume was isotropically resampled and quantized to 64 gray levels followed by extraction of 25 GLCM features. In univariate analysis, median cut-off was used for stratification and Kaplan-Meier draw for statistically significant features. Multivariate machine learning was performed by Variable Hunting as a feature selector and Random Survival Forest (RSF) as a classifier. The performance of our model was evaluated by the Concordance index.

Results: In univariate analysis, two features, namely joint_max (p-value=0.02) and energy (p-value=0.002) were statistically significant. Multivariate analysis was performed by the RSF mode, which the concordance index in the training dataset with 100 bootstrap was 0.56 (95% confidence interval: 0.55 - 0.57) and in the test dataset was 0.73.

Conclusion: Fused metabolic and anatomic images provides joint information for radiomics-based survival analysis. The preliminary results showed that machine learning and fused PET and CT image radiomics analysis could predict survival of NSCLC cancer.

p 038

Optimized and specified the amount of injectable activity in myocardial perfusion imaging (MPI) SPECT

Mahdi Mazinani, Mohammad Ali Tajik Mansouri, Mahsa Sabour, Nader Asadian, Elham Kashian

Department of medical physics, Semnan University of medical science, Semnan, Iran
Raaheaseman Center of Nuclear Medicine, Semnan University of medical science, Semnan, Iran

Background: In Iran, the usual injectable dose of radiopharmaceutical for myocardial perfusion scans is not specified for each patient. However, according to the ALARA principle, it is necessary to determine the amount of injectable radiopharmaceutical to patients to reduce the harmful effects of radiation and to achieve optimal image quality by weight. Therefore, dose optimization is important to preserve the quality of myocardial perfusion images and reduce patient exposure. In previous studies, in different countries, the relationship between injectable radiopharmaceutical and patient weight for the same country has been identified.

Objective: Diagnostic reference levels (DRL) data is not available in our country. Therefore, in this study, we investigate changes in the enumeration of patient outputs (heart count) and its relation to weight based on the amount of injected ^{99m}Tc -sestaMIBI.

Methods: patients who were referred to RAHEASEMAN nuclear medicine Center of Semnan for MPI were selected and patients were injected with ^{99m}Tc -sestaMIBI in 2-day protocol stress/rest according to the protocol obtained by Dijk et al. 41 women and 17 men who had not reported ischemia as a result of the scan were selected. Heart count were calculated for an average of 32 views in SPECT imaging with device siemens evo excel using software cedar Sinai. Data were categorized and analyzed by using excel and origin software.

Results: The mean heart count in men and women is 14,000 and 13,000, respectively. Patients with different weights given a dose of radiotracer according to their weight have the same mean heart count for patients without ischemia.

In females with increasing weight the heart count with slope (-3.8) decreased. This was due to the attenuation of the breast tissue in women.

Conclusion: If the radiopharmaceutical is given by weight, heart count has the same mean in patients with different weights. Moreover, it was concluded that in centers where all patients were given the same amount of radiotracer, obese patients had reduced image quality, and in the lean patients the ALARA principle was not observed. The protocol for injecting radiotracer to patients in this study is based on the average weight of the Dutch people and it is necessary for the Iranians to determine this coefficient as well as the DRL values by the competent authorities.

p 039

The effect of overlap size on image quality improvement in ^{18}F -FDG PET/CT imaging based on phantom study

Setareh Gholami Zahedi, Seyed Mahmoud Reza Aghamiri, Pardis Ghafarian, Mehrdad bakhshayesh-Karam

Radiation Medicine Department, Shahid Beheshti University
Chronic Respiratory Diseases Research Center, National Research Institute of Tuberculosis and Lung Diseases (NRITLD), Shahid Beheshti University of Medical Sciences, Tehran, Iran
PET/CT and Cyclotron Center, Masih Daneshvari Hospital, Shahid Beheshti University of Medical Sciences, Tehran, Iran

Background: whole-body PET using ^{18}F -FDG is a valuable molecular imaging modality in the clinical management of patients with cancer. To improve image quality, overlapping bed position is used to compensate some errors in quantitative parameters especially at the edges of the FOV.

Objective: This study aimed to determine the effect of overlap size for different reconstruction protocols, to improve the image quality of PET/CT images.

Methods: This study consisted of a phantom study with 35cm in diameter with various sphere sizes (10, 13, 17, 22, 28, 37mm). The phantom filled with ^{18}F -FDG solution when 2:1 SBR (sphere to background ratio) was considered. Background activities were 4.62 kBq/cc ;(high) and low 2.38 kBq/cc ;(low). Only 10mm sphere diameter was analyzed in this study. Data were reconstructed with OSEM+PSF and OSEM+PSF+TOF protocols. Contrast to noise ratio (CNR), SUV_{max} and coefficient of variation (COV) were used to evaluate the impact of overlap size (19% and 50%).

Results: For OSEM+PSF protocol with 19% (50%) overlap, the $\text{CNR}_{10\text{mm}}$ were varied from 0.83(2.85) to 2.03 (5.04) in low and high background respectively. It seems interesting that, $\text{CNR}_{10\text{mm}}$ variation was seen 0.08(2.04) and 1.1(1.88) for OSEM+PSF+TOF protocol with 19%

(50%) overlap. The SUV_{max} for 10mm sphere diameter using the OSEM+PSF protocol with 19% (50%) overlap, was 1.22(1.4) to 1.3 (1.45) in low and high background respectively. This variation was also observed 1.09(1.26) and 1.19(1.21) for OSEM+PSF+TOF protocol. The COV (%) values using the OSEM+PSF and OSEM+PSF+TOF protocols with 19% (50%) overlap, was varied from 15.08(10.05) to 11.41(7.67) and 13.84(9.24) and 10.18(6.7) in low and high background respectively.

Conclusion: With increasing of overlap size, although, the CNR_{10mm} and SUV_{max} value was increased in both low and high background activity for OSEM+PSF and OSEM+PSF+TOF protocols. It should be clear that this behavior was seen with more impact for OSEM+PSF+TOF in low background activity. It was also illustrated that increasing overlap size can lead to decrease the COV (%) significantly and the lowest noise level was obtained in OSEM+PSF+TOF protocol.

p 040

Effect of dosimeter height on absorbed dose in dosimeter at various distances from radioactive Iodine-treated patients

Mahin Kokhazadeh, Hossein Rajabi, Etesam Malekzadeh

Tarbiat-Modares University, Farhangian University, Tehran Iran

Background: One of the prevalent applications of radioactive Iodine is in treatment of thyroid cancer and hyperthyroidism in which the patient acts as a source of gamma emissions and leaves patient's family members exposed to ionizing radiation. Hence, for safety of patient's family members as well as other people in touch with him/her, patients who receive high volumes of Iodine dose should be kept in quarantine for some time prior to release. Mostly, the amount of activity in a patient's body must be less than 30 mCi in order to release him/her.

Objective: The purpose of this paper is to study the potential effect of radioactive Iodine distribution in patient's body on the absorbed dose in dosimeter at different heights as well as different distances of dosimeter from the patient's body.

Methods: This study has been carried out using NCAT phantoms with a BMI equivalent to a medium-sized man, Monte-Carlo simulation, and GATE code. In simulations, considering a 200 Mega-decay activity in five organs of the phantom (thyroid, stomach, intestine, blood, and bladder) and placing the dosimeter in 10 different heights (between thyroid and bladder) at three distances of one, two and three meters from the phantom, the absorbed doses in dosimeter were measured in all cases.

Results: Extracted curves from simulation results show that when the distance of dosimeter from the phantom is small, the absorbed dose in dosimeter varies significantly in different heights.

Conclusion: Simulation results show that the position of the dosimeter significantly affects the absorbed dose in the dosimeter. Therefore, current method of determining the amount of activity to release patients has drawbacks and must be modified.

Oral (Radiopharmacy)

Section I: Diagnostic-Radiopharmaceuticals and Theranostics**op 001**

Wednesday, November 27, 2019
08:50-09:00, Laleh hall

Technetium-99m-PEGylated dendrimer-G2-(Dabcyle-Lys6, Phe7) pHBSP: A novel nano radiotracer for molecular and early detecting cardiac ischemic region

Naser Mohtavinejad¹, Mehdi Shafiee Ardestani², Ali khalaj³, Ahmad Bitarafan-Rajabi⁴, Massoud Amanlou³

¹Department of Radiopharmacy, Faculty of Pharmacy, Tehran University of Medical Sciences, Tehran, Iran

²Department of Radiopharmacy, Faculty of Pharmacy, Tehran University of Medical Sciences, Tehran, Iran

³Department of Medicinal Chemistry, Faculty of Pharmacy, Tehran University of Medical Sciences, Tehran, Iran

⁴Echocardiography Research Center, Cardiovascular Interventional Research Center, Department of Nuclear Medicine, Rajaie Cardiovascular Medical and Research Center, Iran University Of Medical Sciences, Tehran, Iran.

Background: One of the major global concern that cause of illness and mortality around the world is a cardiovascular disease (CVD). In cardiac hypoxia and ischemic disorders, EPO-BcR receptor as a tissue-protective is reached at the cell surface to increase cell stability. Protection of myocardium by early detection and precise diagnosis of hypoxic and ischemic is very critical to eliminating ischemia stroke and myocardial infarction (MI). Pyroglutamate helix B surface peptide (pHBSP) binding to EPOR-βcR receptor. During solid phase peptide synthesis, to improving stability, tow lipophilic amino acids Fmoc-(Dabcyle)-Lys-oH and Fmoc-Phe were replacing instead of Fmoc-Arg6, Fmoc-Ala7 respectively, subsequently conjugated PEGylated dendrimer-G2 and Labeling with ^{99m}Tc for detection of cardiac ischemic region.

Methods: Radiochemical purity (RCP) was evaluated by ITLC methods. Also Technetium-99m-PEGylated dendrimer-G2-(Dabcyle-Lys6, Phe7) pHBSP was evaluated for stability in human serum and hypoxic cellular specific binding in myocardium H9c2 cell lines. The biodistribution was investigated in the rat.

Results: By using PEGylated dendrimer-G2 as a chelator, radiochemical purity was more than 94% and the stability in human serum up to 6 h was 89%. The ^{99m}Tc-nanocungocate binding at hypoxic cells than normoxic was very significant (3-fold higher compared to normoxic cells at 1h).

Conclusion: In biodistribution studies, EPO-BcR receptor-positive uptake in the cardiac ischemic region was 3.62 ± 0.44 % ID/g at 30 min p.i. SPECT imaging studies showed that ^{99m}Tc-nanoconjugate had prominent activity uptake in EPO-BcR expressing ischemic heart.

op 002

Wednesday, November 27, 2019
09:00-09:10, Laleh hall

Development of Ga-68 radiolabeled, biotinylated thiosemicarbazone dextran-coated iron oxide nanoparticles as the multimodal PET/MRI probe

Mehdi Akhlaghi¹, Nazila Gholipour^{2,3}, Amin Mokhtari Kheirabadi¹, Parham Geramifar¹, Davood Beiki¹

¹Research Center for Nuclear Medicine, Tehran University of Medical Sciences, Tehran, Iran.

²Chemical Injuries Research Center, Systems Biology and Poisonings Institute, Baqiyatallah University of Medical Sciences, Tehran, Iran.

³Faculty of Pharmacy, Baqiyatallah University of Medical Sciences, Tehran, Iran.

Background: To be benefited more from the advantages of hybrid PET-MRI technology, the use of multi-functional contrast imaging agents is essential. Multi-functional Nanoparticles (NPs) could meet all aspects that are necessary for a multi-functional contrast imaging agent.

Objective: The main goal of this work was fabricating and primary evaluating of multifunctional Nanoparticles which are usable as both PET and MRI contrast agents.

Methods: A bi-functional biotinylated thiosemicarbazone dextran-coated iron oxide (IO@biotin-TSCDex) NPs was fabricated. Aldehyde groups of oxidized dextran coating layer were utilized to conjugate biotin as a tumor targeting agent and thiosemicarbazide as a cation chelator. NPs were characterized for physicochemical (FT-IR, TGA, DLS, zeta-potential, TEM, VSM and T2-MRI)

and biological (cytotoxicity, blood compatibility) properties. Then, they radiolabeled with Ga-68 radioisotope for biodistribution studies after radiochemical stability examinations.

Results: Biotinylated NPs were compatible with red blood cells and did not change the blood coagulation time. They showed a significantly enhanced affinity to biotin receptor-positive 4T1 cells compared to non biotinylated one. The r_2 relaxivity coefficient value of the fabricated NPs was 110.2 mM⁻¹s⁻¹. Although, biotinylated NPs was easily radiolabeled with Ga-68 at room temperature, but the stable radiolabeled NPs was achieved at a higher temperature (60°C). The major accumulation of radiolabeled NPs was in the liver and spleen. However, an uptake of about 5.4% ID/g was observed in the 4T1 tumor site. A blocking experiment with the biotin molecule injected before than of Ga-68 radiolabeled biotinylated thiosemicarbazone dextran coated NPs revealed a significant reduction in radioactivity uptake to about 1.1% ID/g in tumor site.

Conclusion: Results indicated that the accumulation of radiolabeled NPs in 4T1 tumors was influenced by the presence of biotin in the structure of NPs. The final product could be used for detection of biotin receptor-positive tumors via PETMRI.

op 003

Wednesday, November 27, 2019

09:10-09:20, Laleh hall

Synthesis and labelling p-NH₂-Bn-DTPA-(Dabcyl-Lys-6, Phe7)-pHBSP with ^{99m}Tc as radiopeptide scintigraphic agents for detecting cardiac ischemia area

Naser Mohtavinejad¹, Mehdi Shafiee Ardestani², Ali khalaj³, Ahmad Bitarafan-Rajabi⁴, Massoud Amanlou³

¹Department of Radiopharmacy, Faculty of Pharmacy, Tehran University of Medical Sciences, Tehran, Iran

²Department of Radiopharmacy, Faculty of Pharmacy, Tehran University of Medical Sciences, Tehran, Iran

³Department of Medicinal Chemistry, Faculty of Pharmacy, Tehran University of Medical Sciences, Tehran, Iran

⁴Echocardiography Research Center, Cardiovascular Interventional Research Center, Department of Nuclear Medicine, Rajaie Cardiovascular Medical and Research Center, Iran University of Medical Sciences, Tehran, Iran

Background: Coronary heart disease (CHD) and myocardial ischemia are an incident disease with high morbidity; therefore immediate diagnosis can reduce fatality and health care costs. Erythropoietin (EPO) tissue-protective effects in the hypoxic and ischemic situation are because of pyroglutamate helix B surface peptide (pHBSP) which derivate the external 3D structure of the helix B subunit of EPO through binding EPOR-βcR receptor. Accordingly, we designed and synthesized a modified undodecanopeptide of p-NH₂-Bn-DTPA-pHBSP using Fmoc solid-phase peptide synthesis strategies. The aim of this study was improving serum stability by replaced two lipophilic amino acids Lys-(Dabcyle), Phe with Arg6 and Ala7 respectively and investigate the characteristics of p-NH₂-Bn-DTPA-(Lys-Dabcyl6, Phe7)-pHBSP for cardiac ischemic imaging.

Methods: The p-NH₂-Bn-DTPA-(Lys-Dabcyl6, Phe7)-pHBSP was labelled with technetium-99m. Radiochemical purity, serum stability and receptor binding in the hypoxic H9c2 cells line was evaluated. In vivo investigation for biodistribution and SPECT/CT scintigraphy were assessed in a cardiac ischemic rabbit model.

Results: Labelling yield was more than 97% and the serum stability of the radiolabelled peptide up to 6 h was 84%. In vitro propensity of radiolabelled peptide binding to hypoxic cells was significant (p<0.01). ^{99m}Tc-p-NH₂-Bn-DTPA-(Lys-Dabcyl6, Phe7)-pHBSP showed considerably accumulated in the ischemic region in the biodistribution and SPECT/CT scintigraphy study (cardiac ischemic area-to-Lung rate = 3.50 ± 0.05 ID/g % at 30 min).

Conclusion: The in vitro and in vivo results presented that ^{99m}Tc-p-NH₂-Bn-DTPA-(Lys-Dabcyl6, Phe7)-pHBSP can be a suitable candidate for cardiac ischemia early detection.

op 004

Wednesday, November 27, 2019

09:20-09:40, Laleh hall

Radiolabeling and evaluation of ^{99m}Tc-DTPA-Amlodipine for calcium channel imagingTahereh Firuzyar¹, Amir Reza Jalilian²¹Nuclear Medicine and Molecular Imaging Research Center, Namazi Teaching Hospital, Shiraz University of Medical Sciences, Shiraz, Iran²Radiation Application Research School, Nuclear Science and Technology Research Institute (NSTRI), Tehran, Iran

Background: The non-invasive imaging and quantification of L-type calcium in living tissues is of great interest in diagnosis of congestive heart failure, myocardial hypertrophy, irritable bowel syndrome etc. Several [¹¹¹C] radiolabeled 1,4-dihydropyridine antagonist have been suggested as promising agents in molecular imaging. Furthermore covalent attachment of a strong chelating agent, DTPA, with pharmaceuticals provides binding sites to which reduced ^{99m}Tc is strongly bound and show excellent results as a metal radiopharmaceutical for molecular imaging. In this work, a DTPA conjugated amlodipine analog was prepared and radiolabeled with ^{99m}Tc for possible voltage gated calcium channel imaging.

Objective: We here report the synthesis, characterization, and radiochemistry of [^{99m}Tc]-DTPA-AMLO. Apoptosis/necrosis study of DTPA-amlodipine Conjugate, biological evaluation and imaging study was also performed.

Methods: Technetium-99m labeled amlodipine conjugate ([^{99m}Tc]-DTPA-AMLO) was prepared starting freshly eluted (<1 h) ^{99m}Technetium pertechnetate (86.5 MBq) and conjugated DTPA-AMLO at pH 5 in 30 min at room temperature in high radiochemical purity (>99%, RTLC; specific activity: 55-60 GBq/mmol). The calcium channel blockade activity (CCBA) and apoptosis/necrosis assay of DTPA-amlodipine conjugate evaluations were performed for the conjugate. Log P, stability, bio-distribution and imaging studies were performed for the tracer followed by biodistribution studies as well as imaging.

Results: The conjugate demonstrated low toxicity on MCF-7 cells and CCBA compared to the amlodipine. The tracer was stable up to 4 h in final production and presence of human serum and log P (-0.49) was consistent with a water soluble complex. The tracer was excreted through kidneys and liver as expected for dihydropyridine. excluding excretory organs, calcium channel rich smooth muscle cells; including colon, intestine and lungs which demonstrated significant uptake.

Conclusion: Significant uptake of [^{99m}Tc]-DTPA-AMLO was obtained in calcium channel rich organs. The complex can be a candidate for further SPECT imaging for L-type calcium channels.

op 005

Wednesday, November 27, 2019

09:40-09:50, Laleh hall

Folate targeted ^{99m}Tc radiolabeled poly (ethylene glycol)/citrate dendrimer-G3 as the SPECT contrast agent for breast cancer detectionSaede Zahani¹, Mehdi Shafeie-Ardestani¹, Omid Sabzevari^{2,3}¹Department of Radiopharmacy, ²Department of Toxicology and Pharmacology, Faculty of Pharmacy, ³Toxicology and Poisoning research Centre, Tehran University of Medical Sciences, Tehran, Iran

Background: Current screening and staging techniques for breast cancer provide a non-perfect diagnostic yield. In addition, optimal treatment with targeted therapies often requires knowledge about the expression of their targets within the tumor lesions. Molecular imaging of tumor metabolism, proliferation and other tumor specific targets may therefore be of additional value in breast cancer management which can be performed with various imaging modalities. Ligands used for this purpose can be labeled with a positron emitting radionuclide for gamma emitting radionuclide for single photon emission computed tomography (SPECT) imaging. Dendrimers are highly branched, star-shaped macromolecules with nanometer-scale dimensions. Dendrimers are defined by three components: a central core, an interior dendritic structure (the branches), and an exterior surface with functional surface groups. Folic acid receptors are highly overexpressed onto some cancer cells such as breast cancer cell which can be utilized as the target to diagnose these tumors. In the present study we fabricated PEG/citrate dendrimer-G3 decorated with ^{99m}Tc and conjugated with folic acid as the PECT contrast agent for breast cancer detection.

Methods: Radiolabeled PEG/citrate dendrimer conjugated with folate was fabricated based on DCC conjugated chemistry. The fabrication of dendrimers was confirmed by ¹HNMR, LC-MS, and FTIR spectroscopy. Moreover, the fabricated dendrimers were characterized via DLS, zeta sizer, and TEM. The toxicity of the dendrimers was measured by XTT assay kit and the imaging potential efficacy assessed by SPECT animal imaging.

Results: The results showed that PEG and citrate are able to form dendrimeric structure which was revealed by ¹HNMR, FTIR, and, LC-MS spectroscopy. The observed peaks around 2.7 (2J=15.5 Hz, 2 hours), 3.5 (t, 3J=5 Hz, 2 hours), and 5.02 (s, 2 hours) in Figure 1a were related to CH₂COOH functional group of citric acid, OCH₂CH₂, and OCH₂CO functional groups of PEG, respectively. These peaks confirmed the presence of citric acid and PEG in the synthesized dendrimer-G3. The stability evaluation demonstrated that the dendrimers were stable in the biological fluid up to several days. XTT assay showed that the dendrimers were biocompatible with negligible toxicity. The animal study also illustrated that the radio labeled dendrimers were able to provide bright SPECT image applicable for cancer detection in vivo.

Conclusion: The findings showed that the fabricated dendrimers are proper SPECT contrast agent for breast cancer detection.

Op 006

Wednesday, November 27, 2019

09:50-10:00, Laleh hall

Synthesis of gadolinium-based nanoparticles and radio labeling for multimodal imaging in breast cancer

Hakimeh Rezaei Aghdam¹, Mehdi Shafiee Ardestani¹, Seyed Esmail Sadat Ebrahimi²

¹Department of Radiopharmacy, Faculty of Pharmacy, Tehran University of Medical Sciences, Tehran, Iran

²Department of Medicinal Chemistry, Faculty of Pharmacy, Tehran University of Medical Sciences, Tehran, Iran

Background: Synthetic amorphous silica is gaining popularity as the material of choice in the fabrication of nanoparticles for use in imaging diagnostics, medical therapeutics, and tissue engineering because of its biocompatible nature.¹

Objective: Ordered silica nanoparticles are compounds highly organized which have very interesting textural characteristics, such as high thermal stability, well defined pore size, narrow size distribution and high area surface. Their morphology, which make it in a promising material for a range of bio applications such as incorporation of radioisotopes. Combining fluorescence and magnetons with radiation increases tumor cell diagnoses, and improves the life spans and the planning of the therapy of animals bearing breast cancer.²

Methods: SiGdNPs, including the pH stability, and anti-photo bleaching ability. In order to get the best fluorescence properties of the synthetic SiNPs, we optimized the reaction conditions by use of box benken experimental design. Cell culture, Tumor implantation, labeling set up and Statistical analysis were carried out.

Results: The synthesis and main characteristics of Nanoparticles reported that are composed of a polysiloxane network surrounded by Gd, that are covalently grafted to an inorganic matrix. Confirmed by TEM imaging (Supplementary information). In vivo studies tumor model and protocol adjustments, to assess the efficacy of Nanoparticles, a 4T1 breast tumors model was selected. In our study, SPECT was performed it has been demonstrated that Nanoparticles accumulate passively in breast cancer tumors. Infrared Spectroscopy, FL, SEM, TEM, evaluation of the survival rate of cancer cells are carried out. Micro SPECT, CT, PET, OI and MR imaging are carried out.

Conclusion: This study demonstrated the safety and efficacy of Gd-based nanoparticles as a potential pre-clinical contrast agent.

Section II: Conventional topics in radiopharmacy**Various aptamers radiolabeling strategies used in SPECT and PET imaging techniques**

op 007

Wednesday, November 27, 2019

11:00-11:10, Laleh hall

Leila Hassanzadeh

Department of Nuclear Medicine, School of Medicine, Rajaie Cardiovascular, Medical and Research Center & Department of Medicinal Chemistry, School of Pharmacy-International Campus, Iran University of Medical Sciences, Tehran 1449614535, Iran;

Background: Clinical molecular imaging (SPECT & PET) techniques facilitate characterization of biological processes in vivo on a molecular and cellular level. Nucleic acid (DNA or RNA) Aptamers are promising targeting biomolecules which are able to bind different types of targets, such as small ions like Zn²⁺, large targets like proteins, whole cells, bacteria, or viruses. Based on their excellent characteristics like easy solid phase chemical synthesis, high specificity, and small size for high tissue penetration, are used as molecular imaging probe in nuclear medicine.

Objective: Different method of radiolabeling, γ -emitters (99mTc, 123I, 67Ga, and 111In), and positron emitters 18F, 11C, 13N, 15O, 68Ga, 82Rb, 64Cu and 89Zr which are reported in various original articles are reviewed.

Methods: Using bifunctional chelators such as MAG3, DTPA, and DOTA to attach some radionuclides to aptamers are described. The possibility of incorporating positron emitters into oligonucleotide such as labeling via click chemistry, silicon-based chemistry and hybridization-based are considered. Hyperbranched polymers as highly interesting nanocarrier in radiolabeling of aptamers are introduced.

Conclusion: Nucleic acid aptamers are excellent molecular imaging probes because of their high specificity. One of the most prevalent probe design approaches is the incorporation of functional groups in 5' or 3' ends of aptamers. They usually require the covalent attachment of a chelator on their 5' terminal amine and then the chelators strongly conjugate radionuclides and make it possible to be used as molecular imaging agents.

op 008

Wednesday, November 27, 2019

11:10-11:20, Laleh hall

Introduction of carbone's nanoparticles derivatives as a facilitator to troublous radiolabeling process

Ashraf Fakhari^{1,2}, Esmail Gharepapagh^{1,2}, Tahereh Firuzyar³, Azadeh Ostadchinar⁴, Farzaneh azimi⁵, Shahram Dabiri Oskuei^{1,2}

¹Medical Radiation Sciences Research Team, Tabriz University of Medical Sciences, Tabriz, Iran

²Department of Radiology, Medical School, Tabriz University of Medical Sciences, Tabriz, Iran

³Department of Nuclear Medicine, Shiraz University of Medical Sciences, Shiraz, Iran

⁴Department of Chemistry, Faculty of Sciences, Azarbaijan Shahid Madani University, Tabriz, Iran

⁵Department of energy engineering and physic, Amirkabir University of Technology, Tehran, Iran

Background: Graphene Quantum Dots (GQDs) as nanoparticles derived from graphene have been considered as big interest in realm of pharmacy, bioimaging and biosensors due to their incredible properties. Because of owing expanded physical capacity (both side of each GQDs layer) and wide range of functional groups, they bind to wide range of molecules and atoms. In this study we introduced a new aspect of GQDs, through providing gamma emitting radio-complex as 99mTc-(N-GQDs) in order to facilitate radiolabeling of agents lacking potential to chelate of radioisotope.

Objective: In this study we made an attempt to show a new potential of Graphene Quantum Dots (GQDs) nano particles as a multipurpose substrate for developing 99mTc-labeled scintigraphy agents through promoting of either radioisotope chelation and water solubility of ligands simultaneously.

Methods: N-GQDs were synthesized and radiolabeled with technetium-99m to obtain 99mTc-(N-GQDs). The 99mTc-(N-GQDs) was injected to healthy Wistar rats for biodistribution studies. Dosimetry studies were done to find out effective radiation dose of each organs.

Results: The characterization of N-GQDs were showed that the high purity of N-GQDs particles in the size range of 5-10 nm were obtained. ITLC surveys demonstrated that 99mTc-(N-GQDs) were prepared in high radiochemical purity (RCP \geq 95%). Filtration of 99mTc-(N-GQDs) with 0.1 μ m

filter was proved that 77.38 % of particles are less than 0.1 μ m. The biodistribution studies showed that the ^{99m}Tc-(N-GQDs) were eliminated by kidneys. Aggregation of ^{99m}Tc-(N-GQDs) in spleen was considerable because of particles size. The ovaries and uterus showed more concentration of ^{99m}Tc-(N-GQDs) within 2h after injection compared with other organs. Dosimetry studies introduced kidneys as critical organ.

Conclusion: Our study demonstrated Technetium-99m labeling of N-GQDs is feasible and radiolabeling of poor water soluble ligands as well as molecules without effective functional groups can potentially be labeled by Technetium-99m using this system.

op 009

Wednesday, November 27, 2019

11:20-11:30, Laleh hall

Method for synthesis and assessment of biodistribution of ^{99m}Tc labeled erlotinib

Zahra Kalaei¹, Nasim Vahidfar², Mehrshad Abbasi², Saeed Farzanehfard²

¹Department of Radiology, Faculty of Paramedical, Tehran University of Medical Sciences, Tehran, Iran

²Department of Nuclear Medicine, Vali-Asr Hospital, Tehran University of Medical Sciences, Tehran, Iran

Background: Non-small cell lung cancer is the most common cause of cancer-related death worldwide. It has been found that between 10-40% of NSCLC patients have a tumor with mutation in EGFR. Erlotinib is a tyrosine kinase inhibitor approved for the first-line treatment of patients with locally advanced or metastatic NSCLC with EGFR activating mutations.

Objective: In this study, we radiolabeled erlotinib with diagnostic radioisotope ^{99m}Tc and assessed its biodistribution.

Methods: In order to radiolabeling of erlotinib with ^{99m}Tc, 40 mg of erlotinib was dissolved in DMSO in a vial, and then SnCl₂ and ascorbic acid were added to the vial. One mCi of pertechnetate was added and the vial was incubated for 20 min at room temperature. RTLC and HPLC were conducted for quality control studies. Three BALB/C mice were injected 150-200 μ Ci ^{99m}Tc-erlotinib and sacrificed, after dissecting their organs, the organs were weighted and counted by gamma counter. One New Zealand rabbit also was used for imaging studies. It was injected 1 mCi ^{99m}Tc-erlotinib at its marginal ear vein and imaging was done at 41, 187 and 384 min after injection by using a dual head gamma camera.

Results: Based on RTLC and HPLC analysis ^{99m}Tc-erlotinib purity was more than 92% and more than 87% of the radiolabeled compound was stable until 24 h. Biodistribution and imaging studies indicated that most uptake of ^{99m}Tc-erlotinib was in the kidneys. Following images showed that lung uptake was reduced by passing time. Imaging studies also revealed that the thyroid and stomach uptake of ^{99m}Tc-erlotinib were negligible.

Conclusion: In this study, we found that erlotinib can be easily radiolabeled with ^{99m}Tc and it could be a novel diagnostic radiopharmaceutical to detect NSCLC. ^{99m}Tc-erlotinib can help predict the patient's response to treatment with erlotinib as a targeted therapy drug itself.

op 010

Wednesday, November 27, 2019

11:30-11:40, sub hall

In vivo chemistry for bioorthogonal pretargeted imaging

Abdolreza Yazdani^{1,2}, Soraya Shahhosseini², Patricia Edem³, Brian Zeglis⁴, Mathias Herth⁵, John Valliant⁶

¹Iran's National Elites Foundation

²Pharmaceutical Chemistry and Radiopharmacy Department, Shahid Beheshti University of Medical Sciences, Iran

³TRIUMF, Canada's Particle Accelerator Centre, Canada

⁴Department of Chemistry, Hunter College, New York, United States

⁵Department of Drug Design and Pharmacology, University of Copenhagen, Denmark

⁶Department of Chemistry and Chemical Biology, McMaster University, Canada

Background: Bio-orthogonal click reactions between two moieties have become powerful tools with interesting applications in molecular imaging.1 Pretargeted imaging allows the use of short-

lived radioisotopes for imaging of slow clearing targeting agents macromolecules such as antibodies.

Objective: While a number of different bioorthogonal reactions have been reported, the inverse electron demand Diels-Alder (IEDDA) reaction between a radiolabelled tetrazine (Tz) and a nano-sized trans-cyclooctene (TCO) functionalized targeting vector has been established as a promising tool for pretargeted imaging. In addition, pretargeted nuclear imaging based on the ligation between Tz and nano-sized targeting agents functionalized with TCO has recently been shown to improve both imaging contrast and dosimetry in nuclear imaging of nanomedicines.

Methods: Once high yield labeling procedures were established, Tz compounds were administered with TCO functionalized alendronic acid (BP-TCO) in various animal models. Biodistribution and/or imaging studies were then conducted to study the results.

Results: BP-TCO ultimately accumulate intracellularly in osteoclasts and becomes accessible for Tz short after injection. Tz labeled derivative demonstrated selective localization to shoulder and knee joints in a biodistribution studies in different animal studies. Using the same pretargeting approach, imaging studies showed that a tetrazine complex localized to implanted skeletal tumors. For control, active targeting was also performed and the results indicated near identical biodistribution data for the active targeting and pretargeting strategies.

Conclusion: TCO-BP represents an effective ligand for delivering trans-cyclooctene to sites of active bone remodeling and can be utilized to target functionalized tetrazines to bone. TCO-BP is a convenient reagent to assess novel tetrazine derivatives in vivo bioorthogonal pretargeting strategies without having to employ TCO-derived antibodies, which are expensive given the amounts required to perform preclinical pretargeting studies.

op 011

Wednesday, November 27, 2019

09:40-09:50, Laleh hall

Comparative studies of carrier added (CA) and no carrier added (NCA) ¹⁷⁷Lu radionuclide roles in radiolabeling of Dotatate

Nafise Salek, Sara Vosoghi, Simindokht Shirvani Arani

Nuclear Science and Technology Research Institute, Tehran, Iran

Background: The peptides radiolabeled with ¹⁷⁷Lu are including the wide range of the promising radiopharmaceuticals. The NCA form of ¹⁷⁷Lu provides high specific activity that is required in targeted receptor therapy in order to avoid saturation of the targeted receptors.

Objective: In this study, the outstanding quality of NCA radionuclides especially in case of ¹⁷⁷Lu was evaluated by comparing of it with CA radionuclide for radiolabeling of DOTATATE peptide.

Methods: The NCA ¹⁷⁷Lu and CA ¹⁷⁷Lu were obtained by chromatography separation of irradiated ¹⁷⁶Yb (enrichment: 96.4%) and irradiation of ¹⁷⁶Lu (enrichment: 95%) respectively. Radiolabeling of DOTATE with CA and NCA ¹⁷⁷Lu was carried out in the same conditions and time. Then, radiolabeling yield was calculated as a function of the some parameters like the Ligand: metal ratio and stability of compound after production.

Results: In radiolabeling of DOTATE with NCA ¹⁷⁷Lu, the radiochemical purity higher than 98% was obtained for a 7: 1 peptide to metal ratio at pH = 5.4 for 45 min incubation at 95 oC. The NCA¹⁷⁷Lu due to its high specific activity, proved stable over a period over 14 days, displaying labelling results from > 95%. Also radiolabeling of DOTATATE with ¹⁷⁷Lu in form of CA was performed and radiochemical purity of 95% was observed in molar ratio of 1:15 metal to peptide. But The rapid degradation in the quality was detected after 4 days preparation and a labelling yield of only 10 % could be achieved after 15 days.

Conclusion: The results showed the superiority of NCA ¹⁷⁷Lu with respect to CA ¹⁷⁷Lu. Not only the particle ratio showed the advantages of the NCA radionuclide, but also the long-term comparison over a period of 15 days revealed the inferior character of CA.¹⁷⁷Lu with regard to the high requirements regarding the specific activity set by radio-immunotherapy.

Section III: Novel Radiopharmaceuticals for Imaging and Therapy**Op 012**

Wednesday, November 27, 2019

14:10-14:20, Laleh hall

Fibroblast activation protein (FAP) inhibitors: Novel ligands for PET/CT imagingMahshid kiani¹, Davood Beiki²¹Department of Radiopharmacy, Faculty of Pharmacy, Tehran University of Medical Sciences, Tehran, Iran²Research Center for Nuclear Medicine, Tehran University of Medical Sciences, Tehran, Iran

Fibroblast activation protein (FAP) is highly expressed in the microenvironment of more than 90% of epithelial tumors. The fact that overexpression is associated with a worse prognosis in cancer patients led to the hypothesis that FAP activity is involved in cancer development, cancer cell migration, and cancer spread. Therefore, targeting of this compound can be considered a promising strategy for detecting and treating malignant tumors. On the other hand, because FAP shows low expression in most normal organs, it presents an interesting target for imaging with low background activity and selective radionuclide therapy. Recently, a German group presented the development of quinoline-based PET tracers that act as fibroblast-activation-protein inhibitors (FAPIs) demonstrated promising preclinical and clinical. They concluded that ⁶⁸Ga-FAPI PET/CT is a promising new diagnostic method for imaging various kinds of cancer, in particular pancreatic, head and neck, colon, lung, and breast cancer, with tumor-to-background contrast ratios equal to or even better than those of ¹⁸F-FDG. The favorable characteristics of these new ligands include fast tracer kinetics that seem appropriate for imaging patients even less than 1 h after injection; low background uptake in liver, oral mucosa, and brain; and independence from blood sugar. Because the ⁶⁸Ga-FAPI tracers contain the universal DOTA-chelator, a theranostic approach also seems feasible. The focus of the present review is to introduce this novel class of radiopharmaceuticals, which may open new applications for noninvasive tumor characterization and staging examinations.

Op 013

Wednesday, November 27, 2019

14:20-14:30, Laleh hall

Clinical use of ^{99m}Tc-HMPAO-labeled platelets in cerebral sinus thrombosis imagingParvizi Mahdieh¹, Tafakhori Abbas², Farzanefar Saeed³, Abbasi Mehrshad³¹Department of Radiopharmacy, Faculty of Pharmacy, Tehran University of Medical Sciences, Tehran, Iran²Department of Neurology, School of Medicine, Imam Khomeini Hospital Complex, Tehran University of Medical Sciences, Tehran, Iran³Department of Nuclear Medicine, Vali-Asr Hospital, Tehran University of Medical Sciences, Tehran, Iran

Background: Magnetic resonance imaging (MRI) and computed tomography (CT) scans are not always conclusive for the detection of cerebral venous sinus thrombosis (CVST).

Objective: ^{99m}Tc-HMPAO-labeled platelets may be useful in cases with high clinical suspicion.

Methods: Three patients with headache with or without intraparenchymal hemorrhage that were highly suspected to have CVST, despite inconclusive anatomical imaging, were selected for inclusion in this study. Platelets were extracted by two rounds of centrifugation from 49 ml of the patient's whole blood. The platelets were labeled with ^{99m}Tc-HMPAO, and any unbound ^{99m}Tc was removed by centrifugation. The re-suspension of ^{99m}Tc-HMPAO-labeled platelets in cell-free plasma (CFP) was re-injected into the patients. After 2 hours, planar and single-photon emission computed tomography (SPECT) images of the head were obtained.

Results: Extensive clots were detected in all 3 patients, illustrated in the planar images and even clearer in the SPECT images.

Conclusion: We propose that ^{99m}Tc-HMPAO-labeled platelets scan is a favorable imaging method for patients suspected to have CVST with inconclusive CT and MRI results.

op 014

Wendsday, November 27, 2019
14:30-14:40, Laleh hall

Synthesis and radiolabeling of a novel radiopharmaceutical (Technetium-99m)-(DOTA-NHS-ester)-methionine as a SPECT-CT tumor imaging candidate for breast cancer detection

Paria Mojarad¹, Seyed Esmail Sadat Ebrahimi^{1, 2}, Mehdi Shafiee Ardestani³

¹Faculty of Pharmacy, International Campus, Tehran University of Medical Sciences International Campus (TUMS-IC), Tehran, Iran

²Department of Medicinal Chemistry, Faculty of Pharmacy, Tehran University of Medical Sciences, Tehran, Iran

³Department of Radiopharmacy, Faculty of Pharmacy, Tehran University of Medical Sciences, Tehran, Iran

Background: Nowadays, Breast cancer is the most common and deadliest cancer among women, and can easily be cured by early detection. Molecular imaging plays a very important role in the detection of abnormalities, especially, cancers. SPECT/CT, a kind of imaging technique is able to reveal crucial information due to radiopharmaceuticals used.

Objective: The aim of this study is to find a novel radiopharmaceutical for early detection of breast cancer.

Methods: In this study, Technetium-99m-(DOTA-NHS-ester)-Methionine radiopharmaceutical was synthesized using conjugation between DOTA-HNS ester (chelator) and Methionine (marker). Then it was labeled with Technetium-99m. The synthesized Radio drug performed in breast cancer diagnosis using SPECT/CT imaging technique.

LC-mass, HNMR and FTIR applied to confirm conjugation between DOTA-HNS ester chelator and Methionine. Technetium-99m is the most efficient radioactive element which constituted basic element among radio drugs. DOTA-NHS ester is used in this research to increase Technetium-99m conjugating with Methionine. For the final radiopharmaceutical, MTT assay was done for cellular toxicity and radiochemical purity was evaluated by TLC. Biodistribution and cellular uptake were other studies that were done.

Results: LC-mass, HNMR and FTIR confirmed conjugation between DOTA-HNS ester and Methionine. Radiochemical purity of final radiopharmaceutical obtained 94%, which is high. Cellular uptake indicates higher percentage with the use of Methionine as marker. Cellular toxicity was observed to be low in Human embryonic kidney cells 293 (HEK-293). Radiopharmaceutical biodistribution study 90 min after injection, revealed distribution in Tumor was about 5 times more than brain and muscle.

Conclusion: The results of SPECT imaging in the mice having tumors at 90 min showed that 99mTc-labeled methionine-DOTA accumulated in tumoral tissues. High renal activity observed indicates that kidneys provide the primary means of 99mTc-labeled methionine-DOTA excretion because of their high solubility.

op 015

Wendsday, November 27, 2019
14:40-14:50, Laleh hall

^{99m}Tc-radiolabeled J18 -modified peptide for ovarian cancer detection

Zahra Shaghghi^{1,2}, Seyed Jalal Hosseinimehr², Sajad Molavipordanjani²

¹Department of Nuclear Medicine and Molecular Imaging, Clinical Development Research Unit of Farshchian Heart Center, Hamadan University of Medical Sciences, Hamadan, Iran.

²Department of Radiopharmacy, Faculty of Pharmacy, Mazandaran University of Medical Sciences, Sari, Iran

Background: Early detection of ovarian cancer is key to overcome its poor prognosis. Peptides are amino acids fragments possessing ideal properties as probes for molecular imaging

Objective: In this study, we investigated invitro and invivo properties of ^{99m}Tc-HYNIC-(ser)3-J18, an imaging probe for detection ovarian cancer.

Methods: The selected peptide RSLWSDFYASARGP (J18) was conjugated with a SSS-spacer and Hydrazinonicotinamide (HYNIC) creator and radiolabeled with ^{99m}Tc using tricine and EDDA/tricine as the coligands. Bio distribution studies were conducted in normal mice. Cellular specific binding, of both peptides were evaluated in the SKOV-3 cell line.

Results: HYNIC-peptide was labeled with ^{99m}Tc with more than 99% efficiency and showed high stability in buffer and serum. In vitro cell binding on human ovarian cancer cell lines, SKOV-3

indicated the specificity of ^{99m}Tc -HYNIC-(ser)3-J18 toward ovarian cancer cells. In vivo biodistribution in normal mice showed that radiolabeled peptides cleared rapidly from the blood and was excreted significantly via the kidneys and liver, the proportion of which depends to type of coligand using for labeling. The use of EDDA/tricine results in a mixed route of excretion through both liver and kidneys. However, reducing the lipophilicity on the ^{99m}Tc -(tricine)-HYNIC-(ser)3-J18 peptide in direct excretion toward the desired renal route.

Conclusion: The radiochemical and in vitro/in vivo characterizations indicate that the radiolabeled peptides have favorable properties and these be useful radiopharmaceuticals for detection of ovarian cancer in vivo. Although favorable route of excretion of the complex ^{99m}Tc -(tricine)-HYNIC-(ser)3-J18 compared with ^{99m}Tc -(EDDA/tricine)-HYNIC-(ser)3-J18, making ^{99m}Tc -(tricine)-HYNIC-(ser)3-J18 a promising candidate for SPECT imaging of ovarian cancer.

OP 016

Wednesday, November 27, 2019

14:50-15:00, Laleh hall

Reform of DOTMP structure for using in $^{166}\text{Dy}/^{166}\text{Ho}$ in vivo generator as a bone marrow ablation agent

Sara Vosoughi, Nafise Salek, Ali Bahrami Samani

Nuclear Science and Technology Research Institute, Tehran, Iran

Background: One method to deliver Holmium-166 to target tissue is via $^{166}\text{Dy}/^{166}\text{Ho}$ in vivo generator which parent is separated from daughter and then attached to an agent. Production of an efficient radiopharmaceutical for bone marrow ablation requires the formation of a stable complex between bone-targeting agent and radionuclide. Because of their excellent specificity for bone localization, phosphonate ligands are used in this method. In this study, radiolabeling of DOTMP with $^{166}\text{Dy}/^{166}\text{Ho}$ in vivo generator was investigated. Examination of all the labeling conditions revealed that the complex was not stable over time, so MOF-stable organic-metal framework was synthesized and labeled with $^{166}\text{Dy}/^{166}\text{Ho}$.

Objective: Radiolabeling bone marrow seeking agent was done with $^{166}\text{Dy}/^{166}\text{Ho}$ in vivo generator.

Methods: ^{166}Dy with radionuclide purity >99% obtained by neutron bombardment of ^{164}Dy . The method of separation was based on EXC. The various factors affecting DOTMP radiolabeling, like different pH (4,5,7,8 and 9), reaction times (45min, 1,2 and 24 hour), temperatures (25 and 50°C) and ligand values (20,30,50 and 100 mg) were investigated. The obtained results with TLC-HPGe technique showed that complex was not stable over time and the recoil of daughter nucleus occurred. For the synthesis of radio-MOF material, an aqueous solution was prepared of radio-lanthanide ($^{166}\text{Dy}/^{166}\text{Ho}$) spiked (10 mCi)- $\text{Dy}(\text{NO}_3)_3:\text{CuCl}_2:\text{DOTMP}$ in a molar ratio of 2:1:1, at pH=3. The resulting mixture was injected into a vacuum-capped vial. The vial was heated at 80°C for 10hr. Then radio-MOF crystals (RMC) were obtained. Synthesis of colloidal radio-MOF particles (RMP) was conducted by first preparing a deprotonated solution of DOTMP at pH=8 and then by addition of ($^{166}\text{Dy}/^{166}\text{Ho}$)-spiked (10mCi)- $\text{Dy}(\text{NO}_3)_3$:copper chloride solutions while stirring to provide a molar ratio of 2:1:1 for Ln:Cu:DOTMP, respectively. After 15 min, the obtained radio-MOF particles were collected by centrifuging and re-dispersed in water. To do quality control of the products, IR spectra were recorded. CHN and ICP were conducted to determine the estimated chemical formula of the synthesized compounds. Then, the results were confirmed by PIXE analysis. The final product (RMS) consequently was prepared by the protocol obtained for colloidal particles using 10mCi($^{166}\text{Dy}/^{166}\text{Ho}$), 0.1μL of 0.1mmolar CuCl_2 , and 0.1μL of 0.1mmolar DOTMP. The resulting clear solution, which was a very dilute solution of ($^{166}\text{Dy}/^{166}\text{Ho}$)-Cu-DOTMP, was quality-controlled as the final product.

Results: Bone seeking radio-MOF showed high stability in a saline solution and in human serum up to one week. Dynamic light scattering measurements showed a particle size range of 60 to 100nm. We also performed in vitro hydroxyapatite (HA) binding experiments, and it was observed that the product had a very high affinity for the bone-type chemical structure (HA).

Conclusion: Reform of the DOTMP structure and preparation of highly-stable radionuclide phosphonate framework which can be used for bone marrow ablation were performed.

op 017

Wednesday, November 27, 2019
15:00-15:10, Laleh hall

⁶⁸Ga-labeled RGD peptide as an early diagnostic agent for overexpressed $\alpha v \beta 3$ integrin receptors in Non-small cell lung cancer (NSCLC)

Nazanin Pirooznia¹, Khosro Abdi¹, Davood Beiki², Farshad Emami³, Seyed Shahriar Arab⁴, Omid Sbzevari⁵, Zahra Pakdin-Parizi³

¹Department of Radiopharmacy, Faculty of Pharmacy, Tehran University of Medical Sciences, Tehran, Iran

²Research Center for Nuclear Medicine, Tehran University of Medical Sciences, Tehran, Iran

³Nuclear Medicine &, Molecular Imaging Department, Imam Reza International University, Razavi Hospital, Mashhad, Iran

⁴Department of Biophysics, Faculty of Biological Sciences, Tarbiat Modares University, Tehran, Iran

⁵Department of Toxicology & Pharmacology, Faculty of Pharmacy, and Toxicology and poisoning Research Centre, Tehran University of Medical Sciences, Tehran, Iran

Background: The $\alpha v \beta 3$ integrin receptors are overexpressed on proliferating endothelial cells such as those present in growing tumors, as well as on tumor cells of various origins. Specific targeting of $\alpha v \beta 3$ integrin receptors by these RGD-containing peptides makes these short sequences a suitable candidate for cancer imaging and therapy.

Objective: The RGD peptide with high affinity is designed based on molecular docking and modelling. This dimeric RGD radiolabeled peptide has higher affinity for integrin $\alpha v \beta 3$ with selective tumor targeting potential. Peptide labeling with a positron emitter (for imaging) radioisotope was performed with high degree of radiochemical purity and specific activity. Radiolabeled dimeric RGD peptide will have higher sensitivity for early diagnostic purposes and is suitable for follow up procedures.

Methods: DOTA-E(cRGDfK)₂ was radiolabeled with ⁶⁸Ga efficiently. The in vivo and in vitro stability were examined in different buffer systems. Metabolic stability was assessed in mice urine. In vitro specific binding, cellular uptake and internalization was determined. The tumor targeting potential of a ⁶⁸Ga-DOTA-E(cRGDfK)₂ in a s.c. lung cancer xenograft mouse model was studied. In addition, the very early diagnostic potential of the ⁶⁸Ga-labeled RGD peptide was evaluated. Acquisition and reconstruction of the CT and PET image data was also done.

Results: Radiochemical and radionuclide purity for ⁶⁸Ga-DOTA-E(cRGDfK)₂ were >98% and >99%, respectively. Radiotracer showed high in vivo, in vitro and metabolic stability which was determined by ITLC. The Dissociation constant (K_d) of ⁶⁸Ga-DOTA-E(cRGDfK)₂ was 15.28. In average, more than 95% of the radioactivity was specific binding (internalized + surface-bound) in A549 cells. In average, more than 95% of the radioactivity was specific binding (internalized + surface-bound) in A549 cells. Biodistribution data showed that radiolabeled peptides were accumulated significantly in A549 tumor and excreted rapidly by renal system. Tumor uptake peaks were at 1-hour post-injection for ⁶⁸Ga-DOTA-E(cRGDfK)₂. The tumor was clearly visualized in all images.

Conclusion: ⁶⁸Ga-DOTA-E(cRGDfK)₂ can be used as a peptide-based imaging agent allowing very early detection of different cancers overexpressing $\alpha v \beta 3$ integrin receptors and can be a potential candidate in clinical peptide-based imaging for non-small cell lung cancer.

op 018

Wednesday, November 27, 2019
15:10-15:20, Laleh hall

Evaluation and its effectiveness of rhenium-188 radiosynovectomy for chronic hemophilic synovitis

Ghasemali Divband¹, Bagher Azizkalandari², Seyed Hosein Fatemizadeh³, Mohammad E.Zandinezhad⁴, Amir Reza Kachooei⁵, Arash Heidari⁵

¹Research Center of Department Nuclear Medicine, Ghaem Hospital, Mashhad University of Medical Science, Mashhad, Iran

²Radiopharmacy Research Group, Radiation Application Research School, Nuclear Science and Technology Research Institute, Tehran, Iran

³Research center of Nuclear Medicine Department, Ghaem Hospital, Mashhad University of Medical Science, Mashhad, Iran

⁴Sarvar Clinic, Mashhad University of Medical Sciences, Mashhad, Iran

⁵Orthopedic Research Center, Mashhad University of Medical Sciences, Mashhad, Iran

Background: Radiocolloids labelled with less costly and more accessible radionuclides such as Rhenium-188 are of interest to developing countries compared with those labeled with Rhenium-186 and Yttrium-90. This study was aimed to evaluate the efficacy and safety of radiosynovectomy using Rhenium-188 in patients with chronic hemophilic synovitis and recurrent hemarthrosis.

Methods: In this quasi-experimental prospective study, 20 hemophilia patients were evaluated at pre-injection, and at 1, 3, 6, and 12 months after injection. Magnetic resonance imaging (MRI) was done to measure synovial thickness and to calculate Denver score. Joint radiographs were taken to measure the Pettersson score. The Gilbert questionnaire, Functional Independence Score in Hemophilia (FISH) and visual analogue scale (VAS) for pain were completed and the number of bleeding episodes and factor consumption were recorded at each follow-up visit.

Results: The number of bleeding episodes, the amount of factor consumption per month, VAS pain scores, and synovial thickness decreased significantly over time ($P < 0.05$). Gilbert and FISH scores showed significant improvement ($P < 0.05$). However, Pettersson score and Denver score showed no significant changes after injection. Minor complications including temporary pain and swelling occurred in 20% of patients and no major complication was observed after Rhenium-188 injection.

Conclusion: Our results indicated a high clinical impact, efficacy, safety, and low invasion of Rhenium-188 in radiosynovectomy of hemophilic patients. Considering the availability and relatively low cost of Rhenium-188 in developing countries, this can be a good treatment option for hemophilic patients with recurrent hemarthrosis, particularly when the synovial hypertrophy is not massive yet.

op 019

Wednesday, November 27, 2019

15:20-15:30, Laleh hall

Preparation and biological assessment of ⁶⁴Cu-NOTA-Anti ROR1 as a radioimmunoconjugate for diagnosis of ROR1+ breast cancer by PET

Behrooz Alirezapour¹, S. Milani², Fatemeh Ghaemimanesh, Abdohhah Salimi, Reza Hadavi, A.A. Bayat, H. Rabbani, M. Hashemizadeh³

¹Radiation Application Research School, Nuclear Science and Technology Research Institute, Tehran, Iran

²Antigen and Antibody Engineering Department, Monoclonal Antibody Research Center, Avicenna Research Institute, ACECR, Tehran, Iran

³Pars Isotope Company, Tehran, Iran

Background: Radioimmunosciintigraphy (RIS) has attracted considerable clinical application in tumor detection. Receptor-tyrosine-kinase-like orphan receptor 1 (ROR1) is extensively expressed during embryogenesis but it is absent within most mature tissues. However, expression of ROR1 has been reported in multiple human malignancies including breast cancer. High level expression of ROR1 in breast adenocarcinoma was associated with aggressive disease. So breast cancer radioimmunosciintigraphy targeting ROR1 expression is an attractive object in molecular imaging especially nuclear medicine researches. In this study, we have developed an efficient indirect labeling method of anti-ROR1 with ⁶⁴Cu ($T_{1/2} = 12.8$ h, $\beta^+ = 17\%$, $\beta^- = 39\%$, $EC = 43\%$) through using NOTA (p-SCN-Bn-NOTA) bi-functional chelator and performed preliminary biodistribution studies in mouse bearing breast adenocarcinoma.

Methods: Anti-ROR1 was conjugated with NOTA (Macrocylics B-605), the average number of the chelator conjugated per mAb was calculated and total concentration was determined by spectrophotometrically. NOTA- anti-ROR1 was labeled with ⁶⁴Cu then Radiochemical purity and immunoreactivity by 4T1 cell line and serum stability of ⁶⁴Cu-NOTA- anti-ROR1 were determined. The biodistribution studies and radioimmunosciintigraphy were performed in female BALB/c mouse bearing breast carcinoma tumor (⁶⁴Cu-NOTA- Anti-ROR1 i.v., 100 μ l, 20 \pm 5 μ g mAb , 6, 12, 24 and 48 h).

Results: ⁶⁴Cu-NOTA- anti-ROR1 was prepared (RCP $>97.1\% \pm 0.7$, Specific activity 4.3 ± 0.7 μ Ci/ μ g). Conjugation reaction of chelator (80 molar excess ratio) to antibody resulted in a product with the average number of chelators attached to a mAb (c/a) of 5.9 ± 0.8 Labeling yield with ⁶⁴Cu in 400 μ g concentration of bioconjugate was $94.9\% \pm 1.1$. Immunoreaction of ⁶⁴Cu-NOTA- anti-ROR1 complex towards ROR1 antigen was determined by RIA and the complex showed high immunoreactivity towards ROR1. In vitro and in vivo stability of radioimmunoconjugate was

investigated respectively in PBS and blood serum by RTLC method. In vitro stability showed more than $92.2\% \pm 2.2$ in the PBS and $78.5\% \pm 2.7$ in the serum over 48 h. The Immunoreactivity of the radiolabeled anti-ROR1 towards MDA-MB-231 cell line was done by using Lindmo assay protocol. Under these conditions, the immunoreactivity of the radioimmunoconjugate was found to be 0.77. The biodistribution of ^{64}Cu -NOTA- anti-ROR1 complex in the mice with normal and breast tumor at 6, 12, 24 and 48 h after intravenous administration, expressed as percentage of injected dose per gram of tissue (%ID/g). Biodistribution and imaging studies at 24 and 48 h post-injection revealed the specific localization of complex at the site of tumors.

Conclusion: ^{64}Cu -NOTA- anti-ROR1 is a potential compound for molecular imaging of PET for diagnosis and follow up of ROR1 expression in oncology.

op 020

Wednesday, November 27, 2019

15:30-15:40, Laleh hall

Computational, radiolabeling and biological studies: A diagnostic biomolecule for targeting amyloid- β plaques in Alzheimer's disease rat model

Safura Jokar¹, Mostafa Erfani², Mohammad Sharifzadeh³, Davood Beiki⁴

¹Department of Radiopharmacy, Faculty of Pharmacy, Tehran University of Medical Sciences, Tehran, Iran.

²Radiation Application Research School, Nuclear Science and Technology Research Institute (NSTRI), Tehran, Iran.

³Department of Toxicology and Pharmacology, Faculty of Pharmacy; Toxicology and Poisoning Research Centre, Tehran University of Medical Sciences, Tehran, Iran.

⁴Research Center for Nuclear Medicine, Tehran University of Medical Sciences, Tehran, Iran.

Background: Alzheimer's disease (AD) is recognized as one of the most prevalent causes of dementia that about 46 million worldwide people suffer from dementia. Also, it is predicted, this number will arrive to quadruple by 2050. According to pathophysiology evidence, amyloid- β ($\text{A}\beta$) plaques are considered as one of the principal pathological hallmarks of AD in the brain. Therefore, the development of new radiotracers for $\text{A}\beta$ plaques imaging can be useful for the detection of AD. With respect to these findings, we designed and synthesized a derived peptide of $\text{A}\beta_{42}$ C-terminal sequence and radiolabeled with technetium-99m for imaging of $\text{A}\beta$ plaques in Alzheimer's rat Model.

Methods: The derived peptide was prepared using the Fmoc solid-phase method. The peptide was radiolabeled with $^{99\text{m}}\text{Tc}$ complex and the stability studies were performed in plasma serum and cysteine solution. Moreover, binding affinity assay of the radio-peptide to formed $\text{A}\beta$ aggregation was measured. Finally, bio-distribution and imaging studies of radiolabeled peptide were carried out in normal and AD rats.

Results: The peptide was synthesized in great yield (more %98) using the Fmoc solid-phase peptide synthesis method and successfully radiolabeled with $^{99\text{m}}\text{Tc}$ agent in mild condition. Radiochemical purity (more 95%) obtained at an optimal condition and radiolabeled peptide demonstrated high stability against plasma serum and ligand exchange after 24h. According to the obtained results of the stability studies and Log P-value, we encouraged to evaluate brain uptake in normal and AD rats using bio-distribution and imaging studies. Radiolabeled peptide demonstrated a suitable brain uptake in AD rats at 30 min after injection due to the presence of $\text{A}\beta$ plaques in the brain of AD rats.

Conclusion: Our results illustrated that this radiotracer may be valuable in the diagnosis of $\text{A}\beta$ plaques in clinical studies.

Radiopharmacy (Posters)

p 001 **Radiolabeling, biodistribution and nuclear imaging of chitosan microparticle labeled with ^{99m}Tc**

Saleh Salehi Zahabi¹, Samira Rasaneh²

¹Department of Radiology and Nuclear Medicine, Kermanshah University of Medical Sciences, Kermanshah, Iran

²Department of Radiology, Lorestan University of medical sciences Lorestan, Iran.

Background: Due to excellent biocompatibility and biodegradability of Chitosan, have been used extensively in pharmaceutical application and radiopharmaceutical in nuclear medicine.

Objective: The aim of study was evaluate radiolabeling, biodistribution and Imaging of Chitosan microparticle labeled with ^{99m}Tc.

Methods: In this Experimental study synthesized microparticle and then were used DLS and SEM for size distribution and morphology of particle. After radiolabeling with ^{99m}Tc, labeling efficiency and stability was performed. Finally, biodistribution study in Balb/c mice in 15,30,60, and 120 min after injection of 200 μ Ci of radiolabel of chitosan complex with ^{99m}Tc were performed.

Results: Results showed that the microparticle have spherical shape and with average size $35\pm 10\mu\text{m}$. The labeling efficiency of chitosan microparticle with ^{99m}Tc was $93\pm 2\%$, $95\pm 4\%$ and stability obtained $98\pm 2\%$. Biodistribution study showed high accumulation of Chitosan microparticle in lung

Conclusion: The results showed that the ^{99m}Tc-Chitosan microparticles may be considered as a suitable radiopharmaceutical for lung scintigraphy in nuclear medicine, so that suggest more investigations for final conclusion.

p 002 **Comparison of nano-radio-ytterbium and nano-radio-scandium bio-distribution in mice**

Navideh Aghaei Amirkhizi¹, Fariba Johari Daha¹, Leila Moghaddam Banaem², Sodeh Sadjadi¹

¹Applied Radiation School, Nuclear Science and Technology Research Institute, Tehran, Iran

²Material and Nuclear Fuel School, Nuclear Science and Technology Research Institute, Tehran, Iran

The purpose of this study is the evaluation of safety and dose rates of nano radio ytterbium-175 and nano-radio-scandium-46 in the organs of the mice based on biological distribution in two groups of mice, which were administered intravenously by ytterbium-175 and scandium-46 nano radiopharmaceuticals intramuscularly through the caudal vein and in another group directly into the tumor site. To prepare this nano radio pharmaceutical, ytterbium/scandium is encapsulated in the PAMAM dendrimers by synthesis and then irradiated in the Tehran research reactor by 3×10^{12} n/cm².sec neutron flux for two hours outside the reactor core. Quality control tests included nanoparticle analyzes in terms nano particle size, and morphology, as well as radionuclide and radiochemical and chemical properties on the final product are done. After ensuring its purity and properties, it is injected into two groups of mice for in vivo studies. After administration of nano radio ytterbium-175 and nano radio scandium-46, they show the activity in liver, spleen and lungs. This proves that critical organs are liver, spleen and lungs, but the dose rate is not in a high range. The results have showed that nano radio ytterbium-175 and nano radio scandium-46 are suitable for solid tumors therapy.

p 003 **Internal dosimetry of ⁸⁹Zr-trastuzumab radiopharmacy for PET/CT imaging using MCNPX code in the breast cancer**

Saeedeh Izadi Yazdi¹, Mahdi Sadeghi², Elham Saeedzadeh¹, Asghar Haddadi¹

¹Department of Medical Radiation Engineering, Science and Research Branch Islamic Azad University, Tehran, Iran

²Department of Medical Physics, University of Medical Sciences, Tehran, Iran

Background: In recent years the production and use of ^{89}Zr radionuclides have focused on tumor diagnostic for PET imaging. This radionuclide, with a half-life of 78.41 h and 23% positron emission is used to label monoclonal antibodies for tumor imaging. ^{89}Zr Today, it is mainly produced by the $^{89}\text{Y} (p, n) ^{89}\text{Zr}$ reaction by bombarding yttrium metal with cyclotron.

Objective: Internal dosimetry study of ^{89}Zr -trastuzumab radiopharmacy for PET/CT Imaging using MCNP code in the breast cancer.

Methods: In this study, the effective dose for breast cancer patients for PET/CT imaging was investigated. The calculated dose of human organs was calculated using MCNPX code and MIRD analytical method.

Results: The dose of ^{89}Zr -trastuzumab radiopharmacy in different organs of the human body was calculated based on the distribution of information in the mice body using MCNPX simulation code and MIRD analytical method. The highest effective dose reached the liver ($3.43\text{E-}02$ and $4.00\text{E-}02$) mSv and the lowest effective dose reached the brain ($1.15\text{E-}04$ and $3.63\text{E-}04$)mSv respectively.

Conclusion: The results showed that the liver and kidneys are at risk for zirconium-89 radiopharmacy imaging.